ABSTRACT

Title of Dissertation: ELECTRONIC MODIFICATION WITHIN THE WELL-ESTABLISHED CPAM FRAMEWORK AS A MEANS TOWARD INCREASED REACTIVITY

Richard Ray Thompson, Doctor of Philosophy, 2018

Dissertation directed by: Professor Lawrence R. Sita
Department of Chemistry and Biochemistry

Early transition metals (group IV-VI) supported by the pentamethylcyclopentadienyl-amidinate mixed ligand set (CPAM) have been found to enable a number of important chemical transformations including (living) coordinative polymerization of alpha-olefins, fixation of dinitrogen and group transfer chemistry involving oxo, imido and sulfido ligands to unsaturated organic substrates, including carbon dioxide. A great deal of the allure and success associated with these complexes is their modularity, particularly as it concerns the amidinate component which is tunable at both the N-bound substituents as well as the distal position. Accordingly, a great deal of work has established that by reducing the sterics in all three positions engendered higher reactivity. There exists, however, a practical “steric wall” such that the size of substituents can only be contracted so much. Tuning of the electronic character of these well-established systems could prove to be a novel and

potent method for affecting reactivity of these complexes within an already well understood steric environment.

ELECTRONIC MODIFICATION WITHIN THE WELL-ESTABLISHED CPAM FRAMEWORK AS A MEANS TOWARD INCREASED REACTIVITY

by

Richard Ray Thompson

Dissertation submitted to the Faculty of the Graduate School of the
University of Maryland, College Park in partial fulfillment
of the requirements for the degree of
Doctor of Philosophy
2018

Advisory Committee:
Professor Lawrence R. Sita, Chair
Professor Mohamad Al-Sheikhly
Professor Osvaldo Gutierrez
Professor Efrain Rodriguez
Professor Andrei Vedernikov

Acknowledgements

It has been a long, strange trip to be sure. First of all, I need to thank my girlfriend, Christine So, who has supported me throughout my time at UMD. She has fulfilled every role I needed from chauffeur, therapist, editor and friend. I am incredibly lucky to have her in my life.

Dr. Wonseok Hwang and Dr. Tessy Thomas were two of the best labmates, and more importantly, friends I could have had here. Coming into a new lab this late in my career could have been difficult transition; however, it was one which was made much smoother because of these two. Wonseok also patiently taught me much of what I know about polymerization and polymer science.

Dr. Peter Zavalij, the UMD x-ray crystallographer, was crucial to my success as a graduate student in College Park and was someone who was both patient and enthusiastic in discussing the solving of various datasets. He was also incredibly dedicated to getting meaningful structures out of crystals, a highly difficult task.

Prof. Andrei Vedernikov was a great collaborator and resource, teaching me how to run my own calculations, a skill which has been very beneficial for me. I could be a headstrong and overeager student at times but was always greeted with grace by him.

Finally, I am indebted to Prof. Lawrence Sita for allowing me to complete my degree under his tutelage. It was admittedly a complicated situation but I am grateful for the opportunity to work for him. He taught me a lot, including being rigorous and detail-oriented in my work, and how to conduct electro-chemistry. I look back fondly on the two of us setting up the E-chem last fall. It meant a lot to me to receive that amount of one-on-one attention.

Table of Contents

List of Tables

List of Figures

List of Schemes

Chapter 1: Ligand Design as a Means Toward Catalyst Improvement

1.1 Introduction

It could be argued that much of the beauty and utility associated with organometallic-based chemistry and catalysis is due to the cornucopia of elements, geometries and environments which are available. Consequentially a substantive body of work within the field has focused on the development and improvement of novel ligand frameworks which may enforce unusual geometries, electronic structures or bonding motifs. From these fundamental studies have come paradigms in molecular design which further inform catalysis. A primary example of this is the use of sterics within the primary coordination sphere to enforce low-coordination number geometries (i.e. C. N $\leq$ 5) which facilitates substrate binding.[1] Similarly, asymmetry imparted by judicious ligand design has allowed for the catalytic formation of chiral products from achiral or pro-chiral substrates, [2] the impact of which is highlighted by the 2001 Nobel Prize in chemistry awarded to Sharpless, Knowles and Noyori for their work in asymmetric catalysis.

Complimentary to the steric-based, non-bonding strategies mentioned above, the presence of unique bonding interactions between substrate and organometallic species have had an equally important impact on catalysis. The presence of α-agostic interactions within transition-metal catalyzed olefin polymerization proved to be a crucial insight in understanding and describing the mechanism of monomer insertion and polymer propagation.[3] Similarly, independent work from the laboratories of Borovic[4] and Fout,[5] respectively, has shed light on the use of hydrogen-bonding between substrate and the

secondary coordination sphere of the transition metal to impact powerful chemical transformations in biomimetic ways.

A third (and perhaps less developed) means for imparting novel or improved reactivity vis-à-vis ligand design is the electronic modification of the supporting ligands. This allows for tuning of a number of attributes associated with both the ligand and the metal center including donor strength, redox-potential and Lewis acidity, among others, while maintaining approximately the same steric profile, thereby inheriting any and all benefits associated with selective modification of ligand size but with the added control imparted by electronic tuning.

1.2 Inductive Modifications

Inductive modifications of ancillary ligands, while not as deeply investigated as steric perturbations, do have precedent and date back to some of the earliest advancements in organometallic chemistry. The use of highly-fluorinated alkoxy ligands on tungsten alkylidenes and alkylidynes led to some of the first examples of homogenous catalysts for both olefin[6] and alkyne metathesis.[7] It was proposed that the ability of these catalysts to facilitate such important transformations was due to the highly electrophilic metal center generated by the poorly-basic alkoxides. Fluorination of parts (or all) of ancillary ligands found further traction with respect to metathesis chemistry as Johnson found success in generating air-stable, bench-stable molybdenum nitrides which functioned as precatalysts for alkyne-metathesis.[8] This feat is particularly tantalizing as most early transition metal-based metathesis catalysts suffer from extreme sensitivity to water and as such usually must be stored and used under an inert atmosphere. It is interesting to note that the metal-preference for an alkylidyne ligand was reversed when

descending from molybdenum to tungsten.[9] Finally, the groups of Perez[10] and later Caulton[11] were able to accomplish silver-catalyzed carbene insertion into the C-H bonds of light alkanes, including methane and ethane. The use of highly halogenated ancillaries was believed to be critical to their success, inductively generating "super-electrophilic carbenes" capable of activating the robust C-H bonds of alkanes.

At times, observed electronic effects do not trend well with intuition. For example, study of the oxidation potential of 1,1'-dihaloferrocenes along the halogen

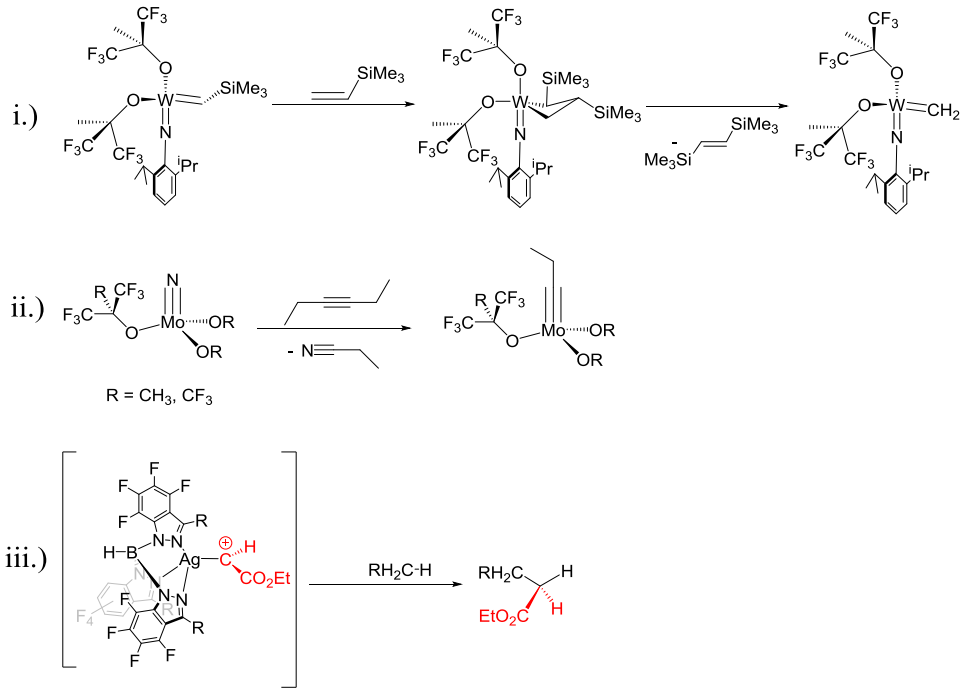

Scheme 1.1. Examples of the beneficial effect of fluorinated ligands in organometallic chemistry from Schrock (i.), Johnson (ii.) and Perez (iii.). Depending on the system, fluorination can impart greater Lewis acidity (i.), increased stability to air and moisture (ii.) or higher electrophilicity at a reactive center (iii.).

series (X = F, Cl, Br, I)[12] found that the difluoro-derivative was actually the easiest to oxidize, despite fluorine being a well-known inductively withdrawing group which should therefore destabilize the ferrocenium cation. Electrochemical, structural and theoretical studies showed that this apparent contradiction was the result of covalent stabilization of the Fe^{2+} oxidation state by the heavier halogen congener metallocenes.

Similarly, oxidation of [Fe(C_5H_5)(C_5F_5)] was found to occur at surprisingly low potentials (0.01 eV vs Fc/Fc^+);[13] this is particularly interesting when compared with the perchloro-analog [Fe(C_5H_5)(C_5Cl_5)], which had an oxidation potential of 0.77 eV.[14]

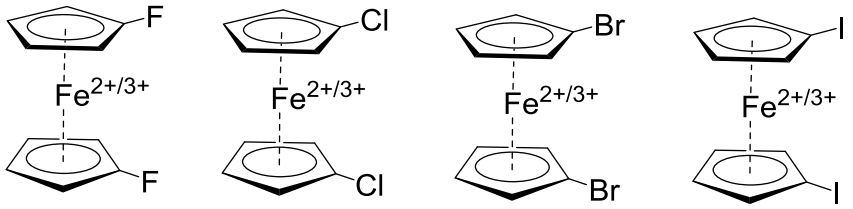

$E_{1/2}$ =	0.239 V	0.316 V	0.319 V	0.287 V

Scheme 1.2. $E_{1/2}$ for the Fe($2^+/3^+$) along the vertical series of 1,1'-dihalo-substituted ferrocenes. Despite F being the most electron-withdrawling the 1,1'-difluoroferrocene is the easiest to oxidize.

It is important to note that one difficulty associated with heteroatom-substitution within ligand sets as a means of electronic tuning is their non-innocence (i.e. ability to independently interact with reagents) and/or vulnerability toward bond-cleavage either during metallation or as a result of forming reactive intermediates throughout a relevant chemical reaction.[15] As such, thoughtful consideration of the type of modification, as well as the regiochemistry of the substitution, is necessary to prevent catalyst inhibition or formation of catalytically inactive species. The final point concerning regiochemistry is further highlighted, particularly as it pertains to aromatic or otherwise delocalized systems, wherein resonance contributions can attenuate or amplify inductive effects based on their placement along the π-system.

1.3 Secondary Bonding Interactions and Spin-State Modifications

While inductive perturbations to ancillary ligands are a powerful method for tuning the spectroscopy, reactivity and redox chemistry of organometallic complexes, an

alternative approach in recent years has been to modulate the orbital and spin-state characteristics of the reactive bonds. Two of the most impressive examples of this are Berry's tetra-formamide-supported diruthenium nitride, $Ru_2(dPhf)_4N$[16] and the dipyrrin-based iron imido/imidyl complexes from Betley.[17]

1.3.1 Diruthenium Nitrides Capable of C-H Activation

Ruthenium nitrides are a common motif in coordination chemistry,[18] likely owing to the high stability of the metal-nitrogen triple bond. A consequence of this stability is its limited reactivity. By incorporating novel electronic features such as three-center-four-electron bonding (3c4e), however, increased reactivity can be forced upon the nitride moiety. Accordingly, photolysis of the mixed valent, diruthenium species, $Ru_2(dPhf)_4N_3$ (dPhf = diphenylformamidinate), at low temperature led to net 2-electron oxidation,

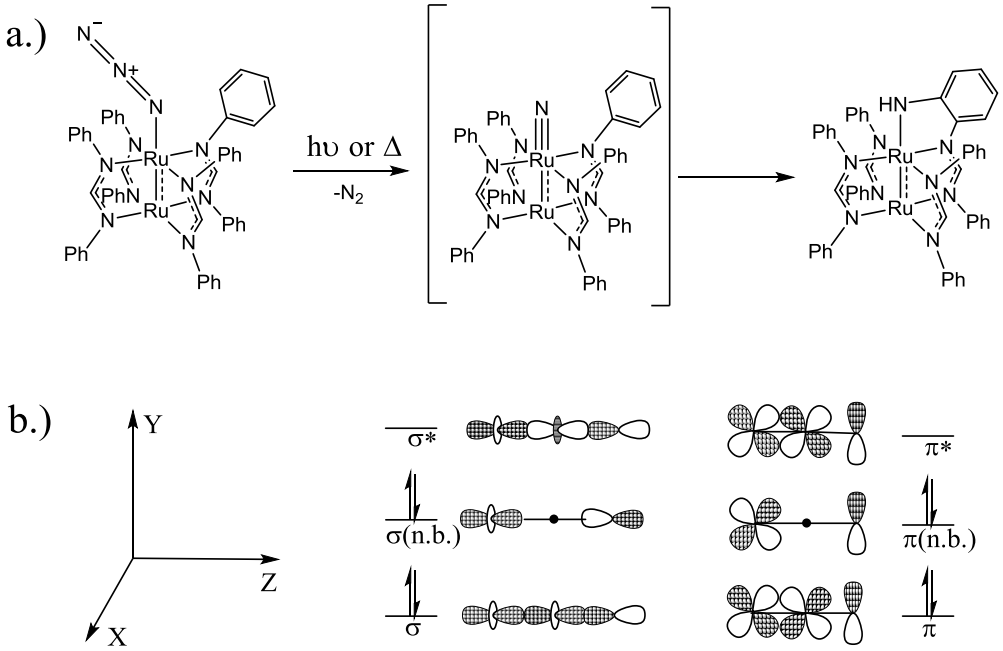

Scheme 1.3. a.) 3c4e bonding along the Ru-Ru-N vector generates the first instance of C-H activation via a transition metal nitride. b.) orbital explanation for the 3c4e bonding along the Ru-Ru-N vector.

concomitant with dinitrogen extrusion, generating a transient Ru_2(III/IV) nitride (Scheme 1.3a). Consideration of the nitride-bound Ru shows that the a Ru(IV) nitride in a pseudo-octahedral ligand field would suggest that such a species should be completely inaccessible due to two electrons occupying the degenerate e_u-set, which corresponds to π * antibonding interactions. The presence of 3c4e interactions along the Ru_2N vector allows for population of non-bonding interactions of both σ- and π-symmetry (Scheme 1.3b). Delocalization along this same vector is also responsible for stabilization of the π* LUMO, thereby generating a "super-electrophilic" nitride, one which allowed for the first instance of C-H bond activation by a transition metal nitride to generate a "tucked-in" amide.

1.3.2 Spin-state Dependent C-H Amination via Iron Imidyls

Iron-ligand multiple bonds have garnered significant interest from numerous sub-disciplines of chemistry including inorganic, organic and biochemistry due to their relevance in alkane-oxidation, especially as it relates to the cytochrome P450 enzyme responsible for such remarkable feats as converting methane to methanol. More specifically, iron imides have gained particular interest due to their isolobal similarity to the oxo in cytochrome P450 but with the benefit of a tunable steric and electronic environment. Further, the importance of C-N bonds in pharmaceutical chemistry cannot be understated and the ability of insert a NR linkage into otherwise unreactive C-H bonds could greatly expedite the synthesis of drug and/or biologically relevant molecules. That said, while a plethora of iron imides exist with a variety of geometries, oxidation states and spin-states;[19] few have been found to replicate the chemistry associated with P450. Unfortunately, though a number have been characterized and found to undergo group

transfer to unsaturated carbon substrates or activate allylic and benzylic C-H bonds;[19c,20] full amination of alkyl substrates has remained largely underdeveloped. The one glowing exception to this is the work of Betley, wherein 3 or 4coordinate iron imido or imidyl species have been found to undergo amination chemistry both intermolecularly and intramolecularly to productively generate heterocyclic products catalytically. The major difference found in Betley's system making it superior to the likes of Holland[20] or Mindiola[21] among others[19] in terms of C-H amination, is the use of a weak-field ancillary ligand. This facilitates either intermediate or high-spin imido/imidyl complexes. The population of antibonding orbitals within the bona-fide imido species generates a nitrogen-center which already has some radical character and therefore is pre-designed to undergo H-atom abstraction. This attribute can be found in other low-coordinate iron imides, including Holland's, hence their shared ability to undergo related C-H activation chemistry. What is unique, however, is the ability of the resulting S = 5/2 amide in Betley's system to facilitate radical rebound via a partially filed π^* orbital which can readily interact with the unpaired spin on the alkyl radical. Kinetics experiments, in conjugation with very thorough spectroscopic and theoretical work, found that by increasing the extent of unpaired spin density on the imidyl nitrogen, lower barriers were observed such that an alkyl imidyl was more potent than its aryl analog, owing to the latter's ability to delocalize spin density throughout the aryl ring.

1.4 Conclusion

The following chapters are concerned with the implementation and study of electronic perturbation to the well-established, versatile and (importantly) highly tunable pentamethylcyclopentadienyl-amidinate mixed ligand set (CPAM), both in the form of

inductive modulation and secondary-bonding interactions. In both instances, marked improvements with respect to the standard system could be observed. While dilation or

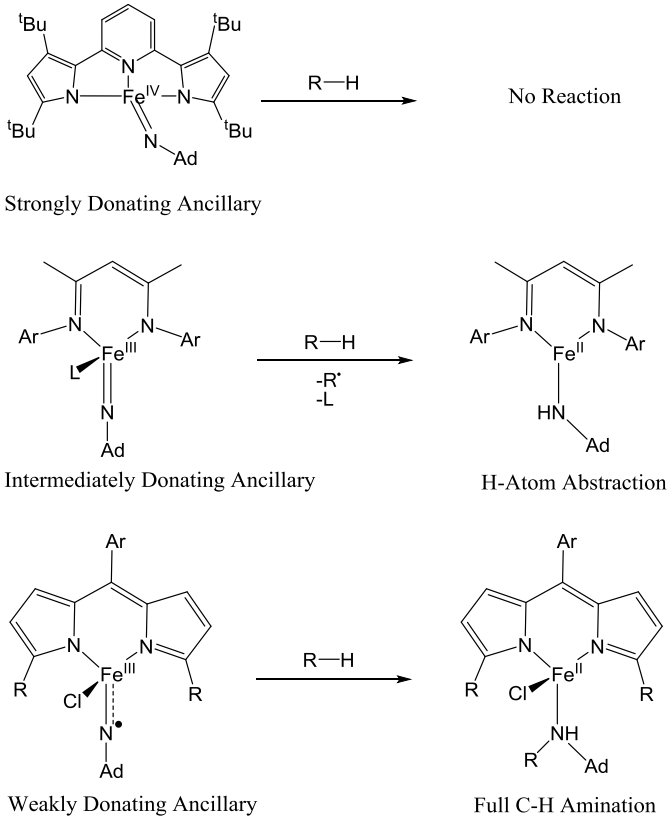

Scheme 1.4. Lowering of ancillary field strength increases the reactivity of Fe-NR ligands.

contraction of substituents within the amidinate framework has been a successful path for controlling reactivity, the accessibility of comparable gains in reaction rate by way of orthogonal electronic tuning could benefit in two ways: (1) Further advancement within the current optimized steric environment; (2) The use of steric environments previously deemed unusable due to drastic declines in activity but which could provide higher regio- or stereoselectivity.

1.5 References

1. (a.) Trnka, T. M.; Grubbs, R. H. *Acc. Chem. Res.* **2001**, *34*, 18-29. (b.) Crabtree, R. *Acc. Chem. Res.* **1979**, *12*, 331-337.
2. (a.) Knowles, W. S. *Acc. Chem. Res.* **1983**, *16*, 106-112. (b.) Kolb, H. C.; VanNieuwenhze, M. S.; Sharpless, K. B. *Chem. Rev.*, **1994**, *94*, 2483-2547.
3. Grubbs, R. H.; Coates, G. W. *Acc. Chem. Rev.* **1996**, *29*, 85-93.
4. (a.) Hammes, B. S.; Young, V. G.; Borovik, A. S. *Angew. Chem. Int. Ed.* **1999**, *38*, 666-669. (b.) MacBeth, C. E.; Golombek, A. P.; Young, V. G. Jr.; Yang, C.; Kuczera, K.; Hendrich, M. P.; Borovik, A. S. *Science*, **2000**, *289*, 938‑941.
5. (a.) Matson, E. M.; Bertke, J. A.; Fout, A. R. *Inorg. Chem.* **2014**, *53*, 4450-4458. (b.) Ford, C.; Park, Y. J.; Matson, E. M.; Gordon, Z.; Fout, A. R. *Science* **2016**, *354*, 741-743.
6. Schaverien, C. J.; Dewan, J. C.; Schrock, R. R. *J. Am. Chem. Soc.* **1986**, *108*, 2771-2773.
7. Freudenberger, J. H.; Schrock, R. R.; Churchill, M. R.; Rheingold, A. L.; Ziller, J.W. *Organometallics* **1984**, *3*, 1563-1573.
8. Gdula, R. L.; Johnson, M. J. A. *J. Am. Chem. Soc.* **2006**, *128*, 9614-9615.
9. Geyer, A. M.; Gdula, R. L.; Wiedner, E. S.; Johnson, M. J. A. *J. Am. Chem. Soc.* **2007**, *129*, 3800-3801.
10. Caballero, A.; Despagnet-Ayoub, E.; Diaz-Requejo, M. M.; Diaz-Rodriguez, A.; Gonzalez-Nunez, M. E.; Mello, R.; Munoz, B. K.; Ojo, W.-S.; Asensio, G.; Etienne, M.; Perez, P. J. *Science* **2011**, *332*, 835-838.

11. Flores, J. A.; Komine, M.; Pal, K.; Pinter, B.; Pink, M.; Chen, C-H; Caulton, K. G.; Mindiola, D. J. *ACS Catal.* **2012**, *2*, 2066-2078.

12. Inkpen, M. S.; Du, S.; Hildebrand, M.; White, A. J. P.; Harrison, N. M.; Albrecht, T.; Long, N. J. *Organometallics* **2015**, *34*, 5461-5469.

13. Sunkel, K.; Weigand, S.; Hoffmann, A.; Blomeyer, S.; Reuter, C. G.; Vishnevskiy, Y. V.; Mitzel, N. W. *J. Am. Chem. Soc*. **2015**, *137*, 126-129.

14. Brown, K. N.; Gulyas, P. T.; Lay, P. A.; McAlpine, N. S.; Masters, A. F.; Phillips, L. *J. Chem. Soc., Dalton Trans.* **1993**, 835-840.

15. Bellows, S. M.; Brennessel, W. W. Holland, P. L. *Eur. J. Inorg. Chem.* **2016**, 3344-3355.

16. (a.) Long, A. K. M.; Yu, R. P.; Timmer, G. H.; Berry, J. F. *J. Am. Chem. Soc*. **2010**, *132*, 12228-12230. (b.) Timmer, G. H.; Berry, J. F. *Chem. Sci.* **2012**, *3*, 3038-3052.

17. (a.) King, E. R.; Hennessy, E. T.; Betley, T. A. *J. Am. Chem. Soc.* **2011**, *133*, 4917-4923. (b.) Hennessy, E.T.; Betley, T. A. *Science*, **2013**, *340*, 591-595. (c.) Iovan, D. A.; Betley, T. A. *J. Am. Chem. Soc.* **2016**, *138*, 1983-1993. (d.) Wilding, M. J. T.; Iovan, D. A.; Betley, T. A. *J. Am. Chem. Soc.* **2017**, *139*, 12043-12049. (e.) Wilding, M. J. T.; Iovan, D. A.; Wrobel, A. T.; Lukens, J. T.; MacMillan, S. N.; Lancaster, K. M.; Betley, T. A. *J. Am. Chem. Soc.* **2017**, **DOI:** 10.1021/jacs.7b08714

18. 42 Examples in the CCDC

19. (a.) Verma, A. K.; Nazif, T. N.; Achim, C.; Lee, S. C. *J. Am. Chem. Soc*. **2000**, *122*, 11013-11014; (b.) Thomas, C. M.; Mankad, N. P.; Peters, J. C. *J. Am. Chem.*

Soc. **2006**, *128*, 4956-4957; (c.) Nieto, I.; Ding, F.; Bontchev, R. P.; Wang, H.; Smith, J. M. *J. Am. Chem. Soc.* **2008**, *130*, 2716-2717; (d.) Klinker, E. J.; Jackson, T. A.; Jensen, M. P.; Stubna, A.; Juhasz, G.; Bominaar, E. L.; Munck, E.; Que, L. *Angew.Chem. Int. Ed.* **2006**, *45*, 7394-7397; (e.) Zhang, H.; Ouyang, Z.; Liu, Y.; Zhang, Q.; Wang, L.; Deng, L. *Angew. Chem. Int. Ed.* **2014**, *53*, 8432-8436.

20. (a.) Cowley, R. E.; Eckert, N. A.; Vaddadi, S.; Figg, T. M.; Cundari, T. R.; Holland, P. L. *J. Am. Chem. Soc.* **2011**, *133*, 9796-9811. (b.) Cowley, R. E.; Holland, P. L. *Inorg. Chem.* **2012**, *51*, 8352-9361.
21. Searles, K.; Fortier, S.; Khusniyarow, M. M.; Carroll, P. J.; Sutter, J.; Meyer, K.; Mindiola, D. J.; Caulton, K. G. *Angew. Chem. Int. Ed.* **2014**, *53*, 14139-14143.

Chapter 2: The Role of Secondary Bonding Interactions in Nitrene Group Transfer for a Vertical Series of Group 14 Substituted Imidos

2.1 Introduction

Transition metal imidos or nitrenes (i.e. M=NR) have played an indispensible role in fields as diverse as small-molecule activation,[1] olefin metathesis[2] and organic synthesis[3] both as spectator ligands and reaction centers. A great deal of the importance

Figure 2.1. Two canonical forms for bonding in a transition metal imido/nitrene complexes.

associated with this moiety lies in the versatility of the substituents decorating the nitrogen atom, allowing for flexibility when tuning the steric profile as well as electronic character of the metal-nitrogen linkage. Sterically, the size of the substituent can range from incredibly bulky 2,6-terphenyl and so-called "super silyl" (-SiR_3; R = CMe_3, $SiMe_3$) groups which bias the imido toward functioning as a terminal ligand or to the parent imido (M=NH) which has relevance in dinitrogen fixation to ammonia.[4] Electronically, a great deal of tuning is also possible, varying from electron-rich alkyl groups, aryl substituents with an array of donating properties, to highly withdrawing groups such as tosyl (para-tolylsulfonyl), nosyl (para-nitrophenylsulfonyl) and triflato (trifluoromethylsulfonyl). Generally speaking, and assuming a closed-shell N-atom, it is possible to divide the bonding in transition metal imidos between the two canonical

forms shown in Figure 2.1. In the case of the alkyl and aryl imidos, the best explanation for the bonding, particularly when involving early transition metals, is a pair of covalent, 2 electron bonds between nitrogen and the metal. Contrastingly, those M=NR interactions with highly electron-poor substitutents (e.g. tosyl, nosyl, etc.) render the N atom so electron-poor that it is often better to view the NR group as a neutral nitrene ligand whose double bond is more in line with acting as a σ donor and π acceptor (i.e. a "Fischer nitrene"). The extreme electrophilicity imparted on the nitrogen in these latter groups has made them highly popular in metal-catalyzed NGT to sp^2 and sp^3 C-H bonds.[5] Finally, recent experimental and computational work suggest that the presence of imidyl radicals, M-NR$^{\cdot}$, are particularly adept at undergoing the same reactions.[6] This comparison becomes even more powerful as it has been shown that there is a stark disparity in reactivity between bona-fide closed-shell imidos and their open-shell, imidyl, analogs; all exist within the same ancillary ligands and oxidation states.[7] Betley has successfully exploited subtle differences in ancillary ligand choice, the poorly-donating dipyrrin ligand, to generate a high-spin, S = 5/2 iron center, despite of the presence of a strong-field imido ligand. The iron anti-ferromagnetically couples to the S = ½ N-center (Figure 2.2) leading to an overall S = 2 complex. The synergetic ability of the N-based radical to undergo H-atom abstraction (HAA) coupled with the high-spin metal center facilitated not only HAA, a feat which occurred in other 3 or 4-coordinate iron imido systems, but the more difficult radical-rebound to facilitate full, metal-catalyzed amination. These differences in orbital population/electronic structure were further exploited to generate a number of N-containing heterocycles catalytically,[3f] the products being highly important precursors for biological and medicinal chemistry. This is a particularly powerful

advancement in the understanding of metal-ligand multiple bonding and one which was exclusively achievable via manipulation of the bonding and electronic structure of the Fe-NR vector.

As stated above, imidos play a crucial role in synthetic chemistry by way of nitrene group transfer (NGT) and are responsible for a myriad of diverse products including amines,[6-8] isonitriles,[9] heterocumulenes[9a,10,11] as well complex heterocycles.[3,5,7,12] A particularly prevalent example of nitrene group transfer is the synthesis of heterocumulenes such as isocyanates or carbodiimides. Both early and late

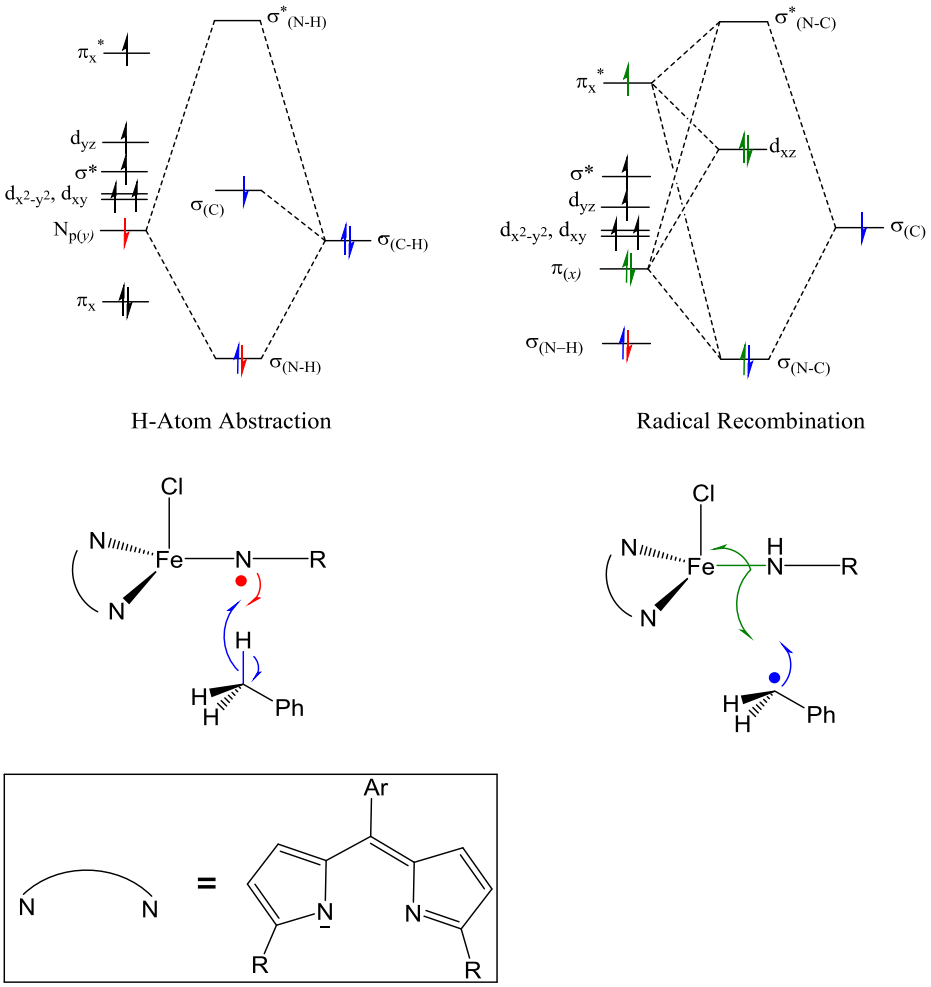

Figure 2.2. Orbital explanation for increased reactivity observed for Betley's iron imidyl for C-H amination.

transition metals systems have been reported, which mediate this transformation from a corresponding organic azide and either carbon monoxide or isonitrile, respectively.[10,11] In rare instances, carbon dioxide can be substituted for the C_1 source to generate the same products, providing encouraging examples of using greenhouse gases to make valuable commodity chemicals.[9a] Such methods for producing these products can also be viewed as more environmentally benign relative to the current routes which oftentimes employ highly dangerous and toxic starting materials such as phosgene.

While several systems are capable of stoichiometric production of carbodiimides,[11] only six systems have been reported that achieve this catalytically, all of which are distinct from one another (Scheme 2.1). The first report of catalytic turnover belongs to Saegusa[10a] with the simple precatalyst, $Fe(CO)_5$, which produced carbodiimide in moderate yields, albeit at high temperatures (90 ^{o}C) and a large excess of the expensive isonitrile reagent, relative to azide. Holland[10a,10b] realized similar results without the high temperatures used by Saegusa, treating his formally Fe(I) dinitrogen (or tris-isonitrile) complex with aryl or alkyl azides and either carbon monoxide or isonitriles. A pair of competition experiments performed by this group showed a slight selectivity (3.8 : 1) for electron-poor azides (4-triflouromethylphenyl azide vs 4-methylphenyl azide) and, unsurprisingly, a small bias toward less bulky isonitriles (2,6-diethylphenyl vs 2,6-diisopropylphenyl).[10c] The Heyduk group[10d] utilized an ingenious combination of a highly nucleophilic imido on zirconium in tandem with a redox-active NNN pincer ligand to catalytically produce either N,N'-di-tert-butyl-carbodiimide or N-adamantyl-N'-tert-butyl-carbodiimide. This was one of the first concrete examples of synthetic chemists complementing traditional organometallic tools (i.e. metal-ligand multiple bond polarity)

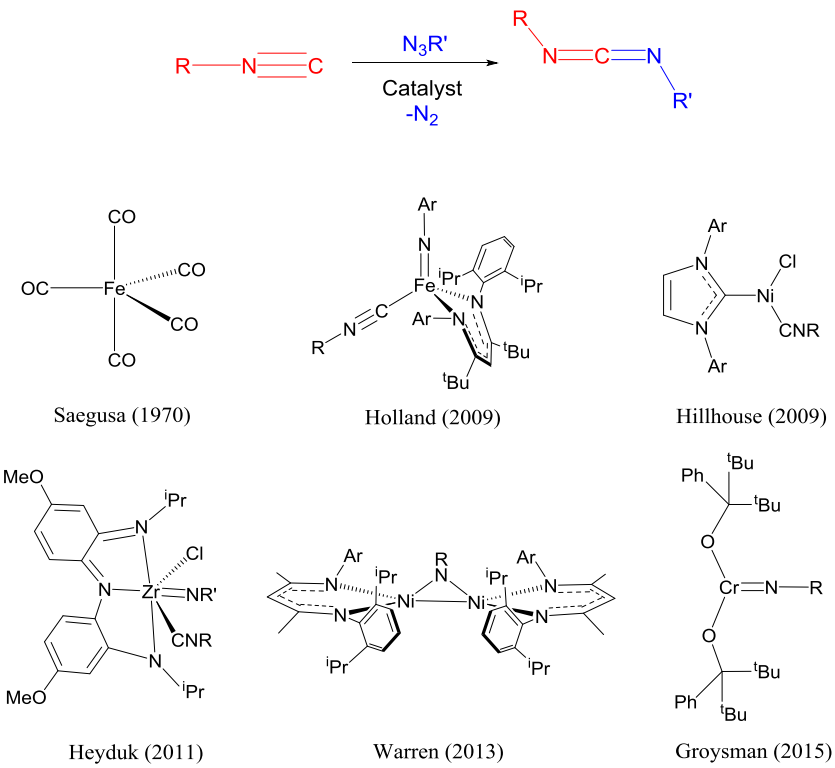

Scheme 2.1. General scheme for catalytic carbodiimide generation and examples of the catalysts.

with the more provocative addition of ligand redox non-innocence to facilitate catalysis (i.e. changes to oxidation state occured at the ligand as opposed to the metal center). Hillhouse[10e] and later Warren[10f] realized catalytic turnover using dinuclear nickel imido species. The latter system showed outstanding scope with respect to both isonitrile as well as organic azide, though it should be noted that it was not compatible with trimethylsilyl azide; instead, it resulted in the formation of a catalytically inactive Ni(II) azide species. It is also worth noting that, unlike the Holland system, the Warren system showed a much higher preference for electron-rich azides. Finally, in 2015 Groysman[10g] found a 3-coordiante Cr(IV) imido capable of generating asymmetric carbodiimides, provided the imido substituent was large enough to prevent catalyst shutdown via a Cr(VI) bis-imido product but not so large as to prevent coupling of the imido with isonitrile. The Groysman system is further interesting, and relevant with respect to the

chemistry of this document, as it invokes an *umploung* mechanism for imido-isonitrile coupling such that the early-transition metal imido acts as the electrophile while the isonitrile is nucleophilic. This highlights that group VI transition metals have a unique position within organometallic chemistry and catalysis that the readily-accessible mid to low oxidation states associated with these metals are able to impart reactivity more associated with the later transition metals. Such duality in reactivity without the use of sophisticated, redox-noninnocent ligands suggests that a renaissance of the (comparably) cheap group VI metals could be on the horizon.

An unfortunate downfall to nearly all of the aforementioned systems, even those which can utilize carbon dioxide as a substrate, is the reliance on organic azides or other "value-added" nitrogen sources. A much more appealing (and atom-economic) route to such species would be one which is capable of generating the same imidos from atmospheric nitrogen. Utilizing the pentamethylcyclopentadienyl (Cp*), amidinate (amidinate = [N(^{i}Pr)C(Me)N(^{i}Pr)]) ligand framework (henceforth referred to as CPAM), it was found by the Sita group[13] that photolytic cleavage of dinitrogen followed by treatment with the appropriate group 14 halide (i.e. CR_3Cl, SiR_3Cl, GeR_3Cl) generated the corresponding metal imido. Upon exposure to carbon monoxide, these dinitrogen-based imidos yielded isocyanate product, as well as a molybdenum bis-carbonyl species, Cp*Mo[N(^{i}Pr)C(Me)N(^{i}Pr)]$(CO)_2$, which, under the right reaction conditions, could be cycled back to close the synthetic cycle. Additional studies found that carbon dioxide could take the place of CO to generate the same product (Scheme 1), albeit under much more forcing conditions (70 psi CO_2, T = 75 ^{o}C) and with a considerably longer reaction time (~ 3 days), counter to higher oxidation state systems wherein the microscopic

reverse of this reaction is seen to occur readily.[14] This is one of the only systems which can, in the same synthetic cycle, fix both dinitrogen as well as carbon dioxide.

While a system capable of producing value-added organic species from carbon dioxide (or monoxide) and dinitrogen is certainly a tantalizing result, the extended

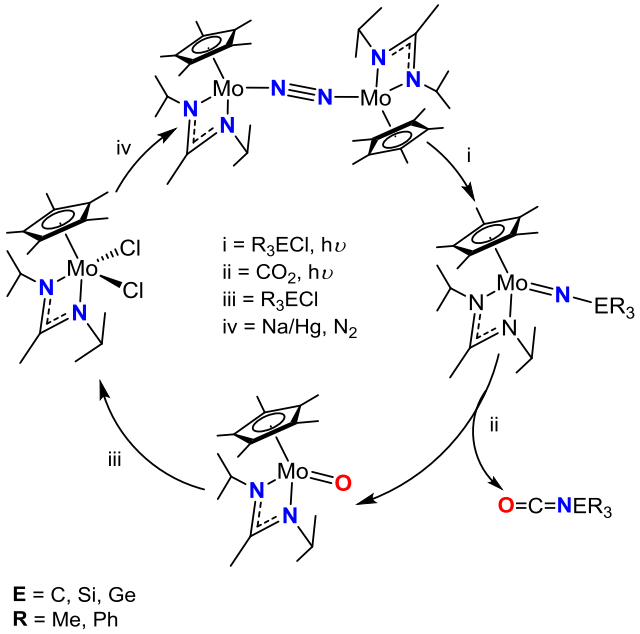

Scheme 2.2. Synthetic cycle converting dinitrogen and carbon dioxide to value-added isocyanates.

reaction times, as well as the forcing conditions under which the reaction occurred, suggests that additional studies on the factors governing the rate of NGT to substrate are in order with the final goal of making the current cycle less energy-intensive and eventually, catalytic. Qualitatively, a non-linear trend in the rate of nitrene group transfer to carbon monoxide based on the N-bound substituent was found such that the silyl imido proceeded the most readily, with the germanyl being slightly slower and finally, the traditional alkyl imido, the most sluggish. To establish a firm, quantitative understanding of NGT in the Cp*Mo[N(^{i}Pr)C(Me)N(^{i}Pr)](NEMe$_3$) (E = C, Si, Ge) system and the origin of the privileged spot which Si occupies in it, kinetics studies were performed, the results of which form the heart of this chapter. A secondary goal of this work was to expand the

scope of products produced by this system and as such, the synthesis of carbodiimides from the corresponding imidos and an aryl isonitrile (2,6-dimethylphenylisonitrile) were used as the model system.

2.2 Results and Discussion

2.2.1 Synthesis of a Vertical Series of Group 14 Carbodiimides

As previously reported, a series of molybdenum imido species of the type, Cp*Mo[N(^{i}Pr)C(Me)N(^{i}Pr)](NEMe$_3$) (E = C (**2.1**), E = Si (**2.2**), E = Ge (**2.3**)) can be produced in fair to modest yield *via* a number of routes,[10h] including fixation of dinitrogen.[13] Treatment of either **2.2** or **2.3** with 3 equivalents of 2,6-dimethylphenylisonitrile at room temperature cleanly converts over the course of 8 hours to the previously reported bis-isonitrile species Cp*Mo[N(^{i}Pr)C(Me)N(^{i}Pr)](CNAr)$_2$ (**2.4**)[15] as well as a new organic product in a 1:1 ratio (Scheme 2.3), as seen by ^{1}H NMR. While **2.1** reacted more sluggishly at room temperature, heating to 65 ^{o}C for 8 h achieved full conversion (Figure 2.3). For the reactions involving **2.1** and **2.2**, the resulting organic product could be identified as the previously reported carbodiimides ^{t}Bu=N=C=NAr (**2.5**) and Me$_3$SiN=C=NAr (**2.6**), respectively.[16] In the case of **2.6**, ^{15}N and ^{29}Si NMR spectroscopy were further enlisted to insure that the isomeric cyanimide had not formed due to trimethylsilyl migration.[17] Gratifyingly, a doublet centered at 1.78 ppm in the ^{29}Si NMR with a $^1J_{29Si\text{-}15N}$ = 14.0 Hz provided additional support for the carbodiimide isomer based on similar coupling constants in the structurally related isocyanate, Me$_3$SiN=C=O.[13] The germanyl derivative (**2.7**) represents both the sole example of a germanium-substituted carbodiimide and only the 2nd example of NGT involving a germanyl-imido, the first of which was also achieved in the Sita laboratory.[13] Neither **2.7**

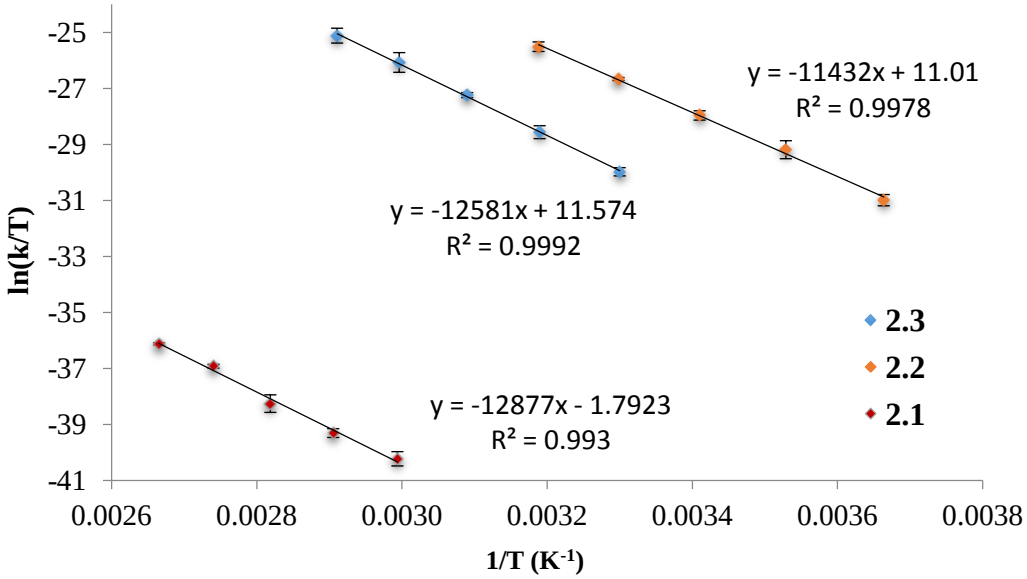

Figure 2.3. Temperature-dependent second-order rate constants with least-squares fit to the linear form of the Eyring equation, $\ln(k/T) = \ln(k_B/h) + \Delta S^{\ddagger}/R - \Delta H^{\ddagger}/R(1/T)$, for the conversion of **2.1** → **2.5**, **2.2** → **2.6** and **2.2** → **2.7**. For each imido, 5 temperature points were acquired in 10 K increments ranging from 273.4 K to 375.4 K and performed in duplicate (error bars shown).

nor the related trimethyl-germanyl isocyanates, which was previously reported, have been isolated cleanly, potentially due to the liability of the N-Ge bond.

2.2.2 Kinetic and Mechanistic Study on Nitrene Transfer

Given the considerable differences in reaction times for the three imidos, in addition to the paucity of data on activation parameters for NGT, an Eyring analysis was performed for the reaction of **2.1**-**2.3** with the isonitrile, 2,6-diisopropylphenyl-isonitrile (Figure 2.3). This study was particularly enticing given the otherwise isostructural nature of the vertical series of group 14 congeners. Kinetics studies were performed under pseudo-first order condition with respect to the imidos, using a 30 fold excess of isonitrile, and monitoring the decay of the EMe_3 resonance by ^1H NMR spectroscopy over the course of the reaction versus an internal (durene) standard (Figure 2.4). The

curves plotting [Imido] versus time confirm 1st order rate dependence as a function of imido. A nonlinear least-squares analysis provided k_{obs} for each run. For each imido, 5 temperature points were acquired in 10 K increments ranging from 0.2 °C to 102.0 °C and

Table 2.1. Experimentally Derived Activation Parameters for Nitrene-Group Transfer

	$\Delta H^{\ddagger}$(kcal/mol)[b]	$\Delta S^{\ddagger}$(cal/(mol K))[b]	$\Delta G^{\ddagger}$ (kcal/mol)[a,b]
2.1	12.88(8)	-50.8(1)	28.0(8)
2.2	11.43(7)	-25.3(1)	19.0(7)
2.3	12.58(6)	-24.2(1)	19.8(6)

[a]Calculated at 298.15 K. [b]Error reported at the 95% confidence interval

performed in duplicate. The derived activation parameters are presented in Table 2.1. The $\Delta G^{\ddagger}$ values of **2.1** (28.0 kcal/mol), **2.2** (19.0 kcal/mol) and **2.3** (19.8 kcal/mol) are in accord with the observed rates of reaction with $k_{Si} > k_{Ge} >> k_{C}$.

Breaking the activation parameters down into both enthalpy ($\Delta H^{\ddagger}$) and entropy of activation ($\Delta S^{\ddagger}$) gives a far better understanding of the factors which control the nitrene group transfer, and more importantly, the ways in which they may be controlled. The order of $\Delta S^{\ddagger}$ values for the three reactions are indicative of greater steric congestion

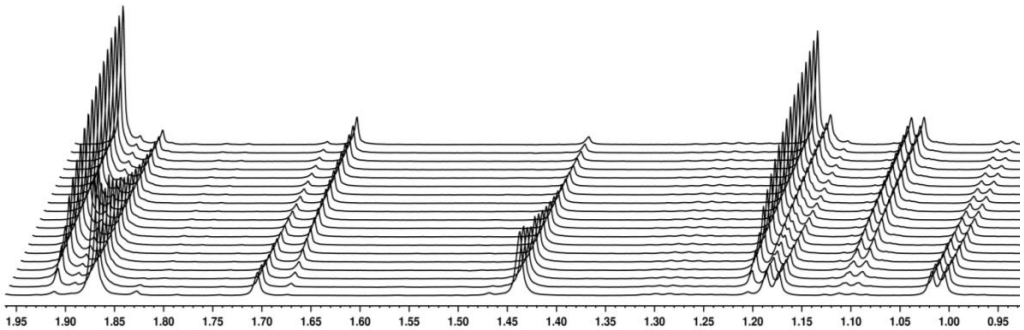

Figure 2.4. NMR stacked plot of group transfer from **2.1** to CNAr to generate **2.4** and **2.5** at 81.6 °C, Δt = 100 min.

which, consequentially, results in a more ordered transition state around the metal center as a result of the shorter N-E bond, which elongates going from C to Si to Ge (Table 2.2). This assessment is supported by viewing the A-values of the nitrogen bound substitutents in which CMe_3 (A = 4.7) is considerably more encumbering than either $SiMe_3$ (A = 2.5)[17] or $GeMe_3$ (A = 2.07),[19] and is further corroborated by the observed N-EMe_3 bond distances of 1.459 (**2.1**), 1.740 (**2.2**) and 1.851 Å (**2.3**).[10h, 13]

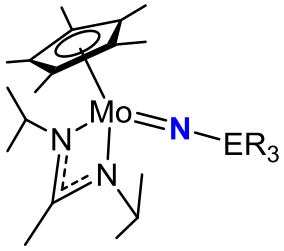

Table 2.2. Comparison of Organic A-Values and N-EMe_3 Bond Distances in 2.1-2.3.

	E = C	E = Si	E = Ge
A-Value	4.7	2.5	2.07
N-EMe_3	1.459 Å	1.740 Å	1.851 Å

More notable (and less obvious) is the non-linear trend in $\Delta H^{\ddagger}$ observed upon changing the congeners along the series, with 12.9 kcal/mol for **1** being higher than either **2.2** (11.5 kcal/mol) or **2.3** (12.6 kcal/mol). These 1.4 and 0.3 differences in $\Delta H^{\ddagger}$ between **2.2** and the other two imidos is likely due to the heightened π-acidity of the Si-Me bonds, which presumably lowers the multiple bond character of the Mo=N bond and consequentially, the barrier for isonitrile insertion. Lappert[20] observed a similar spike in Me_3E-X BDE (E = C, Si, Ge, Sn; X = Br, NMe_2, SBu, Cl, OEt) which was suggested to be due to Si π-acidity strengthening the Si-X bond via donation of the X-group's lone-pair into the accessible d-orbital (or Si-Me σ*). There is a minor contradiction in this logic however; Ge should be a superior π-acceptor due to better accessibility to d-orbitals

or (more likely) mixing into the Ge-Me σ* and thus should drive down the enthalpy of activation even further. To better understand this apparent contradiction, Density Functional Theory (DFT) calculations were enlisted in collaboration with Dr. Andrei Vedernikov.

2.2.3 Computational Investigation

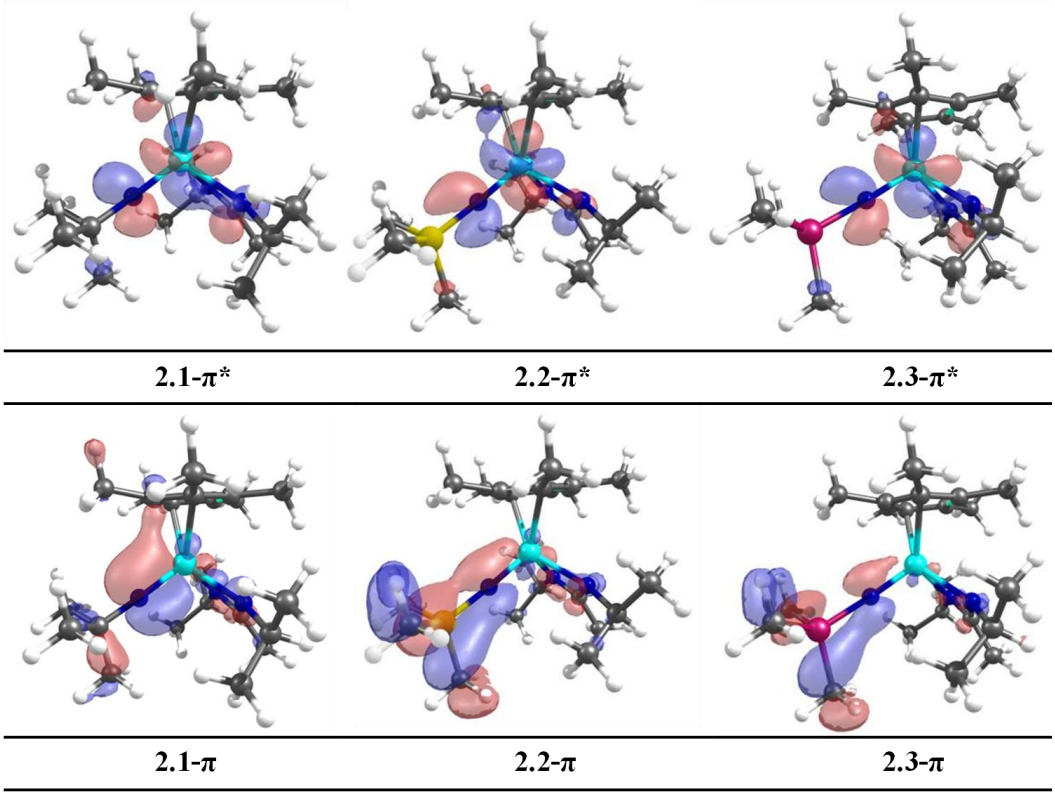

Figure 2.6. Pertinent molecular orbitals for the π bonds of **2.1**-**2.3**. Delocalization of Mulliken density for **2.2** and (to a lesser extent) **2.3** is observed for both the π and π*. Isosurfaces are shown at 0.05. Using the PBE functional and SBK basis set with Priroda program.

The immediate insights from the calculations can be seen wherein one set of the (non-degenerate) bonding and antibonding π-orbitals for each of the three imidos is displayed (Figure 2.6). For **2.1** essentially no contribution of the CMe_3 group on the π-network is observed, as should be predicted. Both **2.2** and **2.3**, however, show significant delocalization of electron density along the Mo=N-EMe_3 vector, supporting their role in

facilitating group transfer. A second observation made from this figure is that while a significant amount of Ge-Me σ* contribution exists for **2.3**, the spatial overlap between the Ge and N is reduced relative to **2.2**. Therefore, while Ge is technically a better π-acid, the longer Ge-N distance leads to reduced orbital overlap and consequentially, less perturbation to the Mo=N multiple bond. The superiority of silicon is further supported by the calculated energies of the respective LUMOs for **2.1-2.3** (all of which are of π* symmetry with respect to the Mo-N vector) wherein **2.2** is the lowest in energy (-1.23 eV vs -0.93 eV for **2.1** and -1.07 eV for **2.3**). It should be noted that the π-effects observed in the LUMO of **2.2** also exist for **2.3**, albeit to a lesser extent. Similar π-effects have been observed by Hillhouse[11i] and Betley,[6a,6b,7] among others; however, in those cases, the asymmetry associated with the N-Ar vector, as well as weaker field strength and reduced coordination, led to different consequences within those systems. While $\Delta H^{\ddagger}$ is the more dominating factor for all three imidos, $\Delta\Delta S^{\ddagger}$ is larger throughout the series; this indicates that while the electronic structure of the reactant(s) is the larger contributor to $\Delta G^{\ddagger}$, change in the sterics of the reaction has a more pronounced effect on the activation barrier.

To further probe the mechanism for nitrene group transfer, DFT calculations were again utilized in collaboration with Dr. Vedernikov. The gas-phase reaction sequence considered, along with the calculated standard Gibbs energies for each step are shown in Figure 2.7. Coordination of the first equivalent of isonitrile (L) to the Mo center is noticeable endergonic for all 3 complexes, **2.1-2.3**, ranging from 5.9 (E= C) to 6.8 (E = Si) kcal/mol. Rate-determining isonitrile insertion into Mo=N bond to produce complexes of the respective η^2-coordinated carbodiimides then occurs with calculated Gibbs

activation energies of **2.1** = 22.1, **2.2** = 17.7, **2.3** = 18.9 kcal/mol in good agreement with the experimental values given in Table 1. The final release of free carbodiimides **2.5-2.7** from their complexes Cp*Mo[N(^{i}Pr)C(Me)N(^{i}Pr)](η^2-ArNCNEMe$_3$) can be broken down into three steps. First, coordination of a second isonitrile ligand produces the weak adducts Cp*Mo[N(^{i}Pr)C(Me)N(^{i}Pr)](L)(η^2-ArNCNEMe$_3$), **INT 2.1-2.3**, which are not sufficiently stable to either isonitrile dissociation (the microscopic reverse of the forward reaction) or carbodiimide dissociation to observe this intermediate. Interestingly, the subsequent carbodiimide dissociation from **INT 2.1-2.3** is itself a two-step procss. The calculations located a second intermediate associated with carbodiimide release, the κ^1-N-isomers Cp*Mo[N(^{i}Pr)C(Me)N(^{i}Pr)](L)(κ^1-N-ArNCNEMe$_3$), which are 10.8 - 12.5 kcal/mol higher energy than **INT 2.1-2.3**. The κ^1-N-isomeric intermediates then undergo a facile and very exergonic dissociation of carbodiimides **2.5-2.7** to produce mono-isonitrile intermediate complexes, which subsequently coordinate the third equivalent of isonitrile to finally form **2.4**. Carbodiimide release and formation of **2.4** was found to be highly favorable thermodynamically. The results of the calculations also predict

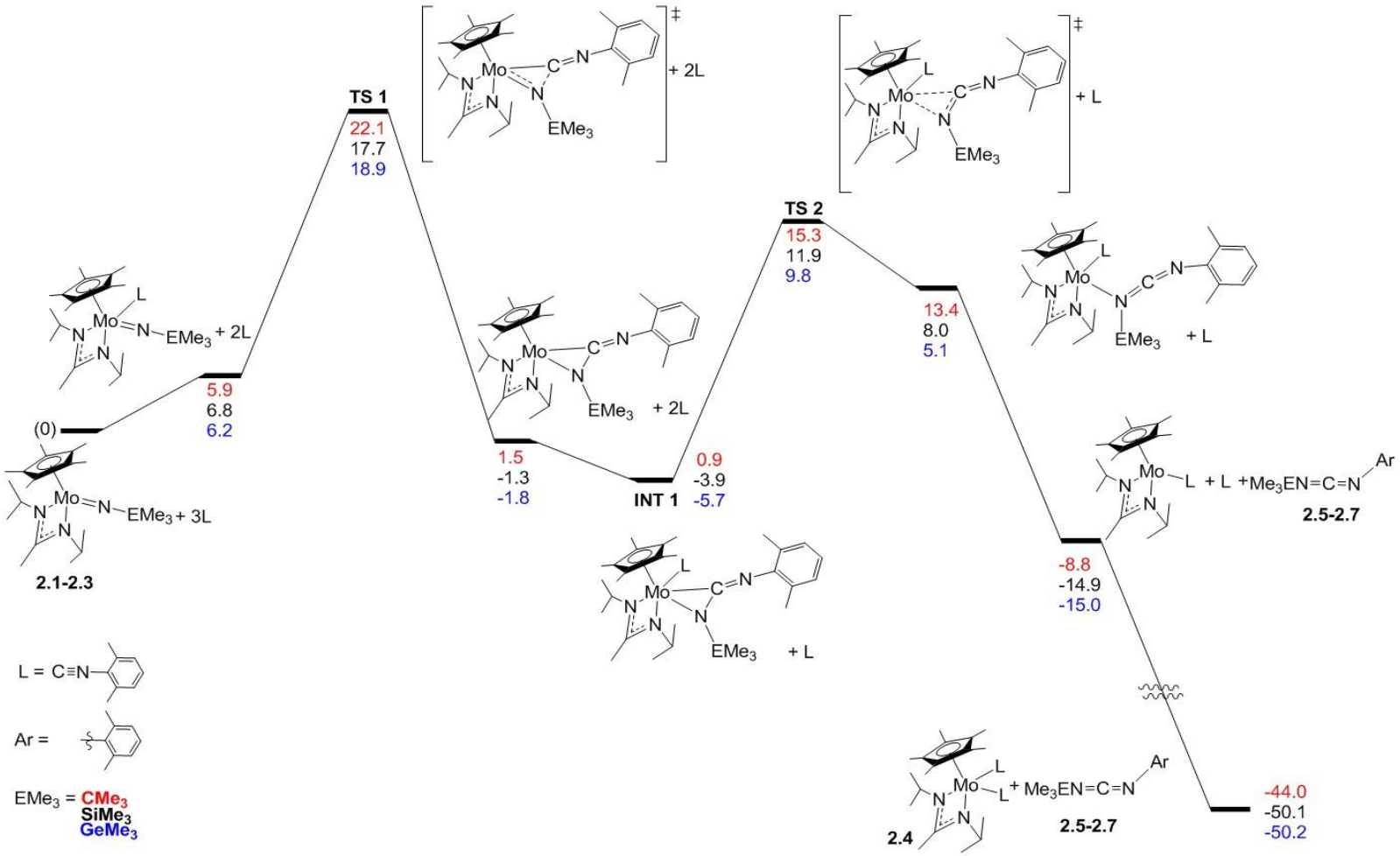

Figure 2.7. Fully-modelled mechanism for NGT from **2.1, 2.2** and **2.3** to isonitrile. Gibbs free energies (kcal/mol, T = 298 K) for minima, maxima and transition states (labeled **TSx**) are shown in bold relative to the imido and 3 equivalents of isonitrile.

the viability of observing Cp*Mo[N(^{i}Pr)C(Me)N(^{i}Pr)](L)(η^2-ArNCNEMe$_3$) in reaction mixtures and that E = Si has the highest barrier of release in agreement with experimental observations.

Finally, the umploung mechanism for C-N coupling wherein the imido nitrogen is electrophilic is further supported when viewing the computed bonding metrics associated with the rate-determining transition state. As can be seen from Table 2.3, the Mo1-N2 distances elongate considerably (greater than 0.1 Å) in all cases, which makes sense given the weakening of the Mo=N double bond. A more subtle change can also be seen

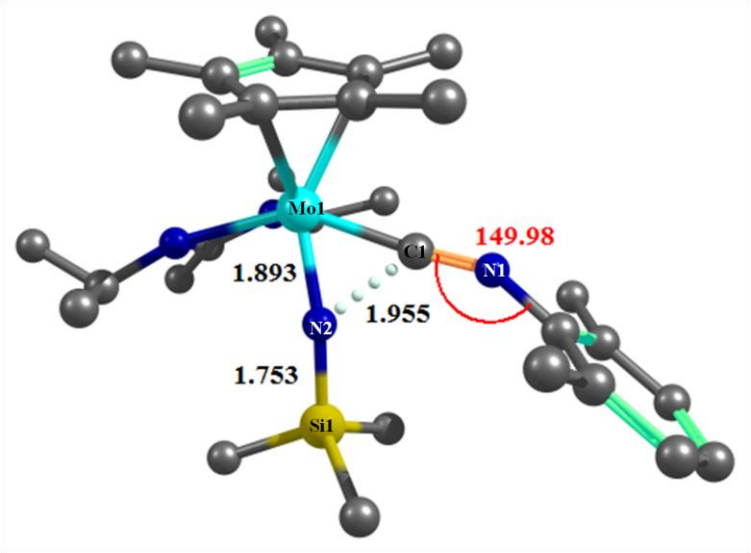

Table 2.3. Metrics in Computed TS for NGT (Change Relative to Imido)

	C1-N2 (Å)	Mo1-N2 (Å)	N2-E1 (Å)
2.1	1.931	1.876 (+0.105)	1.449 (+0.001)
2.2	1.955	1.893 (+0.114)	1.753 (-0.008)
2.3	1.967	1.880 (+0.109)	1.857 (-0.004)

between the N2-E1 distances in the transition state. While the transition state associated with **2.1** shows a small elongation which can be explained on steric grounds (i.e. exceptional crowding about the reaction center), the same bonds associated with **2.2** and **2.3** actually show a minor contraction, suggesting that attack on the nitrogen strengthens

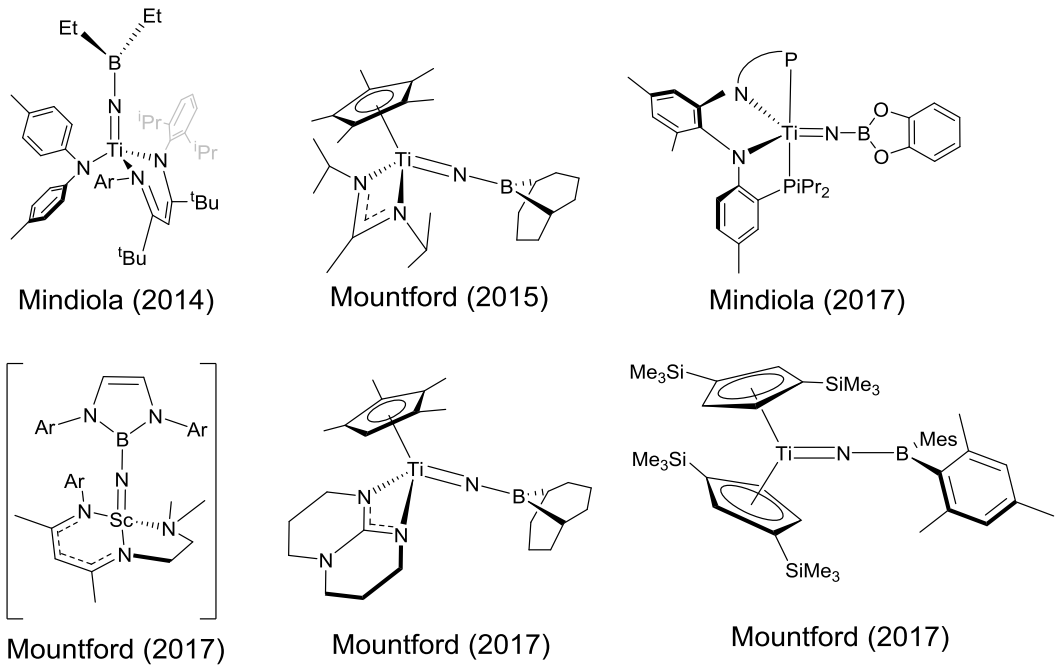

Figure 2.8. Recent examples of borylimidos from the past 3 years.

the bonding interaction along the N-EMe_3 axis due to the LUMOs of **2.2** and **2.3** both having partial N-E π-character.

2.2.4 Computational Investigation of the Theoretical Borylimido in Nitrene Group Transfer

The role of (pure) π-acidity from N-substituents to facilitate NGT has, to our knowledge, never been invoked despite numerous silyl imidos being known. Interestingly, a group-13, hetero-imido renaissance has recently occurred (Figure 2.8),[21] particularly between the groups of Mindiola and Mountford. These species may be capable of even more facile group transfer due to the accessibility of an empty p-orbital. The resulting products are further intriguing given the extended heterocumulene-like structures which would result.

To further probe the effect of π-acidity toward group transfer, a separate, independent computational study was performed under the identical reaction conditions with the hypothetical borylimido, Cp*Mo[N(iPr)C(Me)N(iPr)](NBMe$_2$), (**2.8**) wherein there is an adjacent B-based p-orbital, which is otherwise empty and as such should prove to be a potent π-acid. The structure of this theoretical molecule was optimized and has comparable bond distances and angles relative to the related species, Cp$_2$TiNBMes$_2$ (Mes = 1,3,5-trimethylphenyl), which was recently reported by Mountford,[21e] upon taking into account the larger size of Mo, relative to Ti. The calculated barrier of insertion ($\Delta G^{\ddagger}$ = 12.3 kcal) is over 5 kcal less than the **2.2** analog and nearly 10 kcal less than the same row analog of **2.1**. Admittedly there is a difference in the sterics of the boryl BMe$_2$ group

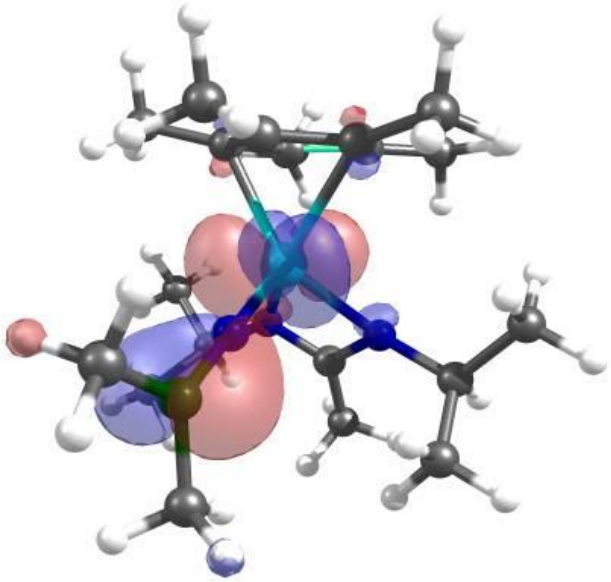

Figure 2.9. Graphical representation of the LUMO of the theoretical borylimido, **2.8**, revealing the complete delocalization of the N-lone pair into the empty, B-based p-orbital.

and the trimethyl-group 14 analogs in **2.1**-**2.3**. It should also be noted that in the optimized structure, the empty p orbital (and consequentially the LUMO) is oriented along the "belt" between the Cp* ring and the amidinate, as opposed to **2.2** or **2.3** wherein the orbital of appropriate orientation is located in the LUMO+1 while the LUMO

is orthogonal. The orientation of the former structure is likely a result of the more pressing steric factors imposed by the diisopropylamidinate over the

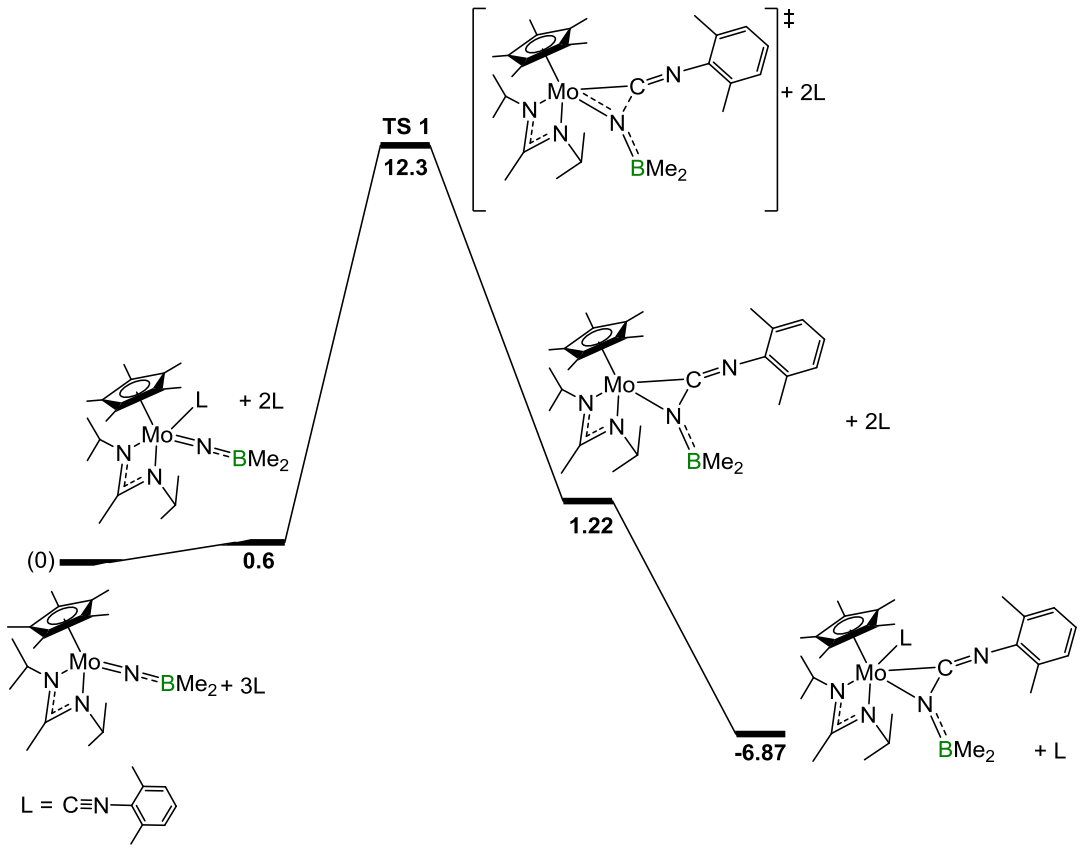

Figure 2.10. Reaction energy diagram for nitrene-group transfer between **2.8** and 2,6-dimethylphenyl-isonitrile.

pentamethylcyclopentadienyl ligand.

The above results have shown the importance of electronic/orbital factors in fine-tuning the barrier for group transfer chemistry. In 2009 Schrock et al. tested a similar hypothesis as it pertained to olefin metathesis with heteroatom-supported alkylidenes including both π donors (alkyoxy, thio, amino and phosphino) as well as π-accepting substitutents (boronic esters).[22] Although it should be noted that these efforts were not done as systematically as here, any deviations in activation energy in there were

attributed to a difference in steric profile, with no real differences attributed to a change in the energy of the π-orbitals vis-a-vis lone pair (or empty p-orbital) interactions. A significant difference between the imido system studied above and the Schrock alkylidenes(s) is the angle between the metal, related ligand (either carbene or imido) and heteroatom. As a consequence of the hybridization of the alkylidene, the necessary metal-carbon-heteroatom angle in most cases approximates to 120^{o}, whereas the imido nitrogen is capable of SP hybridization due to the orthogonal π-bonds and consequentially, can trend toward an 180^{o} metal-nitrogen-heteroatom bond angle. The more acute bond angle in the Schrock system limits the ability of any orbital overlap to perturb the bonding and consequentially the extent of overlap between the metal-carbon π bond with the heteroatom.

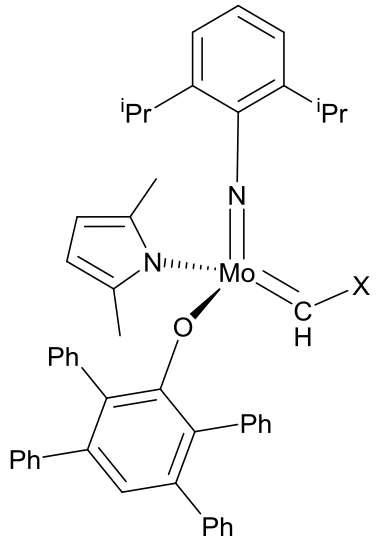

X = $SiMe_3$, O^iPr, SPh, PPh_2, pyrrole, BPin

Figure 2.11. Structure of the heteroatom-substituted alkylidenes investigate by Schrock

2.3 Conclusion

In conclusion, the silyl-substituted imido, Cp*Mo[N(^{i}Pr)C(Me)N(^{i}Pr)](NSiMe$_3$) **(2.2)**, has a privileged spot for NGT as confirmed by both experimental and computational analysis. This unique ease associated with **2.2** is the result of not only reduced steric congestion around the metal center (relative to carbon) due to the longer Si-N bond but, less intuitively, a consequence of perturbed π-bonding between the imido and metal which is more substantial relative to Ge due to the *shorter* Si-N bond. Interestingly, along the series, small changes to the local steric environments of the imido nitrogen result in larger changes as seen by the $\Delta\Delta S^{\ddagger}$ of the reaction while the enthalpy of the reaction(s), $\Delta H^{\ddagger}$, is more substantial but less tunable. The growth of novel, heteroatom-supported imidos with even higher π-acidity than Si may drive down the barrier of reaction further and could produce novel heterocumulene structures. Finally, this work suggests that similar modifications to imido identity and/or ligand environment could dramatically reduce the barrier for NGT to more tantalizing reagents such as CO_2.

To date, the paradigms with which inorganic chemists have approached small molecule activation/functionalization have focused around reducing coordination number and utilizing unusual oxidation states to engender high reactivity. The work which has been presented here suggests that an orthogonal approach wherein tuning the electronics of the metal-ligand multiple bond with π-acids may further facilitate organic transformations.

2.4 Experimental Details

2.4.1 General Considerations

All manipulations with air and moisture sensitive compounds were carried out under N_2 or Ar atmospheres with standard Schlenk or glovebox techniques. Et_2O and THF were distilled from Na/benzophenone under N_2 prior to use. Toluene and pentane were dried and deoxygenated by passage over activated alumina and GetterMax® 135 catalyst (purchased from Research Catalysts, Inc.) within a PureSolv solvent purification system manufactured by Innovative Technologies (model number PS-400-4-MD) and collected under N_2 prior to use. Benzene-d_6 and toluene-d_8 were dried over Na/K alloy and isolated by vacuum transfer prior to use. Celite© was oven dried (150 °C for several days) prior to use. Cooling was performed in the internal freezer of a glovebox maintained at -30 °C. Chemicals were purchased from Sigma Aldrich and used as received. Compounds **2.1**,[1] **2.2**[1] and **2.3**,[2] were prepared according to the previously reported procedures in similar yield and purity. All room temperature ^{1}H NMR were recorded at 400.13 MHz and referenced to $SiMe_4$ using residual ^{1}H chemical shifts of either d_6-benzene (7.16) or d_8-toluene (2.09). Variable temperature ^{1}H NMR studies were recorded at 500 MHz with temperature calibration involving methanol and ethylene glycol standards for low and high temperature studies and referenced using the residual ^{1}H chemical shifts of toluene-d_8 (2.09 ppm).

2.4.2 Synthesis of New Compounds

ArNCNGeMe$_3$ **(2.7)**

2.3 (60 mg, 0.12 mmol) was dissolved in 0.6 ml of C_6D_6 and added to a J. Young NMR tube. To this solution was added 2,6-dimethylphenyl isonitrile (50 mg, 0.38 mmol), which had been dissolved in 0.4 ml of C_6D_6. The red-brown solution slowly changed to emerald green over the course of 8 h at room temperature. ^{1}H NMR (400 MHz, C_6D_6, 25 °C): 0.252 (9H, s, Ge(C*H*$_3$)$_3$), 2.34 (6H, s, 2,6-C*H*$_3$Ar). ^{13}C NMR (125.77 MHz, Tol-d_8, 25 °C): 137.23 (ArN*C*NGe(CH$_3$)$_3$).

2.4.3 Kinetics Experiments

Solutions for Eyring analysis were prepared in a dinitrogen filled glovebox by dissolving 59.5 – 75.5 mmol of 2.1-2.3 in 5 ml of toluene-d_8 to give solutions with concentrations between 11.9 mM – 15.1 mM. For concentration dependence analysis, between 135 – 215.5 mmol tetramethylsilane was added to the solutions containing 2.1-2.3. A separate stock solution was prepared dissolving 305 mmol into either 5 ml (for the reaction done with 2.1) or 10 ml (for the reaction done with 2.2 and 2.3) to give solutions with concentrations of 610 mM and 305 mM, respectively. All solutions were stored and maintained at -30 °C and used immediately after preparation, with aliquots analyzed consecutively until the data set was complete. These solutions were subsequently analyzed at 5 different temperatures within the range of 0 °C to 100 °C in duplicate.

For sample analysis, a J. Young NMR tube was charged with 0.25 ml of stock compound solution followed by 0.25 ml of the stock isonitrile solution, both via separate 1.0 ml syringes, to give an overall volume of 0.50 ml. The NMR tube was pumped out of the glovebox and quickly inserted into a Bruker 500.01 MHz NMR spectrometer that was pre-equilibrated at the desired temperature, with data collection starting simultaneously. Data points were acquired every 10 minutes for solutions of 2.1 and every 5 minutes for

2.2 and 2.3, each with 12 scan per datapoint until a minimum of 3 half-lives were observed.

First-order rate constants for all kinetic runs were determined by a least-squares fit of integration data, to the equation $\ln(A) = -kt + A_0$ using the LINEST function in Excel. and the number of data points included was determined by a standard of linearity ($R^2 > 0.999$) for each kinetic run. Using this standard, up to 3 half-lives of first-order linear data were observed for the compounds examined. All rate constants and initial rates were analyzed in duplicate. Temperature dependent rate constants collected for each compound were least-squares fitted to the Eyring equation, $\ln(k) = \mathrm{Ln}(k_B T/h)\ [(\Delta S^{\ddagger}/R)-(\Delta H^{\ddagger}/RT)]$, using Microsoft Excel. All rate constant, initial rate, and activation parameter errors are reported at the 95% confidence interval.

2.4.4. Computational Details

Theoretical calculations in this work have been performed using density functional theory (DFT) method,[22] specifically functional PBE,[23] implemented in a state-of-the-art program package "Priroda".[24,25] In PBE calculations relativistic Stevens-Basch-Krauss (SBK) effective core potentials (ECP)[26] optimized for DFT-calculations have been used.

Basis set was 311-split for main group elements with one additional polarization *p*-function for hydrogen, additional two polarization *d*-functions for elements of higher periods. Full geometry optimization has been performed without constraints on symmetry. For all species under investigation frequency analysis has been carried out. All minima have been checked for the absence of imaginary frequencies. All transition states possessed only one imaginary frequency. For all reactions where TS's were located the

transition states, corresponding reactants and products were proven to be connected by a single minimal energy reaction path using Intrinsic Reaction Coordinate analysis.

2.5 References

1) For selective examples focusing on C-H and H_2 activation, see the following: (a.) Cummins, C. C.; Baxter, S. M.; Wolczanski, P. T. *J. Am. Chem. Soc.* **1988**, *110*, 8731-8733. (b.) Harlan, C. J.; Tunge, J. A.; Bridgewater, B. M.; Norton, J. R. *Organometallics*, **2000**, *19*, 2365-2372. (c.) Wicker, B.; Fan, H.; Hickey, A. K.; Crestani, M. G.; Scott, J.; Pink, M.; Mindiola, D. J. *J. Am. Chem. Soc.* **2012**, *134*, 20081-20096. (d.) Brown, S. D.; Peters, J. C. *J. Am. Chem. Soc.* **2004**, *126*, 4538-4539. (e.) Walsh, P. J.; Hollander, F. J.; Bergman, R. G. *J. Am. Chem. Soc.* **1988**, *110*, 8729-8731.
2) For selective examples see the following: (a.) Feldman, J.; Davies, W. M.; Schrock, R. R. *Organometallics*, **1989**, *8*, 2266-2268. (b.) Schrock, R. R.; Murdzek, J. S.; Bazan, G. C.; Robbins, J.; DiMare, M.; O'Regan, M. *J. Am. Chem. Soc.* **1990**, *112*, 3875-3886. (c.) Bazan, G.; Khosravi, E.; Schrock, R. R.; Feast, W. J.; Gibson, V. C. *Polym. Commun.* **1989**, *30*, 258-260.
3) For selective examples see the following: (a.) Catino, A. J.; Nichols, J. M.; Forslund, R. E.; Doyle, M. P. *Org. Lett.* **2005**, *7*, 2787-2790. (b.) Doyle, M. P; Hu, W.; Timmons, D. J. *Org. Lett.* **2001**, *3*, 933-935. (c.) Wehn, P. M.; DuBois, J. *J. Am. Chem. Soc.* **2002**, *124*, 12950-12951. (d.) Hinman, A.; DuBois, J. *J. Am. Chem. Soc.* **2003**, *125*, 11510-11511. (e.) Yu, X.-Q; Huang, J.-S.; Zhou, X.-G.; Che, C.-M. *Org. Lett.* **2000**, *2*, 2233-2236. (f.) Hennessy, E. T.; Betley, T. A. *Science* **2013**, *340*, 591-594.

4) (a.) Yandulov, D. V.; Schrock, R. R. *Science* **2003**, *301*, 76-78. (b.) Keane, A. J.; Zavalij, P. Y.; Sita, L. R. *J. Am. Chem. Soc*. **2013**, *135*, 9580-9583.

5) Davies, H. M. L; Manning, J. R. *Nature* **2008**, *451*, 417-420.

6) (a.) Wilding, M. J. Y.; Iovan, D. A.; Betley, T. A. *J. Am. Chem. Soc.* **2017**, *139*, 12043-12049. (b.) King, E. R.; Hennessy, E. T.; Betley, T. A. *J. Am. Chem. Soc.* **2011**, *133*, 4917-4923. (c.) Kuijper, P. F.; Tiekink, M. J.; Breukelaar, W. B.; Broere, D. L. J.; van Leest, N. P.; van der Vlugt, J. I.; Reek, J. N. H.; de Bruin, B. *Chem. Eur. J.* **2017**, *23*, 7945-7952.

7) Wilding, M. J. Y.; Iovan, D. A.; Wrobel, A. T.; Lukens, J. T.; MacMillan, S. N.; Lancaster, K. M.; Betley, T. A. *J. Am. Chem. Soc.* **2017**, **DOI:** 10.1021/jacs.7b08714.

8) (a.) Aguila, M. J.; Badiei, Y. M.; Warren, T. H. *J. Am. Chem. Soc.* **2013**, *135*, 9399-9406. (b.) Wiese, S.; McAfee, J. L.; Pahls, D. R.; McMullin, C. L.; Cundari, T. R.; Warren, T. H. *J. Am. Chem. Soc.* **2012**, *134*, 10114-10121. (c.) Iovan, D. A.; Betley, T. A. *J. Am. Chem. Soc.* **2016**, *138*, 1983-1993. (d.) Cowley, R. E.; Eckert, N. A.; Vaddadi, S.; Figg, T. M.; Cundari, T. R.; Holland, P. *J. Am. Chem. Soc.* **2011**, *133*, 9796-9811.

9) (a.) Kilgore, U. J.; Basuli, F.; Huffman, J. C.; Mindiola, D. J. *Inorg. Chem.* **2006**, *45*, 487-489. (b.)Kriegel, B. M.; Bergman, R. G.; Arnold, J. *J. Am. Chem. Soc.* **2016**, *138*, 52-55.

10) (a.) Saeguesa, T.; Ito, Y.; Shimizu, T. *J. Org. Chem.* **1970**, *35*, 3995-3996. (b.) Cowley, R. E.; Eckert, N. A.; Elhaik, J.; Holland, P. L. *Chem. Commun.* **2009**, 1760-1762. (c.) Cowley, R. E.; Golder, M. R.; Eckert, N. A.; Al-Afyouni, M. H.;

Holland, P. L. *Organometallics* **2013**, *32*, 5289-5298. (d.) Nguyen, A. I.; Zarkesh, R. A.; Lacy, D. C.; Thorson, M. K.; Heyduk, A. R. *Chem. Sci.* **2011**, *2*, 166-169. (e.) Laskowski, C. A.; Hillhouse, G. L. *Organometallics* **2009**, *28*, 6114-6120. (f.) Wiese, S.; Aguila, M. J. B.; Kogut, E.; Warren, T. H. *Organometallics* **2013**, *32*, 2300-2308. (g.) Yousif, M.; Tjapkes, D. J.; Lord, R. L.; Groysman, S. *Organometallics* **2015**, *34*, 5119-5128. (h.) Yonke, B. L.; Reeds, J. P.; Fontaine, P. P.; Zavalij, P. Y.; Sita, L. R. *Organometallics* **2014**, *33*, 3239-3242. (i.) Mindiola, D. J.; Waterman, R.; Lluc, V. M.; Cundari, T. R.; Hillhouse, G. L. *Inorg. Chem.* **2014**, *53*, 13227-13238.

11) (a.) Stokes, B. J.; Richert, K. J.; Driver, T. G. *J. Org. Chem.* **2009**, *74*, 6442-6451. (b.) Stokes, B. J.; Dong, H.; Leslie, B. E.; Pumphrey, A. L.; Driver, T. G. *J. Am. Chem. Soc.* **2007**, *129*, 7500-7501. (c.) Thornton, A. R.; Martin, V. I.; Blakey, S. B. *J. Am. Chem. Soc.* **2009**, *131*, 2434-2435.

12) (a.) Hessell, E. T.; Jones, W. *Organometallics* **1992**, *11*, 1496-1505. (b.) Mindiola, D. J.; Hillhouse, G. L. *Chem. Commun*, **2002**, 1840-1841. (c.) Glueck, D. S., Wu, J. Hollander, F. J.; Bergman, R. G. *J. Am. Chem. Soc.* **1991**, *113*, 2041-2054. (d.) Danopoulos, A. A.; Wilkinson, G.; Sweet, T. K. N.; Hursthouse, M. B. *J. Chem. Soc., Dalton Trans.* **1996**, 3771-3773. (e.) Ishida, Y.; Kawaguchi, H. *J. Am. Chem. Soc.* **2014**, 1*36*, 16990-16993. (f.) Hanna, T. E.; Keresztes, I.; Lobkovsky, E.; Bernskoetter, W. H.; Chirik, P. J. *Organometallics* **2004**, *23*, 3448-3458. (g.) Chomitz, W. A.; Arnold, J. *Chem. Commun.* **2008**, 3648-3650.

13) Keane, A. J.; Farrell, W. S.; Yonke, B. L.; Zavalij, P. Y.; Sita, L. R. *Angew Chem Int. Ed. Engl.* **2015**, *54*, 10220-10224.

14) Chen, G. J.-J.; McDonald, J. W.; Newton, W. E. *Inorg. Chim. Acta.* **1980**, *41*, 49.

15) Fontaine, P. P.; Yonke, B. L.; Zavalij, P. Y.; Sita, L. R. *J. Am. Chem. Soc.* **2010**, *132*, 12273-12285.

16) Keane, A. K., Ph.D. Thesis, University of Maryland-College Park, **2015**.

17) Babcock, J. R.; Sita, L. R. *J. Am. Chem. Soc.* **1998**, *120*, 5585-5586.

18) Anslyn, E. V.; Doughtery, D. A.; *Modern Physical Organic Chemistry*, **2006**, p. 104

19) Kitching, W.; Olszowy, H. A.; Harvey, K. *J. Org. Chem.* **1982**, *47*, 1893-1904.

20) (a.) Baldwin, J. C.; Lappert, M. F.; Pedley, J. B.; Poland, J. S. *J.C.S. Dalton*, **1972**, 1943. (b.) Elschenbroich, Christoph; *Organometallics*, 3rd Ed., Wiley: New York, **2006** p. 173.

21) (a.) Thompson, R.; Chen, C.-H.; Pink, M.; Wu, G.; Mindiola, D. J. *J. Am. Chem. Soc.* **2014**, *136*, 8197-8200. (b.) Stevenson, L. C.; Mellion, S. Clot, E. Mountford, P. *J. Am. Chem. Soc.* **2015**, *137*, 10140-10143. (c.) Grant, L. N.; Pinter, B.; Kurogi, T.; Carroll, M. E.; Wu, G.; Manor, B.; Carroll, P.; Mindiola, D. J. *Chem. Sci.* **2017**, *8*, 1209-1224. (d.) Clough, B. A.; Mellino, S.; Clot, E.; Mountford, P. *J. Am. Chem. Soc.* **2017**, *139*, 11165-11183. (e.) Clough, B. A.; Mellino, S.; Protchenko, A. V.; Slusarczyk, M.; Stevenson, L. C.; Blake, M. P.; Xie, B.; Clot, E.; Mountford, P. *Inorg. Chem.* **2017**, *56*, 10794-10814.

22) Townsend, E. M.; Kilyanek, S. M.; Schrock, R. R.; Muller, P.; Smith, S. J.; Hoveyda, A. *Organometallics* **2013**, *32*, 4612-4617.

23) Parr, R. G.; Yang, W. Density-functional theory of atoms and molecules; Oxford University Press: Oxford, **1989**.

24) Perdew, J. P.; Burke, K.; Ernzerhof, M. *Phys. Rev. Lett.* **1996**, *77*, 3865.

25) Laikov, D. N. *Chem. Phys. Lett.* **1997**, *281*, 151.

26) Laikov, D. N.; Ustynyuk, Yu. A. *Russ. Chem. Bulletin* **2005**, *54*, 820.

27) (a.) Stevens, W. J.; Basch, H.; Krauss, M. *J. Chem. Phys.* **1984**, *81*, 6026; (b.) Stevens, W. J.; Basch, H.; Krauss, M.; Jasien, P. *Can. J. Chem*. **1992**, *70*, 612; Cundari, T. R.; Stevens, W. J. *J. Chem. Phys*. **1993**, *98*, 5555.

Chapter 3: Group IV Complexes Supported by a Novel Trifluoromethylamidinate

3.1 Introduction

The polymerization of olefinic monomers to generate synthetic materials is arguably one of the most powerful and impactful discoveries of the 20th century. For a sense of scale, global demand for polyolefins is expected to reach 200 million tons annually by 2020.[1] Perhaps as a result of the exceedingly high demand, organometallic chemists have spent several decades studying well-defined and tunable homogeneous catalysts which compliment heterogeneous Ziegler-Natta systems. From controlled and rational design of catalysts based on metal-choice, geometry and (most importantly) ligand architecture, remarkable discoveries and improvements have been realized including but not limited to: high stereoselectivity (i.e. isotactic or syndiotactic),[2] extreme branching within the polymer microstructure[3] and precise control of the molecular weight and molecular weight distribution.[4] Understanding the exact factors which control these polymer/polymerization qualities and being able to systematically manipulate them to generate new materials is a crucial discipline in organometallics and catalyst science.

While extensive work has been devoted toward modifying the sterics or geometry of polymerization catalysts,[2] the breadth of work focusing on electronic perturbations is less well-developed. Part of the difficulty in parsing out the role which electronic donation has on catalyst characteristics is the influence the substituents have on the steric profile of the modified catalyst. In order to (partially) overcome this problem, the groups of Collins[5] and Pino[6] investigated, 5,6-substituted and 4,7-substituted indenyl-based metallocene zirconium catalysts, respectively. These complimentary approaches reached a similar conclusion that activity trended with electron-donation from the substitution. Use of the OMe-substituent, however, led to either complete shutdown or high attenuation of catalytic activity depending on the reaction conditions. This anomalous result was rationalized as being due to the lone pair of the oxygen

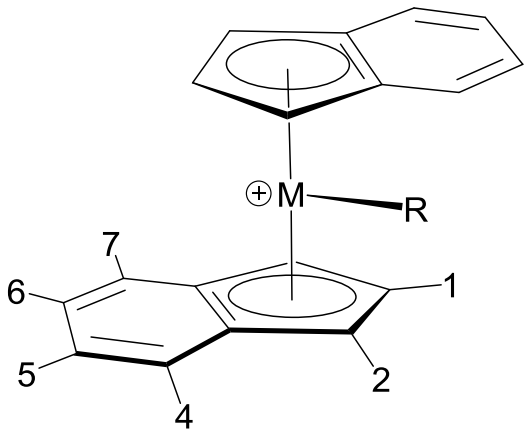

Figure 3.1. Numbering on indenyl-based metallocene catalysts.

coordinating to an Al center from the MAO activator, thereby making it an inductively withdrawing group and thus destabilizing to the cationic propagating center. Similarly, substitution of indenyl ligands in the 1 or 2-position with amino, alkoxy and siloxy groups has been investigated.[7] In the case of amino-indenyls, modest ethylene polymerization activity was observed after an induction period, while the O-based substitutents resulted in rate enhancements over

their unsubstituted counterparts; this again suggests that greater donor strength improves catalyst activity by stabilization of the cationic active site. Despite the findings associated with indenyl-based ligand sets, the use of strongly-donating, bicyclic guanidinates on group 4 metals led to ethylene polymerization catalysts with limited activity and stability.[8,9] It was speculated that the low activities observed were due to facile reduction of the metal center and/or non-innocence on the part of the guanidinate nitrogens to coordinate to Lewis-acidic Al centers in the MAO activator, a similar problem to that which was also observed with the substituted indenyls.

An alternative approach to traditional inductive (and resonance) methods is the introduction of fluoro, trifluoromethyl or, most recently, pentafluorosulfonyl substitutents into the secondary coordination sphere of polymerization catalysts, particularly the ortho-position of the N-bound aryl group in phenoxy-imine (FI) ligand sets (Figure 3.2).[10-22] This method has been utilized by a number of research groups including Fujita, Coates and Marks, with both early and late transition metal catalyst. The benefits of fluorination (over the unsubstituted parent systems) have included introduction of living-character in the catalysis, rate enhancements, increased thermal stability, increased stereoselectivity as well as reduced chain-branching in the polymer microstructure. It has been posited that the presence of attractive C-F---C-H interactions between the ortho-F and β-H of the growing polymer chain disfavors the syn-periplaner conformation which precedes β-H elimination, thereby suppressing deactivation of the propagating species. Such C-F---C-H interactions have been documented both structurally and spectroscopically in model systems, as well as being supported computationally. It is important to note that the absence of fluorination in the ortho-positions removed the living character associated

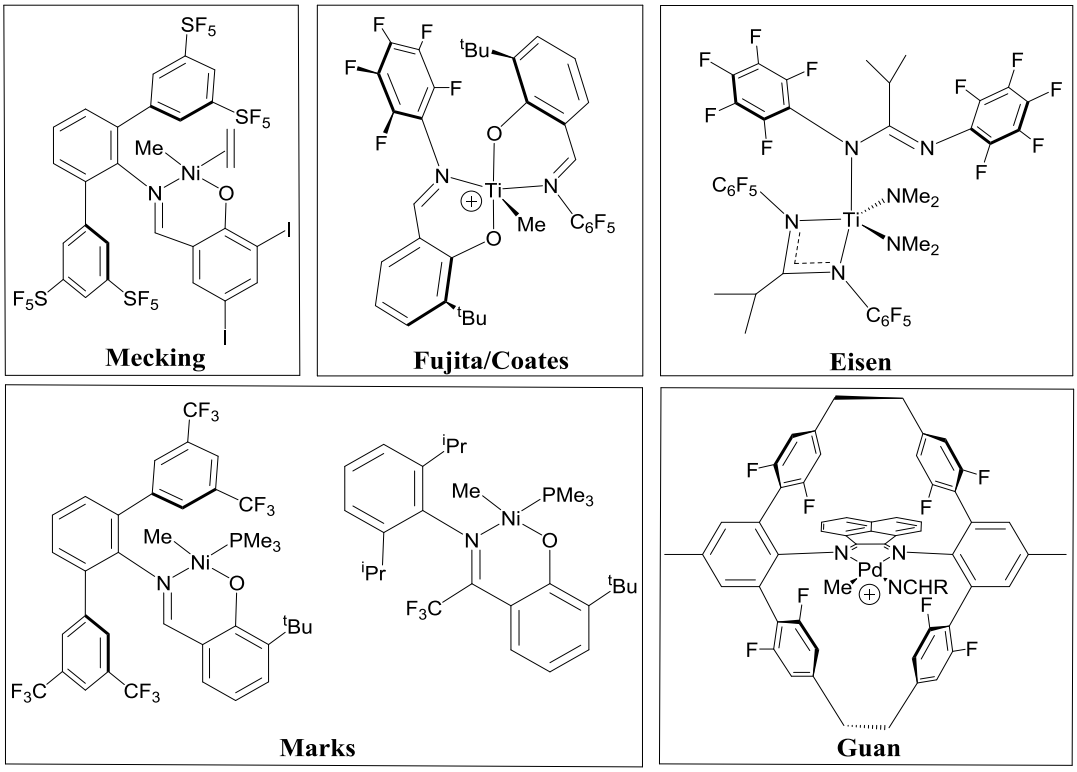

Figure 3.2. Examples of fluorinated ligand sets for polymerization catalysts. Varying fluorinated-derivatives of the FI ligand can be seen supporting the catalysts used by Mecking, Fujita, Coates and Marks.

with these catalysts, highlighting the importance of regio-selective fluorination within the ligand. It was also found that generally increasing the extent of fluorination on the aryl group led to an increase in catalyst activity. Related observations from Eisen et al. found that the presence of meta- and para-fluoro substituents on the N-bound aryl groups of the ancillary amidinate ligands led to suppression of chain-termination and monomer insertion acceleration, respectively, thereby inducing higher polymerization activity. Interestingly, inductive-activation of catalysts is also regio-dependent, as installation of a CF_3 group into the backbone of the FI ligand actually led to diminished activity relative to the parent compound. This suggested that, at least in the Ni-based system studied, pure inductive effects were not responsible for the observed rate enhancements and may well have actually had deleterious effects.

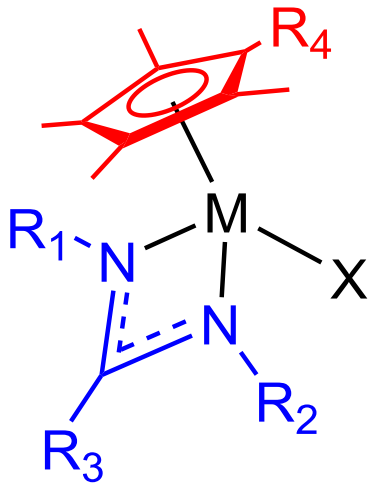

Figure 3.3. Generic example of the CPAM ligand set on a transition metal. R_1 and R_2 constitute the "N-bound" substituents which considerably impact the steric environment around the metal. R_3 is the distal substituent and can impact both the steric and electronic character of the ligand. R_4 is the Cp-based substituent and has be found to impact both sterics and (to a lesser extent) electronics of the metal center (in other systems).

For the past 20 years, the pentamethylcyclopentadienyl-amidinate (CPAM) mixed ligand set has been an effective support for zirconium[24-34] and hafnium-based[35-39] polymerization catalysts, which has imparted on them a number of unique properties including living character within its polymerization as well as readily doing so under chain-transfer conditions. Shrinking of the N-bound sterics led to increases in activity[27] and, provided asymmetric substitution, stereocontrol on the polymer-microstructure giving isotactic polyolefins. Furthermore, modification of the distal position led to considerable changes in catalyst character and consequentially the character of the polymer products.[26,35] Perhaps surprisingly, the use of large distal groups (e.g. tert-butyl, phenyl) led to drastically diminished activity and/or complete catalyst deactivation despite being far away from the reaction center. Alternatively, the use of a sterically unprotecting formidinate (i.e. the distal position is a single hydrogen atom) led to reduced stereocontrol and broadened polydispersity (i.e. the ratio of the weighted average molar

mass of a polymer to the number average molar mass). Due to the sensitivity of the catalysts' structure toward steric modification, there are limited ways to improve its performance. Tethering two propagating centers together to generate dinuclear catalysts has been met with some success.[34]

Electronic modifications have also been tried in the form of the related guanidinate ligands, $N(R^1)C(NR^3_2)N(R^2)$.[40] Conceptually this method should improve catalyst stability via additional electron-donation from the distal nitrogen; furthermore the greater sterics associated with this position should buttress the N-bound substituents, thereby increasing the stereoselectivity of the catalyst, particularly under chain-transfer conditions. Interestingly, all of the presumed benefits of this substitution were not only not realized but in fact led to systems which no longer maintained living character and the stereoselectivity were considerably diminished (Scheme 3.1). It is at first tempting to relate the findings here with that of the bicyclic guanidinates; however, the difference in cocatalyst suggests that the mode of deactivation is dissimilar.

These results, while initially discouraging, point toward electronic modifications

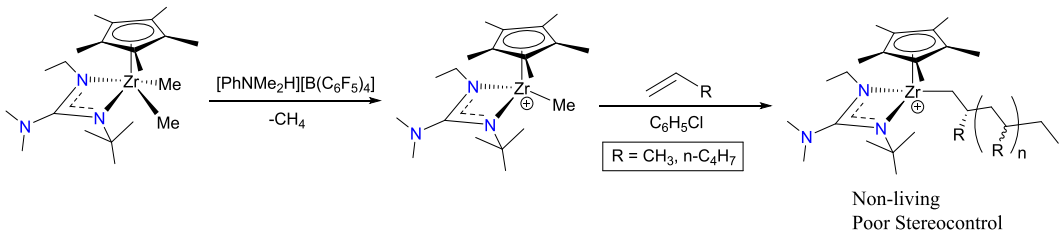

Scheme 3.1. Activation and polymerization of alpha-olefins with CPGU-supported Zr led to a non-living catalyst and one with diminished stereocontrol.

within the amidinate framework being a viable route for affecting catalyst performance. Furthermore, it indicates that, contrary to the breadth of previous literature, the use of inductively withdrawing groups may provide beneficial effects. Intuition suggests that electron-withdrawing ligands should heighten the Lewis acidity of the active metal center

and as such improve the activity of previously established polymerization ligands. Surprisingly, there have been no examples of trifluoromethyl-substituted amidinate ligands and a very limited number of other fluorinated moieties in the distal position.[41-43] It is possible that much of the paucity of such systems may stem from either metal-ligand compatibility problems or the difficulties associated with ligand synthesis. Typical methods for amidinate synthesis involve either nucleophilic attack of alkyl lithiums on carbodiimides[44] or, relatedly, insertion of the same carbodiimide starting materials into a pre-formed metal-ligand bond with the ligand becoming the distal position of the amidinate.[45] Neither of these methods readily lend themselves to synthesis of the trifluoromethyl derivatives as nucleophilic CF_3- groups are more difficult to generate, often relying on reagent mixtures that are condition and transformation dependent. Meanwhile, organometallic CF_3 ligands, while known for early transition metals,[46-50] are themselves a rare commodity. Therefore, an alternative route to accessing such ligands was required, one which focused on generation of the amidine proligand. An added benefit to targeting this alternate route is that it allows access to a much wider variety of potential ligands, as it is not bound by access to carbodiimide precursors which can be either expensive to purchase or difficult to synthesize.

3.2 Results and Discussion

3.2.1 Ligand Synthesis

Amidines **3.1-3.3** (Scheme 3.2) can be generated in moderate to good yields by a two-step process which is an adaptation of the procedure used by Uneyama to generate trifluoromethyl-substituted imindoyl halides[51] and amidines.[52] Treatment of trifluoroacetic acid with triphenylphosphine, triethylamine and the appropriate alkylamine (or aniline) in carbon tetrachloride gave clean conversion to the desired N-alkyl (or aryl)-2,2,2-trifluoroacetimidoyl chloride as observed by ^{19}F NMR. While N-phenyl-2,2,2-trifluoroacetimidoyl chloride was isolated as a pure, colorless oil, due to the volatility of the tert-butyl and isopropyl derivatives, both were generated in-situ and used without further purification. Subsequent treatment of the imidoyl chlorides with two equivalents of amine (the second equivalent functions as a sacrificial base to react with HCl by-product) generated the amidine products. Likely due to pKa considerations of the conjugate acid, the use of NEt_3 as an alternative base was found to be unsuccessful. Though Uneyama reports a mixture of symmetric and asymmetric amidines forming when adding amine directly to the iminoyl chlorides, as well as the use of reaction temperatures above ambient, the generation of **3.1** and **3.2** both occurred at 0 ^oC and cleanly gave a single product without any sign of scrambling. Upon filtration of insoluble by-products, solvent was removed via fractional distillation to give crude products which

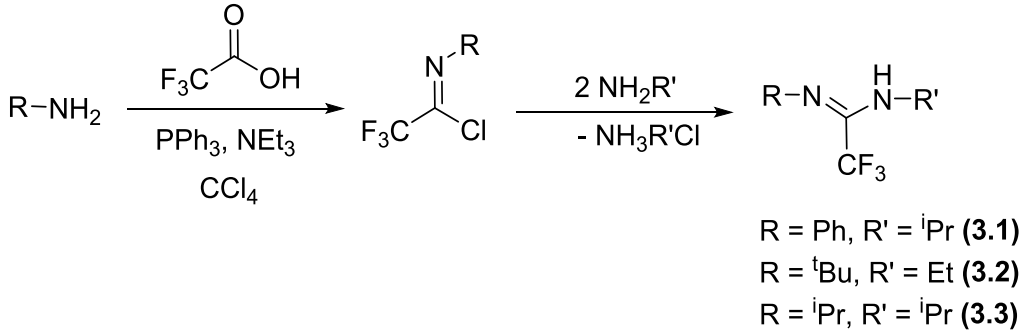

Scheme 3.2. General synthesis of amidine proligands **3.1-3.3.**

were further purified by bulb-to-bulb transfer to give the amidines as foul-smelling, colorless liquids. As stated above, there was no evidence of scrambling during the synthesis of either of the asymmetric amidines **3.1** or **3.2**; however, ^{1}H NMR spectra of **3.1** suggested the presence of two tautamers which rapidly interconvert at room temperature, as evidenced by pairs of broad resonances which coalesced at 60 ^{o}C to give a single, time-averaged species (Figure 3.4).

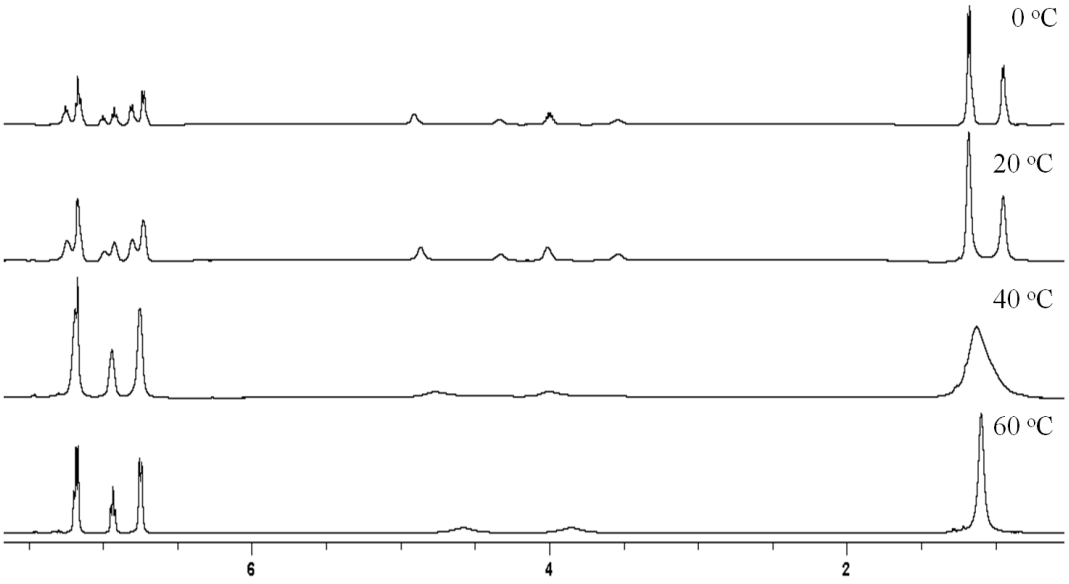

Figure 3.4. Variable temperature ^{1}H NMR spectra of **3.1**.

Metallation of the proligands proceeded readily via treatment of the amidine with $NaN(SiMe_3)_2$ in diethyl ether. All three Na salts, $[Na][N(R^1)C(CF_3)N(R^2)]$ (R^1 = Ph, R^2 = ^{i}Pr (**3.4**), R^1 = ^{t}Bu, R^2 = Et (**3.5**), R^1 = R^2 = ^{i}Pr (**3.6**)) could be isolated in modest yields, interestingly with **3.5** as a dark-red crystalline solid. While the red color of both solid and solutions of **3.5** was perplexing, it likely arose from a low-lying π-π* transition. A number of lithium salts of halogenated-dipyrrin ligands have also been found to be dark-red THF adducts.[53] The dipyrrin moiety is a well-established chromophore and the red-color is associated with π-π* transitions.

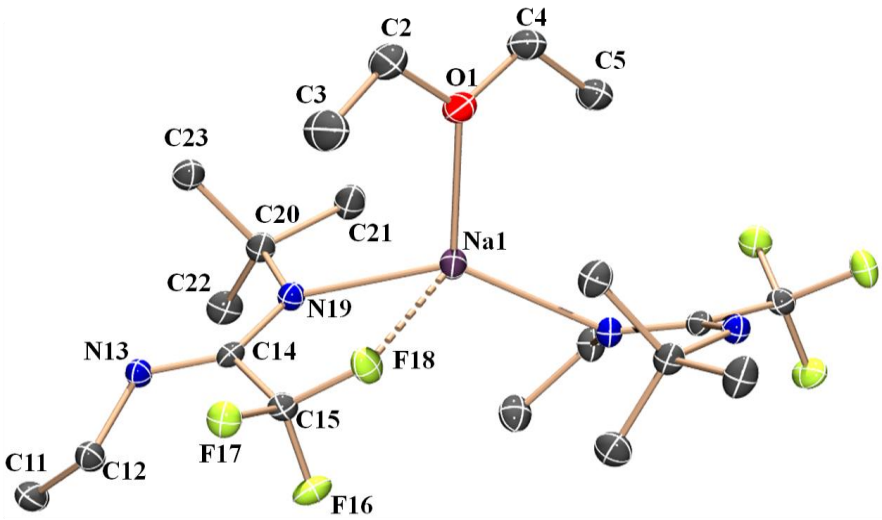

Figure 3.5. Crystal structure of **3.5** with hydrogen atoms omitted for clarity; ellipsoids for the non-hydrogen atoms are shown at the 30% probability level. The asymmetric unit has been expanded partially to highlight the full coordination sphere around Na1.

^{1}H NMR of **3.5** showed sharp resonances for all of the ligand protons, as well as half an equivalent of diethyl ether which was not removed even after prolonged exposure to reduced pressure. The ^{19}F NMR spectrum of **3.5**, however, gave a very broad resonance ($\Delta\nu_{1/2}$= 526 Hz) suggesting that the CF_3 substituent may have somehow been affected by the reaction. To better understand the bonding of the trifluoromethyl-amidinate salt, as well as to confirm that the CF_3 group was still intact, single crystals of it were subjected to X-ray diffraction studies to observe the solid-state structure (Figure 3.5).

3.5 crystallizes in the spacegroup $P2_1/n$ with the screw axis running perpendicular to the infinite coordination polymer formed from two amidinates bridged by Na1. The coordination sphere of the sodium cation is completed by a diethyl ether molecule, as well as a close metal-fluoride contact from the CF_3 distal group (F18-Na1 distance = 2.3621(17)). The broadness associated with the ^{19}F NMR spectra suggests such Na-F contacts are labile but exist in solution. Metal-fluoride contacts are not unprecedented,

particularly as it pertains to alkali metals[54-57] and those observed in **3.5** are relatively short with respect to previously reported sodium fluoride contacts (average Na-F distance = 2.604 Å).[58] Despite the considerable difference in alkyl-substitutents, as well as asymmetry in mode of binding, delocalization throughout the NCN framework of the amidinate can be observed from the C14-N13 and C14-N19 distances of 1.314(3) and 1.322(3) Å, respectively.

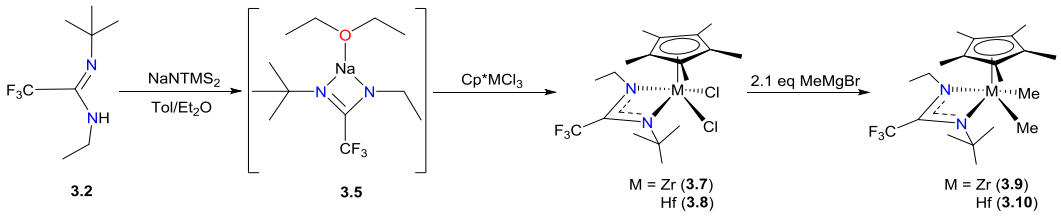

Scheme 3.3. Synthesis of Cp*[^{t}BuNC(CF_3)NEt]MCl_2 (M = Zr; **3.7**, M = Hf; **3.8**) and Cp*[^{t}BuNC(CF_3)NEt]MMe_2 (M = Zr; **3.9**, M = Hf; **3.10**)

Due to the greater sterics (and consequentially, the assumed reduced activity) associated with the isopropyl, phenyl and diisopropyl derivatives, limited work was pursued with these two, opting instead to focus on the tert-butyl, ethyl ligand. This is was further motivated with the direct structural analog, ^{t}BuNC(CH_3)NEt, which enforces a C_1 environment and has seen considerable success in the Sita group for generating isotactic polyolefins.

3.2.2 Synthesis and Characterization of CPAM Complexes Containing a Distal Trifluomethyl group

While **3.5** could be isolated, it was found to be more convenient (and oftentimes higher yielding) to generate it in-situ followed by addition of the pentamethylcyclopentadienyl zirconium (and hafnium) trichloride precursor to yield the dichloride species **7** and **8** (Scheme 3.3) as crystalline solids in moderate-to-good yields.

Comparing the ^{1}H NMR spectra of the two dichlorides, at least one substantial difference became evident. While the methylene of the ligand for **3.7** gave rise to a well-resolved quartet of quartets ($^{3}J_{HH}$ = 7.1 Hz, $^{5}J_{HF}$ = 2.4 Hz) due to coupling to both the adjacent CH_3 as well as longer range coupling to the CF_3 group, **3.8** only showed to 2 broad signals. While long-range H-F coupling was also noted in **3.2**, the origin of the broadness associated with **3.8** is perplexing.

Table 3.1. Selected Bond Lengths (Å) and Angles (°) for the Molecular Structures of 3.7 and 3.8

	3.7	**3.8**
M(1)-N(3)	2.2067(10)	2.1901(13)
M(1)-N(6)	2.2964(10)	2.2770(12)
M(1)-Cl(1)	2.4187(3)	2.4094(4)
M(1)-Cl(2)	2.4318(3)	2.4017(4)
N(3)-C(1)-N(6)	113.35(10)	113.35(14)
N(3)-M(1)-N(6)	59.07(4)	59.52(5)

To see if structural differences between the 2 were responsible for this difference, X-ray diffraction studies were performed on crystalline samples of both. Solid-state structures of **3.7** and **3.8** (Figure 3.6) reveal very similar bond metrics (as well as nearly identical unit cells) between the two metals wherein there is one long (Zr-N: 2.2964(10) Å; Hf-N: 2.2770(12) Å) and one short (Zr-N: 2.2067(10) Å; 2.1901(13) Å) M-N bond, which correspond to the asymmetry in sterics between the ^{t}Bu and Et substituents. The similarity between the two compounds should not come as a surprise, given almost identical atomic, covalent and ionic (4+) radii between the two.

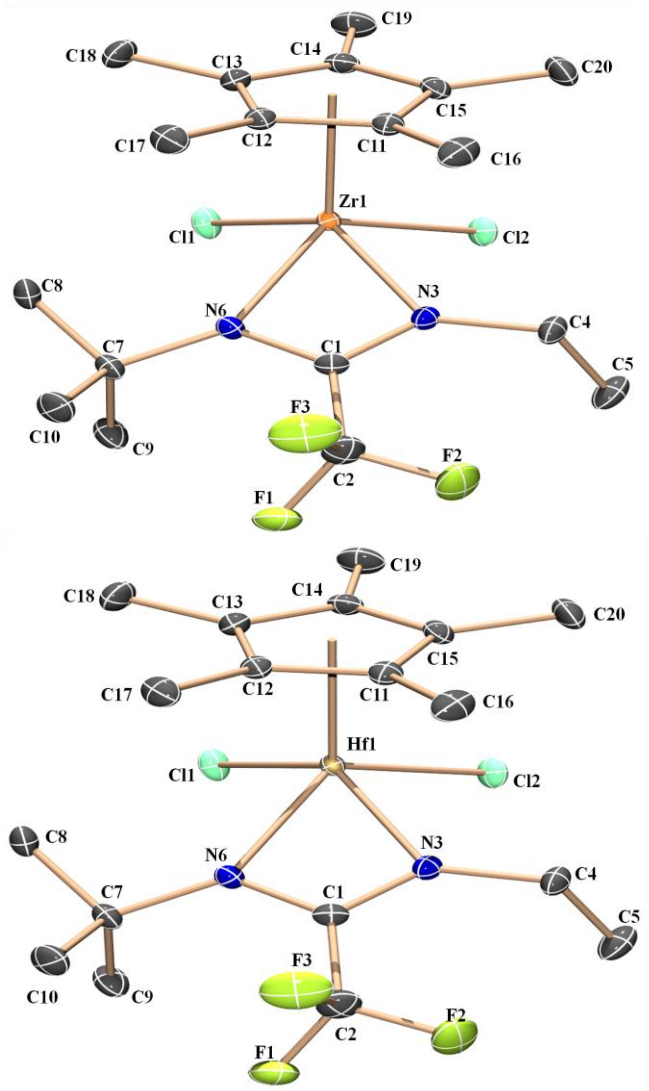

Figure 3.6. Crystal structures of **3.7** and **3.8** with hydrogen atoms omitted for clarity; ellipsoids for the non-hydrogen atoms are shown at the 30% probability level.

3.7 and **3.8** could serve as viable precatalysts for olefin polymerization using MAO activation; however there is extensive evidence that the use of MAO as a cocatalyst can come with a number of unintentional consequences, including ligand transfer as well as coordination of heteroatom lone pairs to Lewis acidic Al centers within the MAO which can modulate the electronic character of such substitutents.[5-7] As such, it was elected that formation of the dimethyl compounds followed by protonolysis with anilinium borate salts would be a preferable route to the cationic species.

Synthesis of the dimethyl compounds **3.9** (Zr) and **3.10** (Hf) could be achieved via straightforward methylation of the dichloride precursors with two equivalents of methyl magnesium bromide in ether to give the final products as yellow oils. The use of MeLi as an alternative methylation reagent was unsuccessful, yielding only intractable materials even when done at -78 ^{o}C. While **3.10** could generally be synthesized cleanly and required minimal purification (purification could be achieved by washing with cold acetonitrile), **3.9** formed with presence of persistent impurities. Further, attempts to purify with cold acetonitrile actually led to partial decomposition and the formation of more impurities. To date, attempts to distill either **3.9** or **3.10** have failed as a method of purification.

The oily nature of **3.9** and **3.10** frustrated any attempt to elucidate a structure-reactivity relationship between these two and their polymerization abilities as well as

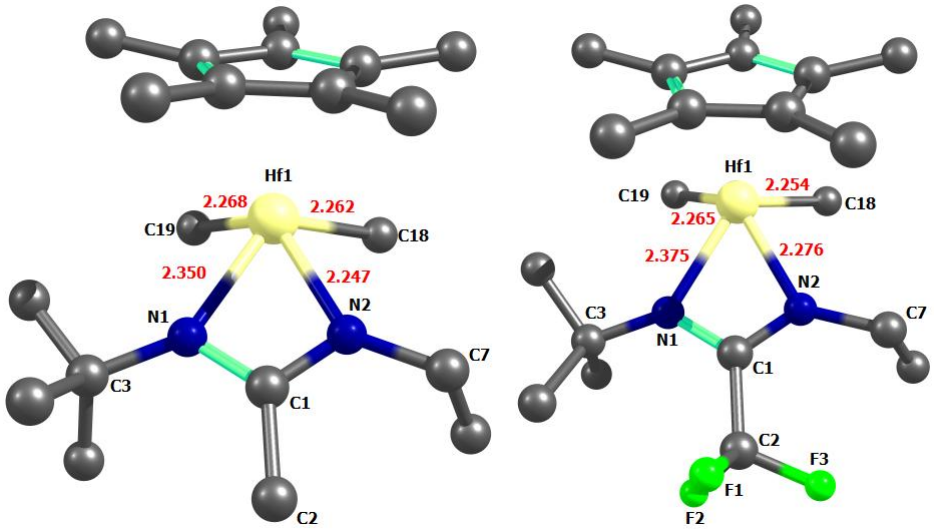

Figure 3.7. Calculated structure of **3.10^{Me}** and **3.10** showing small but meaningful bond elongations between the Hf and both N atoms.

allowing for direct comparisons between the original methyl-amidinate and the trifluoromethyl analog. To partially circumvent this limitation, optimized structures were calculated for both **3.10** and Cp*[N(^{t}Bu)C(Me)N(Et)]HfMe$_2$ (**3.10^{Me}**); the latter has been

previously investigated via X-ray diffraction.[35] Comparing the calculated structure of **3.10^{Me}** with its experimental analog confirmed the fidelity of this approach as most metrics differed by 0.021 Å or less. It is likely that the accuracy of the calculated structure is even greater when it is taken into account that the experimental structure suffered from disorder between the ^{t}Bu and Et sides of the amidinate, thereby only giving an average of the (presumably) different bond lengths. The effect of trifluoromethyl substitution on the bonding in **3.10** can be seen in the elongation of the Hf-N bond distances (+0.025, +0.029 Å) over those in **3.10^{Me}**. Possibly as a result of its greater electrophilicity, the Hf-Me bond distances of **3.10** actually contract slightly (-0.003, -0.008 Å) relative to its methyl-analog. It is possible that perturbations to bonding arose from the greater size of the CF_3 substituent over CH_3, the organic-A values being 2.1 and 1.7, respectively. To indirectly probe this possibility, the angle between the N-bound substitutents and the distal carbon (i.e. C3-C2-C7 in Figure 3.7) were measured. It stands to reason that, as the size of the distal substituent grows, the angle between it and the N-bound substituents should also increase as a result of buttressing. Interestingly, the angles actually contract going from the **3.10^{Me}** to **3.10**, from 110.23^{o} to 106.57^{o}. This suggests that the increase in bond distance is almost exclusively a result of inductive effects, indicating that the CF_3-substituted ligand is a poorer donor, thereby causing the metal center become more electrophilic and Lewis acidic.

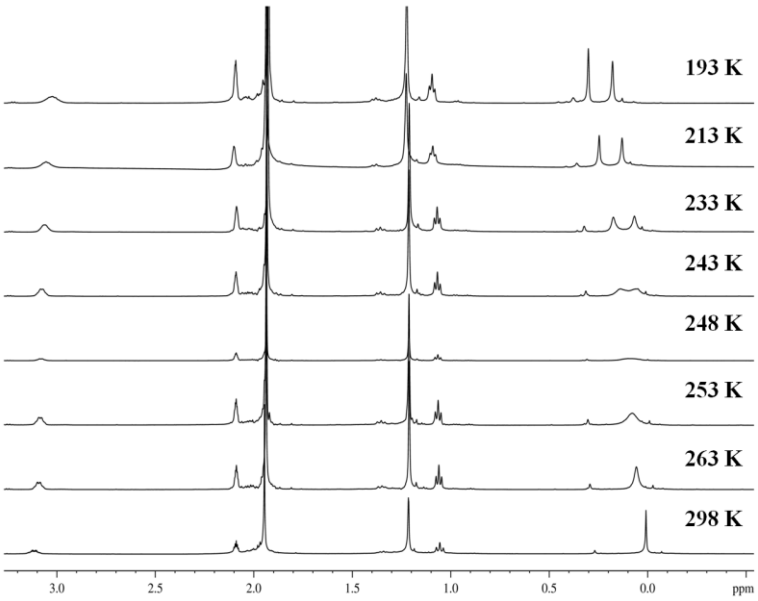

Figure 3.8. Variable-temperature ^{1}H NMR spectra of **3.10**. Coalescence temperature is 243 K.

While the Cp*[^{t}BuNC(X)NEt]M(CH_3)$_2$ (X = CH_3, CF_3) cation is C_1 symmetric and therefore should generate highly isotactic polyolefins, the amidinate ligand can become hemi-labile, facilitating "ring-flipping"[59] which leads to diminished stereoselectivity. Therefore, the elongated bond distances in the **3.10** could be a signal that such species could be responsible for diminished stereocontrol. To more directly probe this possibility, variable temperature NMR studies were enlisted to monitor the temperature (and energetic barrier) at which ring-flipping ceased, making the diastereotopic Hf-Me bonds distinct spectroscopically. As such, a toluene-d_8 solution of **3.10** was prepared and upon cooling, the sharp singlet associated with the six ^{1}H of the spectroscopically equivalent methyl groups broadened out, eventually separating to two separate, sharp singlets at -193 K (Figure 3.8). The coalescence temperature was found to be 248 K which corresponds to a barrier of rotation 9.78 Kcal/mol and is comparable to that found for the distal-methyl analog.

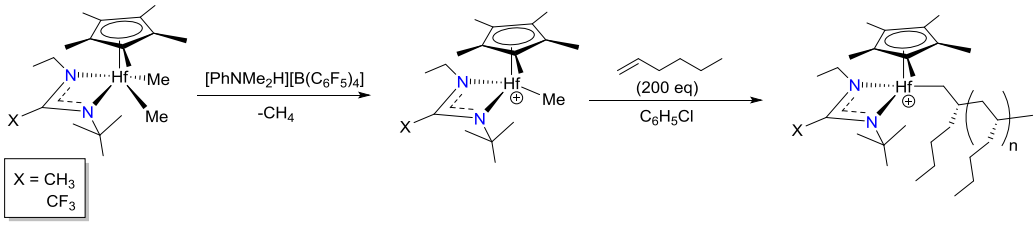

Scheme 3.4. Comparative polymerization studies with Cp*[^{t}BuNC(X)NEt]M(CH_3)$_2$ (X = CF_3, CH_3).

3.2.3 Polymerization studies

Due to the higher yield (as well as more facile purification), **3.10** was first investigated as a potential precatalyst for alpha-olefin polymerization. Previously, the structurally related complex, **3.10^{Me}**, was found to be a living, albeit sluggish ($t_{1/2}$ = 12 h), catalyst for 1-hexene polymerization at -10 ^{o}C. Conversely, **3.10**, upon activation with the borate activator, [NMe_2HPh][$B(C_6F_5)_4$], was capable of producing poly-1-hexene in yields of ~90 % and with Mn of ~20,000 and PDI > 1.1 in considerably less time ($t_{1/2}$ = 2.5 h) at the same temperature. Interrogation of the structure of polymers produced by this catalyst via ^{1}H NMR revealed no signs of olefinic resonance and consequentially no

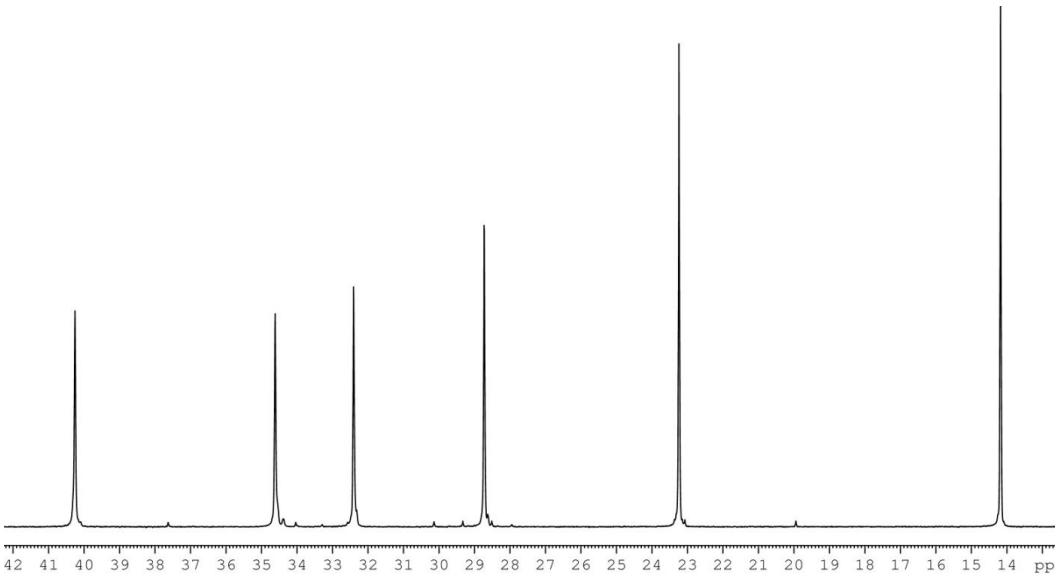

Figure 3.9: ^{13}C NMR of poly-1-hexene produced from **3.10**.

evidence of beta-hydride elimination, further supporting living character for the polymerization. Furthermore, the associated ^{13}C NMR spectrum revealed sharp signals, indicative of high stereoregularity (Figure 3.9).

The qualitative observation of the reduced reaction time encouraged a more thorough kinetic analysis of rate of polymerization between the **3.10** and **3.10^{Me}** catalysts (Scheme 3.4, Figure 3.10). Under identical conditions, the molecular weight of the resulting polymer was measured against time. Initial rate kinetics for **3.10** gave a TOF of

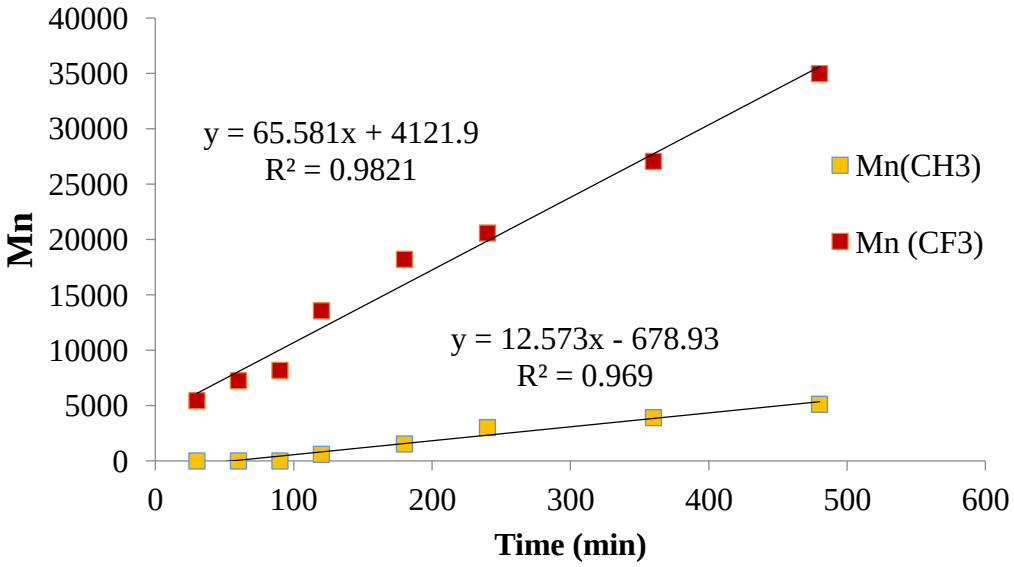

Figure 3.10. Comparison of Mn vs time for 3.10 and 3.10^{Me}

0.013/sec which is contrasted with the analogous **3.10^{Me}** derivative which has a TOF of 0.002/sec. This reveals a nearly 10-fold amplification of rate by way of electronic substitution at the distal position.

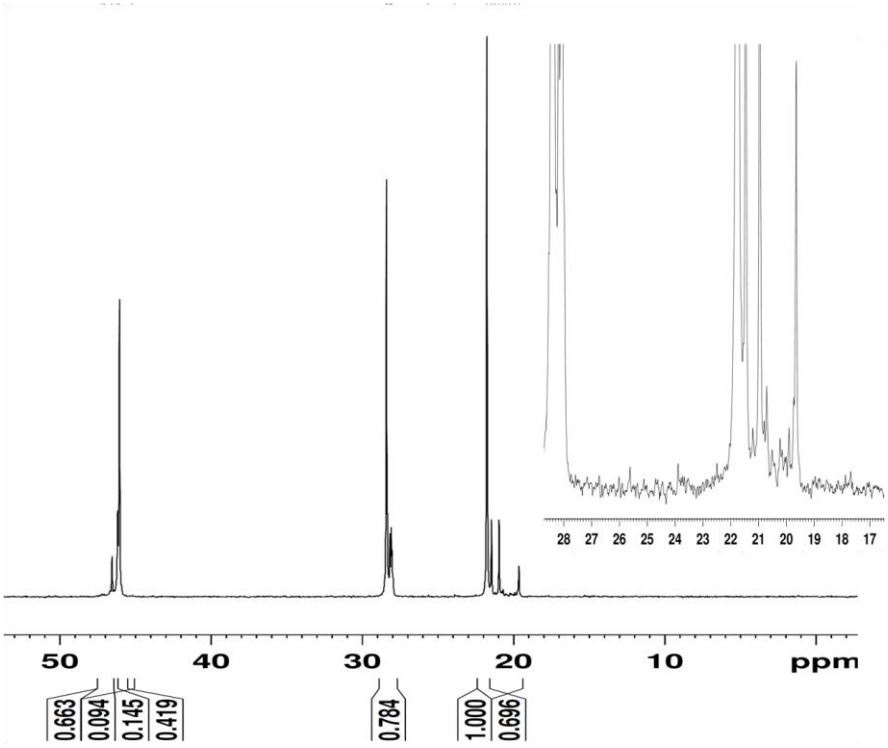

Figure 3.11: ^{13}C NMR of polypropylene produced from **3.10**. Inset is expanded region from 19-29 ppm.

Curious if this rate enhancement, as well as the retention of stereospecificity, was general for smaller alpha olefins, the same polymerization chemistry was attempted with propylene. Accordingly, a constant pressure (5 psi) of the gaseous monomer was bubbled through a -10 ^{o}C toluene solution of **3.10**. After 4.5 h, upon quenching, the polymer product from both **3.10** and **3.10^{Me}** were analyzed by a combination of ^{13}C NMR, differential scanning calorimetry (DSC) and gel permeation chromatography (GPC). First, the polymerization rate utilizing **3.10** was found to be, in agreement with the 1-hexene results, approximately ten times as fast as the analogous **3.10^{Me}**. This amplification in rate, however, did not come at the expense of either stereospecificity or melting point. Polymer produced from **3.10** (Figure 3.11) had a pentad ratio of 0.70 as well as a melting point of 119 °C which is comparable or better than those associated with traditional catalysts. Interestingly, the extent of 2,1-mis-insertions associated with

3.10 was reduced, relative **3.10^{Me}**, to the point that it was almost undetectable. The observation of both rate-enhancement and increased regiocontrol as a result of using a fluorinated ancillary ligand stands counter to the bulk of literature precedent. The difference seen in the trifluoromethyl-substituted CPAM system over other systems may be a result of the mixed ligand imposing sufficient steric bulk that it inhibits close contacts between the metal center and the borate counterion (a source of catalyst inhibition) but still provides a sufficiently large binding pocket for monomer to coordinate. The heightened Lewis acidity of the metal-center over its methyl-amidinate analog encourages monomer coordination, increasing the rate of chain propogation, as well as raises the kinetic barrier of rotation required for 2,1-mis-insertion.

3.3 Conclusion

While historical precedent has suggested that inductively-withdrawing functional groups (e.g. halides and CF_3) attenuate catalyst activity for olefin polymerization, trifluoromethyl-substitution of the distal position within the amidinate ligand of the CPAM framework led to considerable amplification of catalyst activity. This improvement to activity generally came without diminished stereocontrol or broadened polydispersity. Further, increases in regiocontrol have also been observed, essentially obviating any instances of 2,1-mis-insertion and resulting in isotactic polypropylene products whose melting points are comparable or higher than those typically associated with Cp*[N(^{t}Bu)C(Me)N(Et)]$ZrMe_2$ and Cp*[N(^{t}Bu)C(Me)N(Et)]$HfMe_2$. The origin of this rate enhancement likely is a result of increased Lewis acidity of the metal center due to the inductively withdrawing CF_3 substituent. This substitution further benefits from the lack of proximity to the metal, thereby allowing for a purely electronic effect. The

amplified Lewis acidity at the metal center biases the equilibrium between the cationic, propagating center and the olefinic monomer toward monomer binding. The use of electronic perturbation to the CPAM framework therefore has led to catalyst improvements which capitalize on previous, steric-based optimization while further tuning such systems for increased activity.

3.4 Experimental Details

3.4.1 General Considerations

All manipulations were performed under an inert atmosphere of N_2 using standard Schlenk-line or glove-box techniques. All solvents were dried (Na/benzophenone for pentane and diethyl ether, and Na for toluene) and distilled under N_2 prior to use. Benzene-d_6, Toluene-d_8 and 1-hexene were dried over Na/K alloy and vacuum transferred prior to being used. Celite was oven dried at 150 °C for several days before use. Cooling for the reactions was performed in the internal freezer (-25 °C) of the glove box used. ($\eta5$-C_5Me_5)$ZrCl_3$, ($\eta5$-C_5Me_5)$HfCl_3$, $NaN(SiMe3)_2$, and $[PhNMe_2][B(C_6F_5)_4]$ were purchased from Strem Chemicals and used as received. Carbon tetrachloride, triethylamine, tert-butyl amine, ethylamine (2M in THF) and triphenylphosphine were all purchased from Sigma Aldrich and used as purchased. Polymer grade propene and ethene were purchased from Matheson Trigas, and passed over activated Q5 and molecular sieves. GPC analyses were performed using a Viscotek GPC system equipped with a column oven and a differential refractometer both maintained at 45 °C and four columns also maintained at 45 °C. THF was used as the eluent at a flow rate of 1.0 mL/min. M_n, M_w, and M_w/M_n values were obtained using a Viscotek GPC with OmniSEC software

and ten polystyrene standards (Mn=580 Da to 3150 kDa) (Polymer Laboratories). ^{1}H NMR spectra were recorded at either 400MHz or 500 MHz with benzene-d_6 or toluene-d_8. For polymer samples ^{13}C {^{1}H} NMR spectra were recorded at 600MHz using 1,1,2,2-tetrachlorethane-d_2 at 85 °C. Elemental analyses (C, H, and N) were performed by Midwest Microlabs, LLC.

3.4.2 Synthesis of New Compounds

N(Ph)C(CF_3)N(^{i}Pr)H **(3.1)**

A 250 ml round-bottom was charged with a stirbar, 30 ml $CHCl_3$ and 2.00 g (0.963 mmol) of N-phenyl-2,2,2-trifluoroacetimidoyl chloride and chilled to 0 °C with an ice bath to give a pale yellow solution. Dropwise, 1.13 g (1.93 mmol) isopropylamine was added to the stirring solution. The reaction stirred overnight to give a yellow oil concomitant with precipitation of NH_3iPrCl (Note: substitution of the 2nd equivalent of isopropylamine for triethylamine was unsuccessful). All volatiles were removed under reduced pressure, the reaction mixture extracted into pentane and filtered to remove salt impurities. The pentane was removed under reduced pressure, the product rextracted into $CHCl_3$ and filtered through a 4" plug of silica gel to remove colored impurities. The solvent was removed under reduced pressure to yield the amidine as a colorless oil. Yield = 1.35 g (0.586 mol). ^{1}H NMR (500 MHz, $CDCl_3$, 25 °C): 0.95 (6H, br s, CH(C*H*$_3$)$_2$, minor isomer), 1.18 (6H, br s, CH(C*H*$_3$)$_2$, major isomer), 3.54 (1H, br s, C*H*(CH$_3$)$_2$, minor isomer), 4.01 (1H, br s, C*H*(CH$_3$)$_2$, major isomer), 4.33 (1H, br s, N*H*, minor isomer), 4.86 (1H, br s, N*H*, major isomer), 6.73 (2H, br s, Ar-*H*, major isomer), 6.80 (2H, br s, Ar-*H*, minor isomer), 6.92 (1H, br s, Ar-*H*, major isomer), 7.17 (2H, br s, Ar-*H*, major

isomer) , 7.24 (2H, br s, Ar-*H*, minor isomer). ^{19}F NMR (376.1 MHz, $CDCl_3$, 25 °C): -64.52 (CF_3, major), -70.48 (CF_3, minor).

N(^{t}Bu)C(CF_3)N(Et)H **(3.2)**

To a 1000 ml, 3-neck round-bottom flask was added 75.4 g (0.287 mol) of PPh_3, 10.8 g (0.094 mol) trifluoroacetic acid, 100 ml CCl_4 and a large stirbar. This solution was chilled to 0 °C using an ice bath and 11.3 g (0.113 mol) triethylamine was then added and the solution was stirred for 30 minutes at which point 8.3 g (0.113 mol) tert-butylamine was added. The ice-bath was removed and the reaction refluxed for 3 hours, leading to a gradual conversion of the colorless solution to a yellow slurry. The reaction mixture was then cooled to room-temperature and 50-100 ml of pentane was added to precipitate additional solid impurities ($NHEt_3Cl$, PPh_3, $P(O)Ph_3$) and then the reaction mixture was filtered, washing the solids with additional pentane until most of the color had left it and the washings were colorless. (Note: It may be necessary to filter a second time to remove additional precipitates from the yellow filtrate.) The solution was then cooled to 0 °C and 120 ml of ethylamine (2 M THF solution) was added. The reaction stirred overnight to produce a pale yellow solution concomitant with precipitation of NH_3EtCl salt (Note: substitution of the 2nd equivalent of ethylamine for triethylamine was unsuccessful). The solution was filtered to remove salt byproducts. All solvents were removed by fractional distillation (pentane, 36 °C; THF, 66 °C; CCl_4, 76 °C) to yield a yellow liquid with a strong, unpleasant odor. This liquid was then further purified by vacuum transfer to yield pure amidine as a colorless liquid. (Note: Typically 0.5 eq of THF transfers with the free amidine although it does not affect subsequent chemistry and removal of the solvent under reduced pressure leads to considerably diminished yields.) Yield = 9.2 g (0.047

mol). ^{1}H NMR (400 MHz, $CDCl_3$, 25 °C): 1.15 (3H, t, J = 7.2 Hz, CH_2CH_3), 1.34 (9H, s, $C(CH_3)_3$), 3.40 (2H, m, $^{3}J_{HH}$ = 7.2 Hz, $^{5}J_{HF}$ = 2 Hz, CH_2CH_3), 4.40 (1H, br s, NH). ^{13}C NMR (125.77 MHz, C_6D_6, 25 °C): 141.42 (q, $^{2}J_{CF}$ = 27.7 Hz, ^{t}BuN*C*NEt), 117.73 (q, $^{1}J_{CF}$ = 291.8 Hz, CF_3), 51.67 ($C(CH_3)_3$), 43.70 (CH_2CH_3), 17.96 (CH_2CH_3). ^{19}F NMR (376.1 MHz, $CDCl_3$, 25 °C): -66.54 (CF_3).

N(^{i}Pr)C(CF_3)N(^{i}Pr)H **(3.3)**

To a 1000 ml, 3-neck round-bottom flask was added 75.4 g (0.224 mol) of PPh_3, 8.5 g (0.074 mol) trifluoroacetic acid, 100 ml CCl_4 and a large stirbar. This solution was chilled to 0 °C using an ice bath and 9.1 g (0.136 mol) triethylamine was then added and the solution was stirred for 30 minutes at which point 5.3 g (0.136 mol) isopropylamine was added. The ice-bath was removed and the reaction refluxed for 3 hours, leading to a gradual conversion of the colorless solution to a yellow slurry. The reaction mixture was then cooled to room-temperature and 50-100 ml of pentane was added to precipitate additional solid impurities ($NHEt_3Cl$, PPh_3, $P(O)Ph_3$) and then the reaction mixture was filtered, washing the solids with additional pentane until most of the color had left it and the washings were colorless. It may be necessary to filter a second time to remove additional precipitates from the yellow filtrate. The solution was then cooled to 0 °C and 10.6 g (0.272 mol) isopropylamine was added. The reaction stirred overnight to produce a pale yellow solution concomitant with precipitation of NH_3^{i}PrCl salt (Note: substitution of the 2nd equivalent of ethylamine for triethylamine was unsuccessful). The solution was filtered to remove salt byproducts. All solvents were removed by fractional distillation (pentane, 36 °C; THF, 66 °C; CCl_4, 76 °C) to yield a yellow liquid with a strong, unpleasant odor. This liquid was then further purified by bulb to bulb transfer (40

mmHg, 80 °C) to yield pure amidine as a colorless liquid. Yield = 6.4 g (0.043 mol). ^{1}H NMR (400 MHz, $CDCl_3$, 25 °C): 1.10 (6H, d, J = 6.1 Hz, CH(C*H*$_3$)$_2$), 1.15 (6H, d, J = 6.5 Hz, CH(C*H*$_3$)$_2$), 3.81 (^{1}H, m,$^{3}J_{HH}$ = 6.1 Hz, $^{5}J_{HF}$ = 3.0 Hz, C*H*(CH$_3$)$_2$), 3.90 (1H, m, J = 6.5 Hz, C*H*(CH$_3$)$_2$), 4.32 (1H, br s, N*H*). ^{13}C NMR (125.77 MHz, C_6D_6, 25 °C): 140.88 (q, $^{2}J_{CF}$ = 27.7 Hz, ^{t}BuN*C*NEt), 118.21 (q, $^{1}J_{CF}$ = 290.5 Hz, *C*F$_3$), 49.52 (*C*H(CH$_3$)$_2$; Major), 47.22 (*C*H(CH$_3$)$_2$; minor), 45.87 (*C*H(CH$_3$)$_2$; minor), 42.69 (*C*H(CH$_3$)$_2$; minor), 25.81 (CH(*C*H$_3$)$_2$; Major), 24.63 (CH(*C*H$_3$)$_2$; minor), 23.55 (CH(*C*H$_3$)$_2$; minor), 22.08 (CH(*C*H$_3$)$_2$; minor). ^{19}F NMR (376.1 MHz, $CDCl_3$, 25 °C): -66.5 (CF_3, Major), -69.1 (CF_3, Minor).

[Na][N(^{t}Bu)C(CF_3)N(Et)](OEt$_2$)$_{0.5}$ **(3.5)**

To a 250 ml round-bottom flask was added 0.730 g (3.72 mmol) of **3.2**, 100 ml of Et_2O and a magnetic stirbar to give a colorless solution. $NaNTMS_2$ (0.683 g, 0.372 mmol) was dissolved into 10 ml of Et_2O to give a yellow solution. Both solutions were chilled to -25 °C. Dropwise, the $NaNTMS_2$ solution was added to the stirring amidine initially leading to a pale yellow solution which gradually gave way to golden yellow. After 4 h the solution had turned blood-orange in color and all volatiles were removed to give a dark red, oily solid which was dissolved into minimal pentane and chilled to -25 °C and stored overnight to give dark-red, crystalline material. Yield = 0.402 g (0.153 mmol). ^{1}H NMR (400 MHz, C_6D_6, 25 °C): 1.09 (3H, t, J = 6.8 Hz, O(CH$_2$C*H*$_3$)$_2$), 1.19 (3H, t, J = 7.2 Hz, CH$_2$C*H*$_3$), 1.41 (9H, s, C(C*H*$_3$)$_3$), 3.26 (2H, q, J = 7.2 Hz, C*H*$_2$CH$_3$), 3.56 (2H, q, J = 6.8 Hz, O(C*H*$_2$CH$_3$)$_2$). ^{13}C NMR (125.77 MHz, C_6D_6, 25 °C): 153.72 (q, $^{2}J_{CF}$ = 21.4 Hz, ^{t}BuN*C*NEt), 122.49 (q, $^{1}J_{CF}$ = 286.76 Hz, *C*F$_3$), 66.13 (O*C*H$_2$CH$_3$), 51.21

($C(CH_3)_3$), 43.81 (CH_2CH_3), 32.01 ($C(CH_3)_3$) 19.77 (CH_2CH_3), 15.55 (OCH_2CH_3). ^{19}F NMR (376.1 MHz, C_6D_6, 25 °C): -66.63 (CF_3).

$Cp^*Zr[N(^tBu)C(CF_3)N(Et)]Cl_2$ **(3.7)**

To a 250 ml round-bottom flask was added 0.430 g (2.19 mmol) of **3.2**, 10 ml of Et_2O and a magnetic stirbar to give a colorless solution. $NaNTMS_2$ (0.402 g, 2.19 mmol) was dissolved into 10 ml of toluene to give a yellow solution. Both solutions were chilled to -25 °C. Dropwise, the $NaNTMS_2$ solution was added to the stirring amidine solution initially leading to a pale yellow solution which gradually gave way to golden yellow. Upon stirring for 0.5 h, the solution took on a more orange hue at which point the solution was chilled again to -25 °C. To this chilled, stirring solution was added 0.730 g (0.219 mmol) Cp^*ZrCl_3 as a yellow powder leading to an immediate color change to yellow. The reaction was stirred for 0.5 h at which point all volatiles were removed under reduced pressure to give an oily yellow-brown solid. Extraction of the product into pentane followed by filtration removed insoluble salt by-products gave a yellow filtrate which readily crystallized upon removal of solvent. Concentration of the pentane solution and storage at -25 °C readily gave pale yellow, crystalline material. Yield = 0.465 g (0.94 mmol). ^1H NMR (400 MHz, C_6D_6, 25 °C): 1.56 (3H, t, J = 7.1 Hz, CH_2CH_3), 1.33 (9H, s, $C(CH_3)_3$), 1.96 (15H, s, $C_5(CH_3)_5$), 3.30 (qq, $^3J_{HH}$ = 7.1 Hz, $^5J_{HF}$ = 2.4 Hz, CH_2CH_3). ^{13}C NMR (125.77 MHz, Toluene-d_8, 25 °C): 157.72 (q, $^2J_{CF}$ = 31.4 Hz, ^{t}BuN*C*NEt), 124.54 ($C_5(CH_3)_5$), 117.55 (q, $^1J_{CF}$ = 291.8 Hz, CF_3), 55.69 (*C(CH3)3*), 44.45 (q, $^4J_{CF}$ = 3.8 Hz, CH_2CH_3), 32.55 (q, $^5J_{CF}$ = 3.8 Hz, C(CH3)3) 17.00 (q, $^5J_{CF}$ = 2.5 Hz, CH_2CH_3), 12.79 ($C_5(CH_3)_5$). ^{19}F NMR (376.1 MHz, C_6D_6, 25 °C): -59.29 (CF_3). Anal. Calcd for $C_{18}H_{29}F_3N_2Cl_2Zr$: C, 43.89; H 5.73; N, 5.69. Found: C, 43.63; H, 5.62; N, 5.52.

$Cp^*Hf[N(^tBu)C(CF_3)N(Et)]Cl_2$ **(3.8)**

To a 250 ml round-bottom flask was added 0.430 g (1.40 mmol) of **3.2**, 100 ml of Et_2O and a magnetic stirbar to give a colorless solution. $NaNTMS_2$ (0.402 g, 1.40 mmol) was dissolved into 10 ml of toluene to give a yellow solution. Both solutions were chilled to -25 °C. Dropwise, the $NaNTMS_2$ solution was added to the stirring amidine solution initially leading to a pale yellow solution which gradually gave way to golden yellow. Upon stirring for 0.5 h, the solution took on a more orange hue at which point the solution was chilled again to -25 °C. To this chilled, stirring solution was added 0.590 g (0.140 mmol) Cp^*HfCl_3 as a purple powder leading to an immediate color change to yellow. The reaction was stirred for 1.0 h and then all volatiles were removed under reduced pressure to give an oily beige-brown solid. Extraction of the product into a 1:1 pentane:toluene mixture followed by filtration removed insoluble salt by-products and gave an off-white filtrate. All volatiles were removed and the product dissolved in minimal pentane. Storage of this solution at -25 °C readily gave white, crystalline material. Yield = 0.465 g (0.802 mmol). ^{1}H NMR (400 MHz, C_6D_6, 25 °C): 1.56 (3H, t, J = 6.8 Hz, CH_2CH_3), 1.32 (9H, s, $C(CH_3)_3$), 2.03 (15H, s, $C_5(CH_3)_5$), 3.32 (br d, CH_2CH_3). ^{13}C NMR (125.77 MHz, C_6D_6, 25 °C): 157.88 (q, $^2J_{CF}$ = 32.7 Hz, ^{t}BuN*C*NEt), 124.76 ($C_5(CH_3)_5$), 121.20 (q, $^1J_{CF}$ = 289.3 Hz, CF_3), 55.73 ($C(CH_3)_3$), 44.25 (q, $^4J_{CF}$ = 3.8 Hz, CH_2CH_3), 32.97 (q, $^5J_{CF}$ = 2.5 Hz, $C(CH_3)_3$) 17.25 (q, $^5J_{CF}$ = 2.5 Hz, CH_2CH_3), 12.88 ($C_5(CH_3)_5$). ^{19}F NMR (376.1 MHz, C_6D_6, 25° C): -56.74 (CF_3). Anal. Calcd for $C_{18}H_{29}F_3N_2Cl_2Hf$: C, 37.29; H 5.04; N, 4.83. Found: C, 36.94; H, 5.04; N, 4.87.

$Cp^*Zr[N(^tBu)C(CF_3)N(Et)]Me_2$ **(3.9)**

To 30 ml scintillation vial was added 0.185 g (0.379 mmol) of **3.7**, 20 ml of Et_2O and a magnetic stirbar to give a pale yellow solution which was then chilled to -27 °C. To this solution was added, dropwise, 0.35 ml of a 2.48 M solution of MeMgBr in Et_2O. Addition of the Grignard led to a bleaching of the solution as well as precipitation of salt byproduct. Upon stirring for 0.5 h, all volatiles were removed, the crude product extracted into pentane and salt impurities removed by filtration. All solvent was removed to give crude **3.9** as a bright yellow oil.

^{1}H NMR (400 MHz, C_6D_6, 25 °C): 0.28 (6H, s, Zr(CH_3)$_2$), 1.02 (3H, t, J = 6.8 Hz, CH_2CH_3), 1.19 (9H, s, C(CH_3)$_3$), 1.87 (15H, s, C_5(CH_3)$_5$), 3.07 (qq, $^3J_{HH}$ = 6.8 Hz, $^5J_{HF}$ = 2.4 Hz, CH_2CH$_3$). ^{19}F NMR (376.1 MHz, C_6D_6, 25 °C): -59.7 (CF_3).

Cp*Hf[N(^{t}Bu)C(CF_3)N(Et)]Me_2 **(3.10)**

To 30 ml scintillation vial was added 0.220 g (0.379 mmol) of **3.8**, 20 ml of Et_2O and a magnetic stirbar to give a pale yellow solution which was then chilled to -27 °C. To this solution was added, dropwise, 0.35 ml of a 2.48 M solution of MeMgBr in Et_2O. Addition of the Grignard led to a bleaching of the solution as well as precipitation of salt byproduct. Upon stirring for 0.5 h, all volatiles were removed, the crude product extracted into pentane and salt impurities removed by filtration. All solvent was removed to give pure **3.10** as a dark-yellow oil. Yield = 0.190 g (0.353 mmol). ^{1}H NMR (400 MHz, C_6D_6, 25 °C): 0.08 (6H, s, Hf(CH_3)$_2$), 1.06 (3H, t, J = 7.1 Hz, CH_2CH_3), 1.23 (9H, s, C(CH_3)$_3$), 1.96 (15H, s, C_5(CH_3)$_5$), 3.13 (qq, $^3J_{HH}$ = 7.1 Hz, $^5J_{HF}$ = 2.4 Hz, CH_2CH$_3$). ^{13}C NMR (125.77 MHz, C_6D_6, 25° C): 157.82 (q, $^2J_{CF}$ = 30.2 Hz, ^{t}BuN*C*NEt), 119.81 (q, $^1J_{CF}$ = 291.8 Hz, CF_3), 119.98 (C_5(CH_3)$_5$), 55.48 (Hf(*C*H$_3$)$_2$), 54.41 (*C*(CH$_3$)$_3$), 42.54 (q,

$^{4}J_{CF}$ = 3.8 Hz, *C*H_2CH$_3$), 33.09 (q, $^{5}J_{CF}$ = 1.3 Hz, C(*C*H_3)$_3$) 18.15 (CH_2*C*H_3), 12.17 (C_5(*C*H_3)$_5$). ^{19}F NMR (376.1 MHz, C_6D_6, 25 °C): -59.7 (CF_3).

3.4.3 General polymerization of Alpha-Olefins

General polymerization of propene in chlorobenzene

A solution of the precatalyst (0.020 mmol) in 0.5 mL chlorobenzene at -10 °C was added to the [PhNMe_2][B(C_6F_5)$_4$] (0.026 mmol) and agitated until dissolved. The resulting mixture was added to 19.5 mL chlorobenzene at -10 °C in a 250 mL Schlenk flask. The flask was charged to 5 psi with propene gas while stirring. The pressure and stirring was maintained for the duration of the reaction where upon it was quenched with 1.0 mL of methanol and precipitated into 600 mL acidic methanol to isolate the polymer product. The polymer was collected and dried under vacuum. The resulting polymers were characterized by DSC, GPC, and ^{13}C NMR.

General polymerization of 1-hexene

A solution of the precatalyst (0.020 mmol) in 0.5 mL chlorobenzene at -10 °C was added to the [PhNMe_2][B(C_6F_5)$_4$] (0.026 mmol) and agitated until dissolved. The resulting mixture was added to 19.5 mL chlorobenzene and 200 eq 1-hexene at -10 °C in a scintillation vial. The stirring and temperature was maintained for the duration of the reaction where upon it was quenched with 1.0 mL of methanol and precipitated into 600 mL acidic methanol to isolate the polymer. The final poly(1-hexene) was extracted with pentane before being dried under vacuum. The polymer was collected and dried under vacuum. The resulting polymers were characterized by DSC, GPC, and ^{1}H/^{13}C NMR.

3.4.5. Computational Details

Theoretical calculations in this work have been performed using density functional theory (DFT) method,[60] specifically functional PBE,[61] implemented in a state-of-the-art program package "Priroda".[62,63] In PBE calculations relativistic Stevens-Basch-Krauss (SBK) effective core potentials (ECP)[64] optimized for DFT-calculations have been used.

Basis set was 311-split for main group elements with one additional polarization *p*-function for hydrogen, additional two polarization *d*-functions for elements of higher periods. Full geometry optimization has been performed without constraints on symmetry. For all species under investigation frequency analysis has been carried out. All minima have been checked for the absence of imaginary frequencies.

3.5 References

1. Nexant, I. **2007**; Vol. 2012.
2. Coates, G. W. *Chem. Rev.* **2000**, *100*, 1223–1252.
3. Guan, Z.; Cotts, P. M.; McCord, E. F.; McLain, S. J. *Science* **1999**, *283*, 2059–2062.
4. Domski, G. J.; Rose, J. M.; Coates, G. W.; Bolig, A. D.; Brookhart, M. *Prog. Polym. Sci.* **2006**, *32*, 30–92.
5. Lee, I.; Geuthier, W. J.; Ball, J. M.; Iyengar, B.; Collins, S. *Organometallics* **1992,** *11*, 2115-2122.
6. Piccolrovazzi, N.; Pino, P.; Consiglio, G.; Sironi, A.; Moret, M. *Organometallics* **1990,** *9*, 3098-3105.
7. Leino, R.; Lehmus, P.; Lehtonen, A. *Eur. J. Inorg. Chem.* **2004,** 3201-3222.

8. Coles, M. P.; Hitchcock, P. B. *Organometallics* **2003,** *22,* 5201-5211.
9. Andell, O.; Maaranen, J. World Patent No. WO99/10353, **1999**.
10. Iwashita, A.; Chan, M. C. W.; Makio, H.; Fujita, T. *Catal. Sci. Technol.* **2014,** *4,* 599-610.
11. Kenyon, P.; Mecking, S. *J. Am. Chem. Soc.* **2017,** *139,* 13786-13790.
12. J. Saito, M. Mitani, J. Mohri, Y. Yoshida, S. Matsui, S. Ishii, S. Kojoh, N. Kashiwa, T. Fujita, *Angew. Chem., Int. Ed. Engl.* **2001,** *40,* 2918-2920.
13. M. Mitani, J. Mohri, Y. Yoshida, J. Saito, S. Ishii, K. Tsuru, S. Matsui, R. Furuyama, T. Nakano, H. Tanaka, S. Kojoh, T. Matsugi, N. Kashiwa, T. Fujita, *J. Am. Chem. Soc.* **2002,** *124,* 3327-3336.
14. J. Saito, M. Mitani, J. Mohri, S. Ishii, Y. Yoshida, T.Matsugi, S. Kojoh, N. Kashiwa, T. Fujita, *Chem. Lett.* **2001,** *30,* 576-577.
15. J. Saito, M. Mitani, M. Onda, J. Mohri, S. Ishii, Y.Yoshida, T. Nakano, H. Tanaka, T. Matsugi, S. Kojoh, N.Kashiwa, T. Fujita, *Macromol. Rapid Commun*. **2001,** *22,* 1072-1075.
16. Tian, J.; Hustad, P. D.; Coates, G. W. *J. Am. Chem. Soc.* **2001,** *123,* 5134-5135.
17. Mason, A. F.; Tian, J.; Hustad, P. D.; Lobkovsky, E. B.; Coates, G. W. *Isr. J. Chem.* **2002,** *42,* 301-306.
18. Edson, J. B.; Wang, Z.; Kramer, E. J.; Coates, G. W. *J. Am. Chem. Soc.* **2008,** *130,* 4968-4977.
19. Weberski, M. P.; Chen, C.; Delferro, M.; Zuccaccia, C.; Macchioni, A.; Marks, T. J. *Organometallics* **2012,** *31,* 3773-3789.

20. Weberski, M. P.; Chen, C.; Delferro, M.; Marks, T. J. *Chem. Eur. J.* **2012,** *18*, 10715-10732.

21. Makio, H.; Kashiwa, N.; Fujita, T. *Adv. Synth. Catal.* **2002,** *344*, 477-493.

22. Elkin,T.; Aharonovich, S.; Botoshansky, M.; Eisen, M. S. *Organometallics* **2012,** *31*, 7404-7414.

23. The exception to this was the living-systems wherein fluorination solely occurred in either the 2- or 2,6-positions.

24. Jayaratne, K. C.; Sita, L. R. *J. Am. Chem. Soc.* **2000**, *122*, 958-959.

25. Jayaratne, K. C.; Keaton, R. J.; Henningsen, D. A.; Sita, L. R. *J. Am. Chem. Soc.* **2000**, *122*, 10490-10491.

26. Keaton, R. J.; Jayaratne, K. C.; Fettinger, J. C.; Sita, L. R. *J. Am. Chem. Soc.* **2000**, *122*, 12909-12910.

27. Keaton, R. J.; Jayaratne, K. C.; Henningsen, D. A; Koterwas, L. A.; Sita, L. R. *J. Am. Chem. Soc.* **2001**, *123*, 6197-6198.

28. Zhang, Y.; Keaton, R. J.; Sita, L. R. *J. Am. Chem. Soc.* **2003**, *125*, 9062-9069.

29. Zhang, Y.; Sita, L. R. *J. Am. Chem. Soc.* **2004**, *126*, 7776-7777.

30. Zhang, Y.; Reeder, E. K.; Keaton, R. J.; Sita, L. R. *Organometallics.* **2004**, *23*, 3512-3520.

31. Harney, M. B.; Keaton, R. J.; Fettinger, J. C.; Sita, L. R. *J. Am. Chem. Soc.* **2006**, *128*, 3420-3432.

32. Harney, M. B.; Zhang, Y.; Sita, L. R. *Angew. Chem. Int. Ed.* **2006**, *45*, 2400-2404.

33. Harney, M. B.; Zhang, Y.; Sita, L. R. *Angew. Chem. Int. Ed.* **2006**, *45*, 6140-6144.

34. Wei, J.; Hwang, W.; Zhang, W.; Sita, L. R. *J. Am. Chem. Soc.* **2013**, *135*, 2132-2135.

35. Kissounko, D. A.; Zhang, W.; Harney, M. B.; Sita, L. R. *Adv. Synth. Catal.* **2005**, *347*, 426-432.

36. Zhang, W.; Sita, L. R. *J. Am. Chem. Soc.* **2008**, *130*, 442-443.

37. Zhang, W.; Wei, J.; Sita, L. R. *Macromolecules* **2008**, *41*, 7829-7833.

38. Wei, J.; Zhang, W.; Wickman, R.; Sita, L. R. *Angew. Chem. Int. Ed.* **2010**, *49*, 9140-9144.

39. Wei, J.; Zhang, W.; Sita, L. R. *Angew. Chem. Int. Ed.* **2010**, *49*, 1768-1772.

40. Blakely, C. G., Ph.D. Thesis, University of Maryland-College Park, **2013**.

41. Knapp, C.; Lork, E.; Watson, P. G.; Mews, R. *Inorg. Chem.* **2002**, *41*, 2014-2025.

42. Wedler, M.; Knosel, F.; Noltemeyer, M.; Edelmann, F. T.; Behrens, U. *J. Organomet. Chem.* **1990**, *388*, 21-45.

43. Recknagel, A.; Knosel, F.; Gornitzka, H.; Noltemeyer, M.; Edelmann, F. T.; Behrens, U. *J. Organomet. Chem.* **1991**, *417*, 363-375.

44. Krasnopolski, M.; Hrib, C. G.; Seidel, R. W.; Winter, M.; Becker, H.; Rogalla, D.; Fischer, R. A.; Edelmann, F. T.; Devi, A. *Inorg. Chem.* **2013**, *52*, 286-296.

45. Sita, L. R.; Babcock, J. R. *J. Am. Chem. Soc.* **1998**, 5228-5230.

46. Davidson, J. L.; Green, M.; Nyathi, J. Z.; Stone, F. G. A.; Welch, A. J. *J. Chem. Soc., Dalton Trans.* **1977**, 2246-2255.

47. Koola, J. D.; Roddick, D. M. *Organometallics* **1991**, *10*, 591-597.

48. Loizou, D. C.; Castillo, J. Oki, A. R.; Hosmane, N. S.; Morrison, J. A. *Organometallics* **1992**, *11*, 4189-4193.

49. Taw, F. L.; Scott, B. L. Kiplinger, J. L. *J. Am. Chem. Soc.* **2003**, *125*, 14712-14713.

50. Huang, H.; Hughes, R. P.; Rheingold, *Organometallics* **2010**, *29*, 1948-1955.

51. Tamura, K.; Mizukami, H.; Maeda, K.; Watanabe, H.; Uneyama, K. *J. Org. Chem.* **1993**, *58*, 32-35.

52. Uneyama, K.; Kobayashi, M. *J. Org. Chem.* **1994**, *59*, 3003-3014.

53. Scharf, A. B.; Betley, T. A. *Inorg. Chem.* **2011**, *50*, 6837-6845.

54. Dureen, M. A.; Welch, G. C.; Gilbert, T. M.; Stephan, D. W. *Inorg. Chem.* **2009**, *48*, 9910-9917.

55. Krummenacher, I.; Cummins, C. C. *Polyhedron* **2012**, *32*, 10-13.

56. Rasika Dias, H. V.; Jin, W.; Kim, H.; Lu, H. *Inorg. Chem.* **1996**, *35*, 2317-2328.

57. Cole, M. L.; Evans, D. J.; Junk, P. C.; Smith, M. K. *Chem. Eur. J.* **2003**, *9*, 415-424.

58. Groom, C. R.; Bruno, I. J.; Lightfoot, M. P.; Ward, S. C. *Acta. Cryst.* **2016,** *B72*, 171-179.

59. Koterwas, L. A.; Fettinger, J. C.; Sita, L. R. *Organometallics* **1999**, *18*, 4183-4190.

60. Parr, R. G.; Yang, W. Density-functional theory of atoms and molecules; Oxford University Press: Oxford, **1989**.

61. Perdew, J. P. ; Burke, K.; Ernzerhof, M. *Phys. Rev. Lett.* **1996**, *77*, 3865.

62. Laikov, D. N. *Chem. Phys. Lett.* **1997**, *281*, 151.

63. Laikov, D. N.; Ustynyuk, Yu. A. *Russ. Chem. Bulletin* **2005**, *54*, 820.

64. (a.) Stevens, W. J.; Basch, H.; Krauss, M. *J. Chem. Phys*. **1984**, *81*, 6026; (b.) Stevens, W. J.; Basch, H.; Krauss, M.; Jasien, P. *Can. J. Chem*. **1992**, *70*, 612; Cundari, T. R.; Stevens, W. J. *J. Chem. Phys*. **1993**, *98*, 5555.

Chapter 4: Extension of Trifluoromethylamidinates on Tantalum toward Dinitrogen Coordination and Cleavage

4.1 Introduction

The facile synthesis of the N,N'diisopropyl-trifluoromethylamidine, **3.3**, while not especially useful for group IV-based polymerization chemistry, is highly intriguing for both group V and group VI-based dinitrogen and interrelated group transfer chemistry. As was seen in Chapter 3, the trifluoromethyl-substituted amidinates maintain approximately the same steric profile as their methyl analogs, but with a considerably different electronic character. The impact of such a marked change in ligand properties is hard to predict but many aspects of it should improve features within the pre-existing system. Presumably, generating a more electrophilic metal center ligand should lower the reduction potential necessary to reach the M(II) oxidation state associated with dinitrogen complexes capable of full N-N triple bond scission.[1] Depending on the extent of this effect, such chemistry could occur at potentials which would facilitate the use of environmentally benign (and abundant) reductants such as zinc or magnesium metal. To date, the bulk of reduction chemistry which is relevant to dinitrogen fixation has focused on the use of either incredibly powerful alkali metal-based reductants[2] (which may be incompatible with other reagents within reaction mixtures), or expensive organometallic reagents[3] (which make scaling of such systems problematic). Therefore, attenuating the reduction potential necessary for formation of dinitrogen complexes would be advantageous on a number of fronts.

What is more difficult to predict, and likely more interesting to study, would be the effect that such electron-poor ligands have on the kinetics of dinitrogen activation. Previous work by Dr. Andrew Keane found that the barrier for N_2 cleavage by the series complexes with the form, $\{Cp^*[N(^iPr)C(X)N(^iPr)]Ta\}_2(\mu_{1,1}\text{-}N_2)$ (X = Me, NMe_2, Ph), was heavily influenced by the size of the distal substituent with larger groups inhibiting the reaction.[2c] These observations led to the hypothesis that the rate-limiting step involved rearrangement of the (crystallographically characterized) end-on bridging mode of the dinitrogen ligand to a mutually side-bound bridging mode. Indirect evidence supporting this hypothesis was provided by crystal structures of the related d^0, Zr and Hf analogs which feature a side-on binding motif in a sort of "arrested state of dinitrogen cleavage."[4] The concept of end-on to side-on rearrangement preceding N_2-cleavage stands counter to the more widely accepted "zig-zag" transition state put forward by Cummins[5] and supported by a number of other groups.[6] It is possible that enhanced Lewis acidity of the metal center(s) supported by the trifluoromethyl-amidinate could help to bias the mode of binding toward side-on; this would substantially lower the barrier toward cleavage, as no rearrangement process would need to occur.

Finally, the electron-withdrawing nature of the ancillary ligand should impart greater electrophilicity onto the nitrido (or imido by way of EMe_3Cl functionalization) ligand which result from full rupture of the N-N triple bond. The results of Chapter 2 suggest that the mechanism for NGT invokes an electrophilic nitrogen-center; therefore, imparting greater electrophilicity should enhance the current reactivity associated with this system and possibly open new modes of reactivity not yet observed in this system, such as aziridination or R-H bond activation (R = H, C).[7] It should be noted that there is

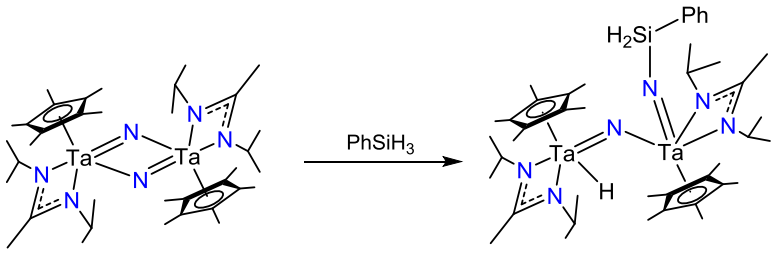

Scheme 4.1. Si-H addition across a N_2-derived bridging Ta nitride. Further attempts at functionalization were unsuccessful.

precedence for Si-H addition across the Ta-N bond of $\{Cp^*[N(^iPr)C(Me)N(^iPr)]Ta(N)\}_2$ to generate Ta(1)-H and Ta(2)=N-SiH_2Ph however further functionalization was unsuccessful (Scheme 4.1).[8] The introduction of the electron-withdrawing amidinate could facilitate such chemistry with more robust E-H bonds.

4.2 Results and Discussion

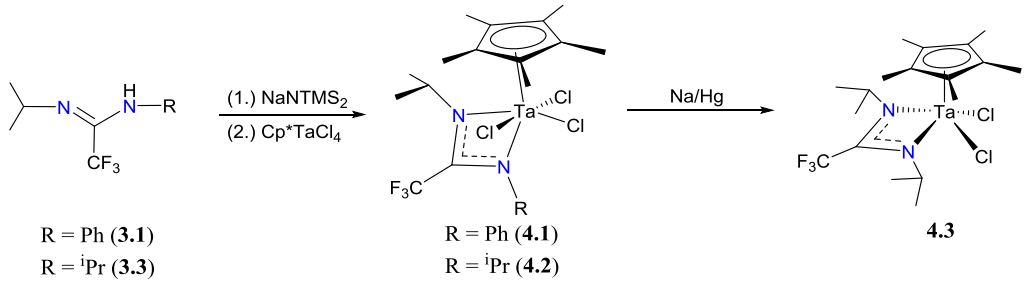

R = Ph (**3.1**)
R = ^{i}Pr (**3.3**)

R = Ph (**4.1**)
R = ^{i}Pr (**4.2**)

4.3

Scheme 4.2. Formation and **4.1**, **4.2** and **4.3**.

Preliminary studies have shown that the same metalation strategy associated with the group IV metals translates for group V as well. As such, treatment of either **3.1** or **3.3** with a slight excess of $NaNTMS_2$ in Et_2O generated a yellow solution of "$[Na][N(^iPr)C(CF_3)N(R)]$." Addition of solid Cp^*TaCl_4 to these ethereal solutions at low-temperatures produced crystalline $Cp^*[N(^iPr)C(CF_3)N(R)]TaCl_3$ (R = Ph, **4.1**; ^{i}Pr = **4.2**) in moderate to good isolated yields (Scheme 4.2). Due to its more direct structural analogy with previous work, as well as reduced steric profile, **4.2** was focused on.

^{1}H NMR spectra of **4.2** suggest two distinct isopropyl environments based on the presence of two well-resolved doublets and, more importantly, two methine environments separated by 0.73 ppm (4.27 and 5.05 ppm); the more downfield signal indicates not only a distinct environment but one which may be shifted due to partial interaction with the ring current of a proximal Cp ligand. This spectroscopic evidence suggests an overall geometry of **4.2** which can be thought of as distorted octahedral (wherein the Cp-ring occupies one position) with the amidinate binding with one N-arm trans to the Cp* ring and one cis. The remaining 3 chloride ligands arrange themselves in a meridonal fashion. Such an assessment is further supported by the presence of similar chemical shifts being observed in the related methyl analog, Cp*[N(^{i}Pr)C(Me)N(^{i}Pr)]TaCl$_3$ (**4.2^{Me}**);[9] X-ray diffraction studies performed on single crystals of **4.2** confirmed this structure (Figure 4.2, Table 4.1). Excitingly, this gave access to a direct structural comparison between the analogous methyl and trifluoromethyl derivatives which are otherwise chemically identical.

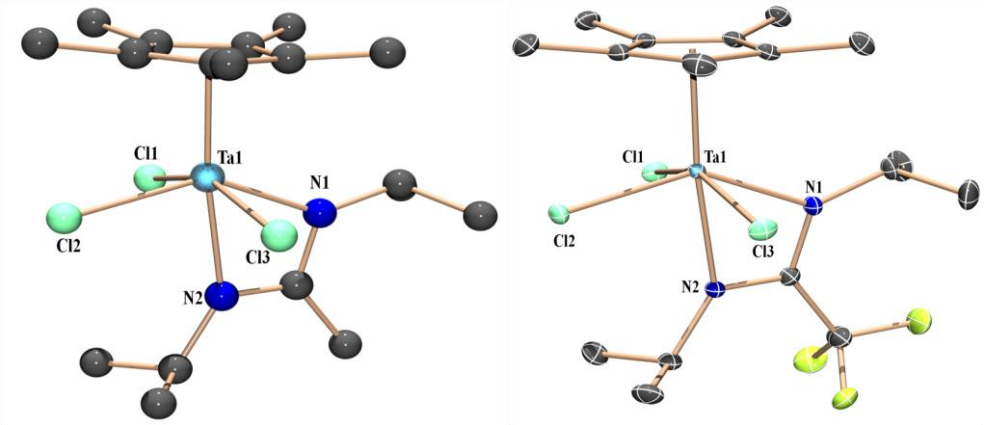

Figure 4.1. Structure of **4.2^{Me}** (left) and **4.2** (right) with hydrogen atoms omitted for clarity, ellipsoids for the non-hydrogen atoms are shown at the 30% probability level.

Analyzing the primary spheres of **4.2** and **4.2^{Me}** shows similar bond distances and angles about the Ta with the expectation of the Ta1-N1 bond which is elongated by 0.06 Å in **4.2** (the chloride trans to this bond, Cl2, saw a smaller 0.02 contraction). Comparison of the space-filling models for **4.2** and 4.2^{Me} shows the methine associated with N1 in **4.2** experiences a marked steric interaction with the CF_3 ligand, suggesting that the elongation of Ta1-N1 in **4.2** is steric in nature.

Table 4.1. Selected Bond Lengths (Å) and Angles (°) for the Molecular Structures of **4.2^{Me}** and **4.2**

	4.2^{Me}	**4.2**
Ta(1)-N(1)	2.094(5)	2.1548(16)
Ta(1)-N(2)	2.194(6)	2.2234(16)
Ta(1)-Cl(1)	2.4372(13)	2.4310(3)
Ta(1)-Cl(2)	2.3821(17)	2.3605(3)
N(1)-Ta(1)-N(2)	60.2(4)	60.04(6)

Reduction of **4.2** successfully led to formation of the Ta(IV) dichloride species, Cp*[N(^{i}Pr)C(CF_3)N(^{i}Pr)]$TaCl_2$ (**4.3**), without degradation of the CF_3 substituent. This latter point is important in that it shows that, at least with Na/Hg as the reductant, the C-F bonds are sufficiently robust toward reduction. ^{1}H spectra of **4.3** are extremely broadened, corroborating its assignment as a paramagnetic, d^1 species. X-ray diffraction

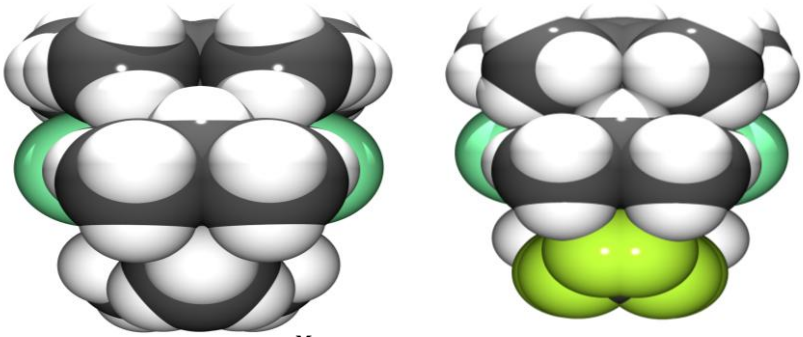

Figure 4.2. Space-filling models of **4.2^{Me}** and **4.2**, highlighting the increased steric pressure exerted by the CF_3-group in **4.2**. The CF_3-group of **4.2** is disordered over 2 positions.

studies confirmed the expected structure and connectivity and again gave an opportunity to directly compare the influence of CF_3 versus its methyl analog, Cp*[N(^{i}Pr)C(Me)N(^{i}Pr)]TaCl$_2$ (**4.3^{Me}**).[10] As can be seen from Figure 4.3, the bulk structures of **4.3** and **4.3^{Me}** have nearly identical 4-legged piano stool geometries. Further, the primary coordination sphere about the Ta centers in both structures is highly similar, showing limited deviation in bond distances or angles (Table 4.2). Interestingly, the Ta-Cp*centroid distance for **4.3** (2.066 Å) is contracted relative to the methyl analog (2.071 Å), likely a direct consequence of the greater electrophilicity on the part of the former's

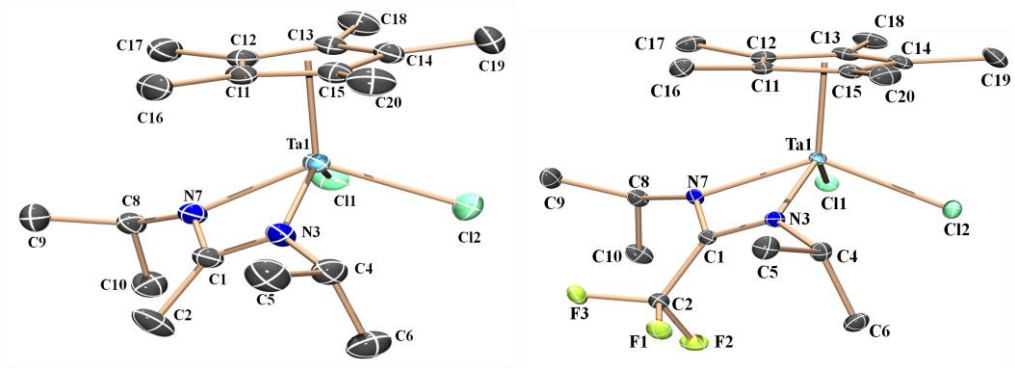

Figure 4.3. Structure of **4.3^{Me}** (left) and **4.3** (right) with hydrogen atoms omitted for clarity, ellipsoids for the non-hydrogen atoms are shown at the 30% probability level.

metal center.

Attempts to reduce **4.3** by multiple equivalents of Na/Hg in hopes of producing a dinitrogen analog of those studied by Dr. Keane have thus far been met with mixtures of numerous diamagnetic products; many of these appear to be of low-symmetry, likely indicating some form of ligand degradation. This is not entirely unexpected as KC_8 has been found to be the preferable reductant for the formation of group V dinitrogen complexes.

Table 4.2. Selected Bond Lengths (Å) and Angles (°) for the Molecular Structures of **4.3**^{Me} and **4.3**

	4.3$^{Me, a.}$	**4.3**
Ta(1)-N(3)	2.123(3)	2.143(2)
Ta(1)-N(7)	2.129(3)	2.144(2)
Ta(1)-Cl(1)	2.4046(11)	2.4033(7)
Ta(1)-Cl(2)	2.4140(11)	2.4072(8)
Ta(1)-Ct^{Cp*}	2.071	2.066
N(3)-Ta(1)-N(7)	61.82(12)	61.94(8)

[a.] Bonding metrics are taken from one of the crystallographically independent (but metrically similar) molecules found in the unit cell.

4.3 Conclusion

Though the substitution of a trifluoromethyl group in the distal position of amidinate ligands has proven to be an effective means to perturb the electronic structure of CPAM-based group IV metal systems (and one which has yielded positive results in terms of increasing reactivity at the metal-center), preliminary studies focused on related Ta and Mo systems have been met with mixed results. Synthesis of the tantalum tri- and dichloride was found to be possible without degradation of the ligand scaffold, opening up the possibility to monitor the effect that a more electron-poor metal center has on previously established dinitrogen chemistry. Attempts to append the CF_3 ligand to molybdenum has of yet proven more difficult and suggests that there are limits to its robustness.

4.4 Experimental Details

4.4.1 General considerations

All manipulations were performed under an inert atmosphere of N_2 using standard Schlenk-line or glove-box techniques. All solvents were dried (Na/benzophenone for pentane and diethyl ether, and Na for toluene) and distilled under N_2 prior to use.

Benzene-d_6 and Toluene-d_8 were dried over Na/K alloy and vacuum transferred prior to being used. Celite was oven dried at 150 °C for several days before use. Cooling for the reactions was performed in the internal freezer (-25 °C) of the glove box used. (η5-C_5Me_5)$TaCl_4$ was purchased from Strem Chemicals and used as received. $NaNTMS_2$ was purchased from Sigma Aldrich and used as purchased.

4.4.2 Synthesis of new compounds

Cp*[N(^{i}Pr)C(CF_3)N(^{i}Pr)]$TaCl_3$ **(4.1)**

To a 30 ml scintillation vial was added 0.230 g (0.10 mmol) of **3.1**, 5 ml of toluene and a magnetic stirbar to give a colorless solution. $NaNTMS_2$ (0.220 g, 0.12 mmol) was dissolved into 10 ml of toluene in a separate scintillation vial to give a colorless solution. Both solutions were chilled to -25 ^{o}C. Dropwise, the $NaNTMS_2$ solution was added to the stirring amidine solution, initially leading to a pale yellow solution which gradually gave way to tea-color. Upon stirring for 1 h the solution was returned to the -25 ^{o}C freezer. To the chilled solution was added 0.460 g (0.10 mmol) of Cp*$TaCl_4$ to generate bright yellow suspension which gradually changed to yellow-orange and finally to red-orange. The reaction was stirred for 2 h at which point all volatiles were removed under reduced pressure to give orange crystalline solids. The solids were re-dissolved in minimal toluene and filtered through a 2" celite plug on a medium porosity fritted funnel. Volatiles were removed under reduced pressure until solid began to form on the walls of the flask, at which point the solution was stored at -25 ^{o}C overnight to give orange crystalline product. Yield = 0.417 g (0.64 mmol). ^{1}H NMR (400 MHz, C_6D_6, 25 °C): 1.27 (6H, d, J = 8.0 Hz, CH(CH_3)$_2$), 2.12 (15H, s, C_5(CH_3)$_5$),

4.25 (m, J = 8.0, C*H*(CH_3)$_2$), 6.93 (t, J = 8.0, *m*-Ph), 7.19 (*p*-Ph, overlaps with C_6D_6 signal), 7.85 (t, J = 8.0, *m*-Ph).

Cp*[N(^{i}Pr)C(CF_3)N(^{i}Pr)]$TaCl_3$ **(4.2)**

To a 30 ml scintillation vial was added 0.33 g (1.68 mmol) of **3.3**, 5 ml of Et_2O and a magnetic stirbar to give a colorless solution. $NaNTMS_2$ (0.34 g, 1.85 mmol) was dissolved into 20 ml of Et_2O in a separate scintillation vial to give a colorless solution. Both solutions were chilled to -25 ^{o}C. Dropwise, the $NaNTMS_2$ solution was added to the stirring amidine solution, initially leading to a pale yellow solution which gradually gave way to golden yellow. Upon stirring for 1 h the solution was returned to the -25 ^{o}C freezer. To a 250 ml round-bottom flask was added 0.660 g (0.144 mmol) of Cp*$TaCl_4$, 50 ml of toluene and a magnetic stirbar to give a yellow suspension which was chilled to -25 ^{o}C. Dropwise, the ethereal solution was added to the stirring aromatic suspension leading to a gradual color change from bright yellow to yellow-orange and finally to red-orange. The reaction was stirred for 2 h at which point all volatiles were removed under reduced pressure to give red-orange crystalline solids. The solids were re-dissolved in minimal toluene and filtered through a 2" celite plug on a medium porosity fritted funnel. Volatiles were removed under reduced pressure until solid began to form on the walls of the flask, at which point the solution was stored at -25 ^{o}C overnight to give orange crystalline product. Yield = 0.550 g (0.890 mmol). ^{1}H NMR (400 MHz, Tol-d_8, 25 °C): 1.15 (6H, d, J = 6.6 Hz, CH(C*H*$_3$)$_2$), 1.85 (6H, d, J = 6.7 Hz, CH(C*H*$_3$)$_2$), 2.15 (15H, s, C_5(C*H*$_3$)$_5$), 4.27 (m, J = 6.7 C*H*(CH_3)$_2$), 5.05 (br s, C*H*(CH_3)$_2$). ^{13}C NMR (125.77 MHz, Tol-d_8, 25 °C): 158.56 (q, $^2J_{CF}$ = 34.0 Hz, ^{i}PrN*C*N^{i}Pr), 130.63 (*C*$_5$(CH_3)$_5$), 120.13 (q, $^1J_{CF}$ = 280.0 Hz, *C*F_3), 55.20 (*C*H(CH_3)$_2$), 52.62 (*C*H(CH_3)$_2$), 22.19 (q, $^5J_{CF}$ = 3.8 Hz,

$CH(CH_3)_2$) 20.65 ($CH(CH_3)_2$), 12.76 ($C_5(CH_3)_5$). ^{19}F NMR (376.1 MHz, C_6D_6, 25 °C): -61.53 (CF_3).

$Cp^*[N(^iPr)C(CF_3)N(^iPr)]TaCl_2$ **(4.3)**

To 30 ml scintillation vial was added 0.210 g (0.340 mmol) of **4.2**, 15 ml of THF and a magnetic stirbar to give an orange solution which was then chilled to -25 ^oC. To this solution was added 1.5 g of 1.0% Na/Hg amalgam. Gradually the color of the solution darkened to ruby-red. Upon stirring for 2 h, all volatiles were removed, the crude product was extracted into pentane and salt impurities were removed by filtration. The solution was concentrated and stored overnight at -27 ^oC to yield dark red crystals of **4.3**.

4.5 References

1. (a.) Scharf, A. B.; Betley, T. A. *Inorg. Chem.* **2011**, *50*, 6837-6845. (b.) Bogart, J. A.; Lewis, A. J.; Boreen, M. A.; Lee, H. B.; Medling, S. A.; Carroll, P. J.; Booth, C. H.; Schelter, E. J. *Inorg. Chem.* **2015**, *54*, 2830-2837. (c.) Inkpen, M. S.; Du, S.; Hildebrand, M.; White, A. J. P.; Harrison, N. M.; Albrecht, T.; Long, N. J. *Organometallics* **2015**, *34*, 5461-5469. (d.) Chen, C.; Bellows, S. M.; Holland, P. L. *Dalton Trans.* **2015**, 16654-16670.
2. (a.) Rodriguez, M. M.; Bill, Eckhard, B.; Brennessel, W. W.; Holland, P. L. *Science* **2011**, *334*, 780-783. (b.) Anderson, J. S.; Rittle, J.; Peters, J. C. *Nature.* **2013**, *501*, 84-87. (c.) Keane, A. J.; Yonke, B. L.; Hirotsu, M.; Zavalij, Sita, L. R. *J. Am. Chem. Soc.* **2014**, *136*, 9906-9909. (d.) Searles, K.; Carroll, P. J.; Chen, C.; Pink, M.; Mindiola, D. J. *Chem. Commun.* **2015**, *51*, 3526-3528. (e.) Kuriyama,

S.; Arashiba, K.; Nakajima, K.; Matsuo, Y.; Tanaka, H.; Ishii, K.; Yoshizawa, K.; Nishibayashi, Y. *Nat. Commun.* **2016**, *7*, 12181-12189.

3. (a.) Yandulov, D. V.; Schrock, R. R. *Science* **2003**, *301*, 76-78. (b.) Arashiba, K.; Miyake, Y.; Nishibayshi, Y. *Nat. Chem.* **2011**, *3*, 120-125. (c.) Chalkely, M. J.; Del Castillo, T. J.; Matson, B. D.; Roddy, J. P.; Peters, J. C. *ACS Cent. Sci.* **2017**, *3*, 217-223.
4. Hirotsu, M.; Fontaine, P. P.; Zavalij, P. Y.; Sita, L.R. *J. Am. Chem. Soc.* **2007**, *129*, 12690-12692.
5. Laplaza, C. E.; Johnson, M. J. A.; Peters, J. C.; Odom, A. L.; Kim, E.; Cummins, C. C.; George, G. N.; Pickering, I. J. *J. Am. Chem. Soc.* **1996**, *118*, 8623-8638.
6. (a.) Tran, B. L.; Pinter, B.; Nichols, A. J.; Konopka, F.; Thompson, R.; Chen, C.; Krzystek, J.; Ozarowski, A.; Telser, T.; Baik, M.; Meyer, K.; Mindiola, D. J. *J. Am. Chem. Soc*. **2012**, *134*, 13035-13045. (b.) Scheibel, M. G.; Askevold, B.; Heinemann, F. W.; Reijerse, E. J.; de Bruin, Bas; Schneider, S. *Nat. Chem.* **2012**, *4*, 552-558.
7. (a.) Schoffel, J.; Rogachev, A. Y.; DeBeer, S.; Burger, P. *Angew. Chem. Int. Ed.* **2009**, *48*, 4734-4738. (b.) Long, A. K. M.; Yu, R. P.; Timmer, G. H.; Berry, J. F. *J. Am. Chem. Soc*. **2010**, *132*, 12228-12230.
8. Hirotsu, M.; Fontaine, P. P.; Epshteyn, A.; Zavalij, P. Y.; Sita, L. R. *J. Am. Chem. Soc*. **2007**, *129*, 9284-9285.
9. Decker, J. M.; Geib, S. J.; Meyer, T. Y. *Organometallics* **1999**, *18*, 4417-4420.
10. Epshteyn, A; Zavalij, P. Y.; Sita, L. R. *J. Am. Chem. Soc*. **2006**, *128*, 16052-16053.

Chapter 5: Implications of Research and Future Work

5.1 Implications of Discoveries

The CPAM ligand set has been a staple of the Sita research group for 20 years and have been found to be a "Jack-of-all-trades" in that it by making minor changes in metal choice and/or substitution within the amidinate framework, a myriad of chemical transformations have been accomplished including catalytic (living) coordinative polymerization of alpha-olefins, dinitrogen cleavage and group transfer of oxo, imido and sulfide ligands to unsaturated organic substrates. A surfeit of these successes can be credited to attenuating the sterics associated with the amidinate. As such, there is a "steric wall" wherein the size of the ligand can only reduced so much and therefore there is a limit to the enhancements that such a method can provide. Electronic tuning of the system has proven to be a versatile and (sometimes) orthogonal means for further improvement.

The qualitative and quantitative establishment of a "silyl-substituent effect" within organometallic chemistry, or more generally, a ligand-based secondary-bonding effect, suggests a means for amplifying the reactivity of imidos in nitrene group transfer. A secondary result of this study shows the relevance of electrophilic reaction centers in mid-valent molybdenum-mediated atom (or group transfer) reactions. This suggests that oxidation state depend reactions could occur at the same complex(es) thereby establishing a "single-catalyst, many products" paradigm that is unique to the CPAM system.

Enhanced electrophilicity due to ligand modulation has also been found to be an important modulation via the amidinate ligand. While a number of other groups have found that the introduction of inductively-withdrawing substituents led to reduced activity in polymerization catalysts of both early and late transition metals, in the work shown here, the use of trifluoromethyl-derivatized amidinates led to increases in both catalyst activity as well as regiocontrol without diminished stereocontrol.

5.2 Future Work

The introduction of the trifluoromethyl-substituted amidinates is an exciting addition to the previously established ligand modifications within the CPAM framework. Further, its investigation and impact have only just begun to be explored. While there are a number of routes which could be investigated three of the most promising will be briefly discussed.

5.2.1 Expanding the ligand library

The modality associated with the synthesis of amidines **3.1**-**3.3** speaks to a much wider variety of accessible proligands. Amidines with reduced steric profiles relative to **3.1**-**3.3** could profit from not other the electronic effects which have already been established but may actually access steric-environments not yet seen. The symmetric amidinate, $[N(Et)C(CF_3)N(Et)]^-$, would be analogous to the methyl and phenyl analogs which have already proven to produce significant improvements over their diisopropyl relatives. Further, the use of methylamine solutions (similar to the ethylamine used to generate **3.2**) would give access to both the symmetric amidinate, $[N(Me)C(CF_3)N(Me)]^-$, which would presumably gain even greater benefits from its reduced size as well as the

methyl analog of **3.2**, $[N(^tBu)C(CF_3)N(Me)]^-$, which would not only promise increased activity but also increased stereoselectivtiy given the even larger differentiation between the bulky tert-butyl group and the much smaller methyl.

5.2.2 The use of Cp*[N(ᵗBu)C(CF₃)N(Et)]Zr(R)Cl as a pre-initiators for olefin polymerization

One of the more frustrating discoveries from the work of Chapter 3 was the oily nature of the dimethyl species **3.9** and **3.10** and consequentially the difficulty associated with their purification. At times, mixed alkyl-halide species have been serendipitously

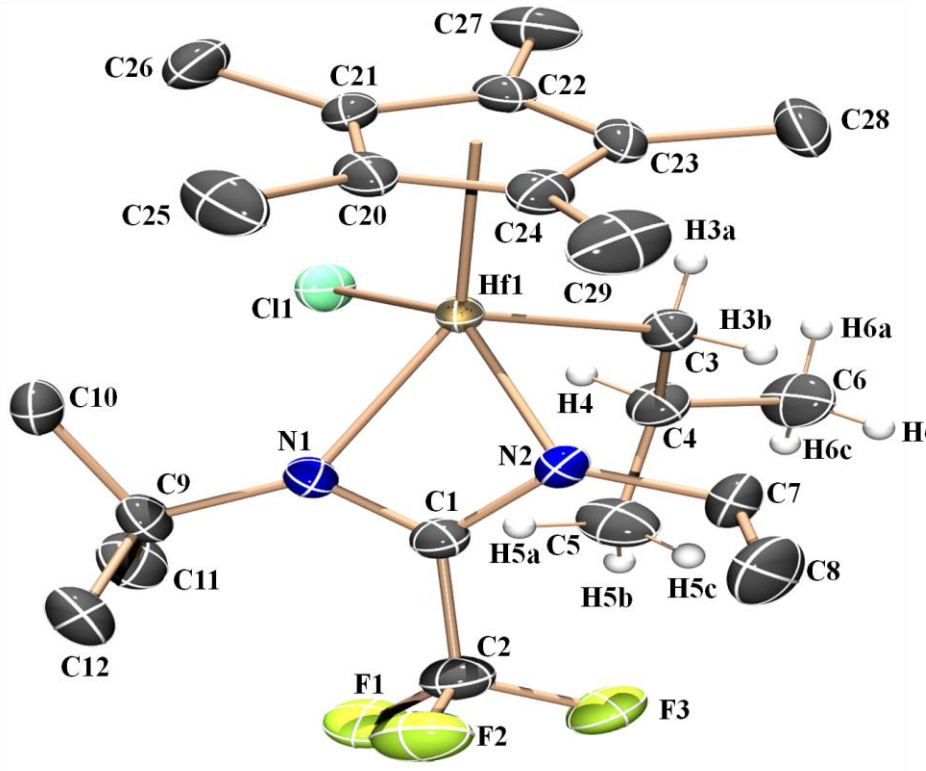

Figure 5.1. Structure of the mixed alkyl-halide, Cp*[N(ᵗBu)C(CF₃)N(Et)]Hf(ⁱBu)Cl.

isolated enroute to the dialkyls and have been found to be crystalline (Figure 5.1). Presumably, intentional and rational synthesis of the species,

Cp*[N(^{t}Bu)C(CF_3)N(Et)]Zr(R)Cl, should be easily achievable given the appropriate alkyl-magnesium chloride. Treatment of this crystalline solid with either silylium borate activators (e.g. [SiR_3][$B(C_6F_5)_4$]) or K[$B(C_6F_5)_4$] with 18-crown-6 (to avoid the use of coordinating, ethereal solvent) would generate the desired cationic, propagating species and one which should be capable of outperforming those associated with both **3.10** and Cp*[N(^{t}Bu)C(Me)N(Et)]$ZrMe_2$.

5.2.3 Extension to group VI

As was highlighted by the introduction of Chapter 2, molybdenum complexes supported by the CPAM ligand set have been found to be capable of undergoing a number of important chemical transformations including dinitrogen fixation and group transfer to unsaturated organic substrates, including carbon dioxide. Unfortunately, many of these reactions require extended reaction times and forcing conditions. The introduction of a trifluoromethyl-amidinate could lead to more electrophilic complexes and ones which could facilitate these transformations with lower barriers.

Appendix

Supporting kinetics data for Chapter 2

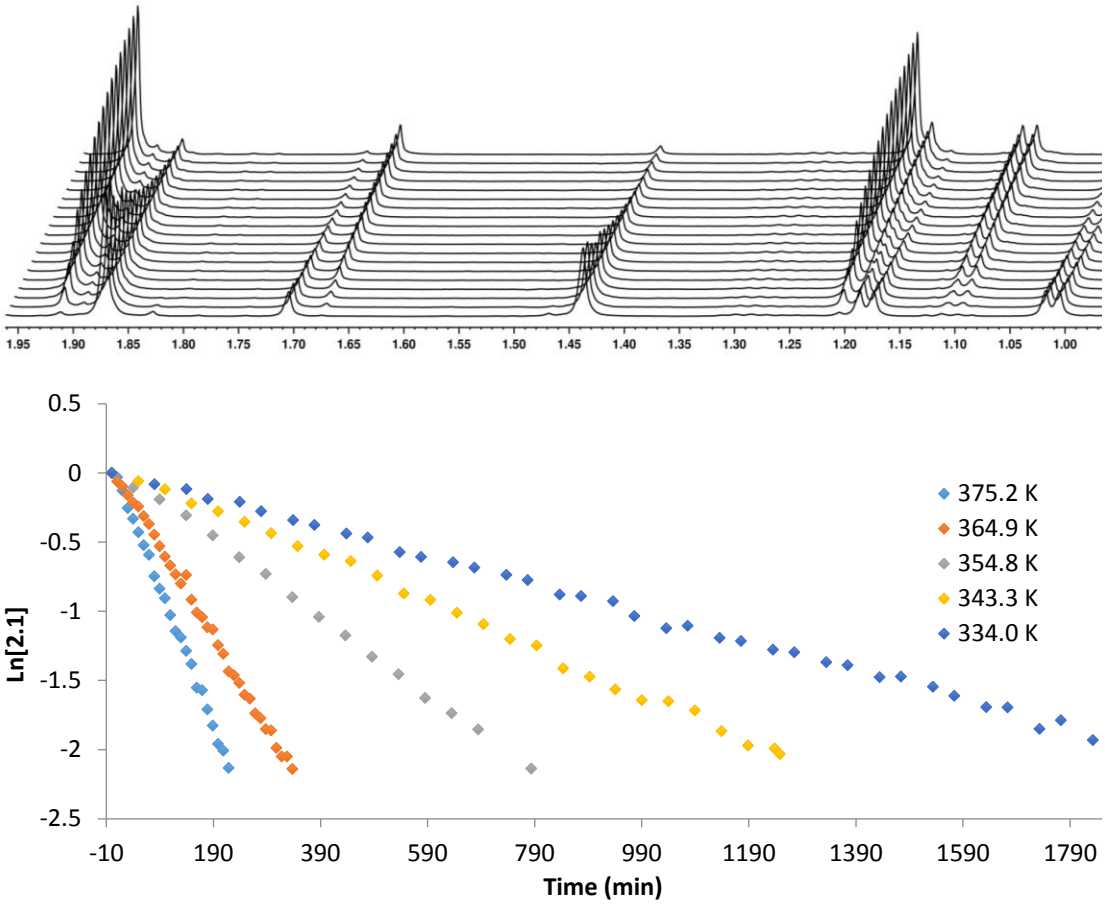

Figure A1. (Top) ^{1}H NMR stacked plot of group transfer from **2.1** to CNAr at 81.6 ^{o}C, Δt = 100 min. (Bottom) Temperature dependent normalized first order ln(A) = -kt + A_o plots.

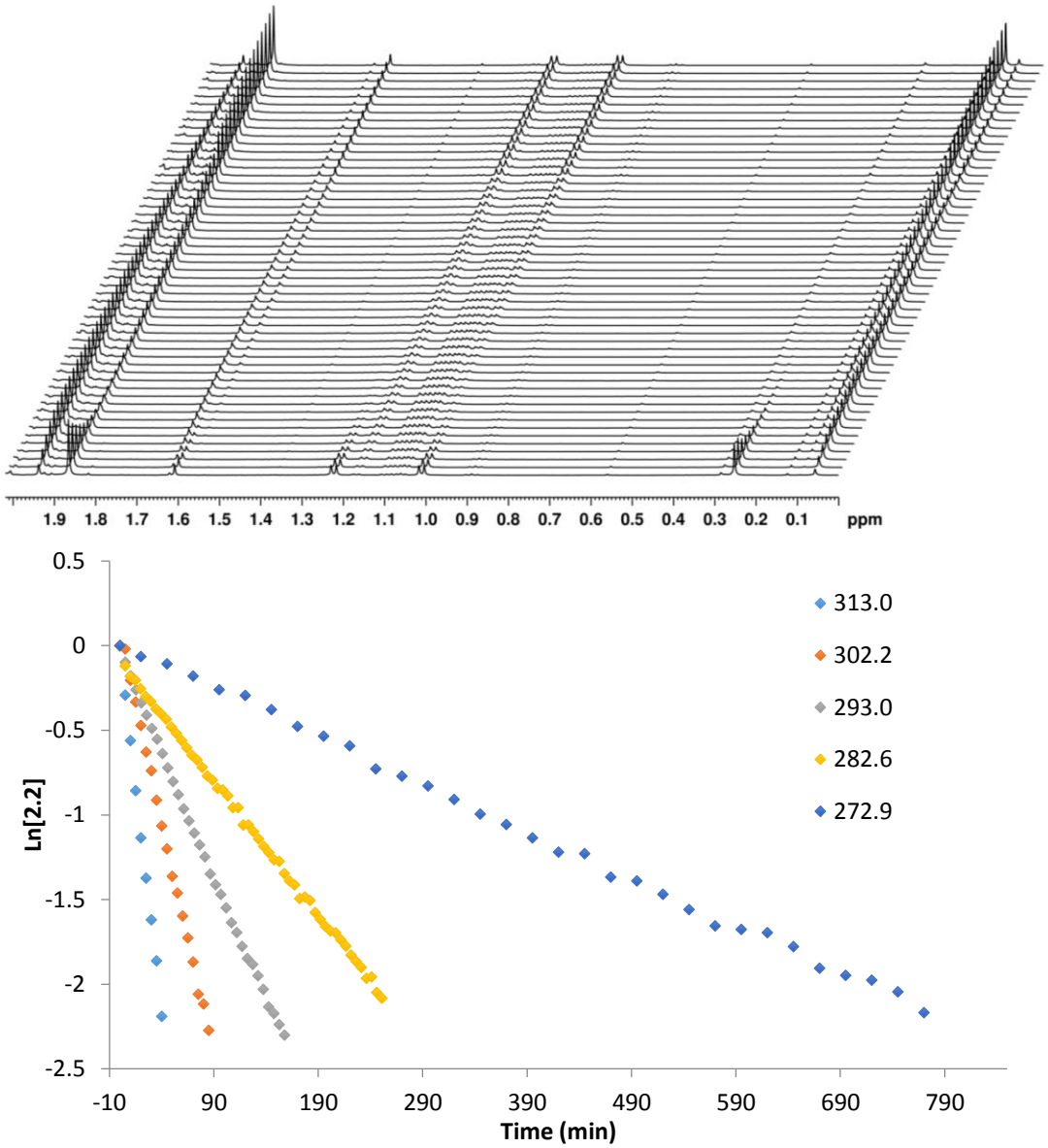

Figure A2. **(**Top) ^{1}H NMR stacked plot of group transfer from **2.2** to CNAr at -0.22 ^{o}C, ΔT = 50 min for the first 16 points and 100 after. (Bottom) Temperature dependent normalized first order ln(A) = -kt + A_o plots.

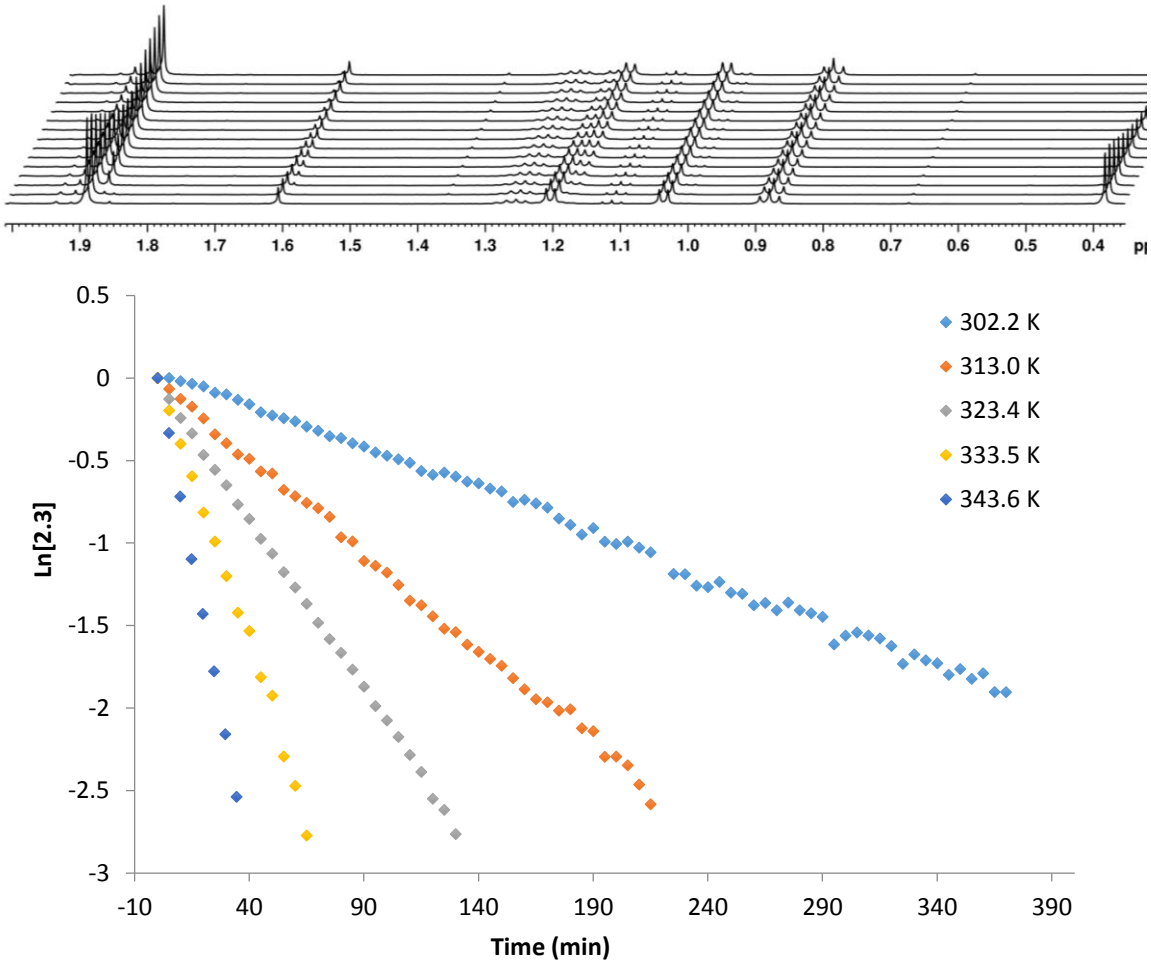

Figure A3. **(**Top) ^{1}H NMR stacked plot of group transfer from **2.3** to CNAr at 80^{o}C, Δt = 50 min. (Bottom) Temperature dependent normalized first order ln(A) = -kt + A_o plots.

Bibliography

1. (a.) Trnka, T. M.; Grubbs, R. H. *Acc. Chem. Res.* **2001**, *34*, 18-29. (b.) Crabtree, R. *Acc. Chem. Res.* **1979**, *12*, 331-337.
2. (a.) Knowles, W. S. *Acc. Chem. Res.* **1983**, *16*, 106-112. (b.) Kolb, H. C.; VanNieuwenhze, M. S.; Sharpless, K. B. *Chem. Rev.*, **1994**, *94*, 2483-2547.
3. Grubbs, R. H.; Coates, G. W. *Acc. Chem. Rev.* **1996**, *29*, 85-93.
4. (a.) Hammes, B. S.; Young, V. G.; Borovik, A. S. *Angew. Chem. Int. Ed.* **1999**, *38*, 666-669. (b.) MacBeth, C. E.; Golombek, A. P.; Young, V. G. Jr.; Yang, C.; Kuczera, K.; Hendrich, M. P.; Borovik, A. S. Science, 2000, 289, 938‑941.
5. (a.) Matson, E. M.; Bertke, J. A.; Fout, A. R. *Inorg. Chem.* **2014**, *53*, 4450-4458. (b.) Ford, C.; Park, Y. J.; Matson, E. M.; Gordon, Z.; Fout, A. R. *Science* **2016**, *354*, 741-743.
6. Schaverien, C. J.; Dewan, J. C.; Schrock, R. R. *J. Am. Chem. Soc.* **1986**, *108*, 2771-2773.
7. Freudenberger, J. H.; Schrock, R. R.; Churchill, M. R.; Rheingold, A. L.; Ziller, J.W. *Organometallics* **1984**, *3*, 1563-1573.
8. Gdula, R. L.; Johnson, M. J. A. *J. Am. Chem. Soc.* **2006**, *128*, 9614-9615.
9. Geyer, A. M.; Gdula, R. L.; Wiedner, E. S.; Johnson, M. J. A. *J. Am. Chem. Soc.* **2007**, *129*, 3800-3801.
10. Caballero, A.; Despagnet-Ayoub, E.; Diaz-Requejo, M. M.; Diaz-Rodriguez, A.; Gonzalez-Nunez, M. E.; Mello, R.; Munoz, B. K.; Ojo, W.-S.; Asensio, G.; Etienne, M.; Perez, P. J. *Science* **2011**, *332*, 835-838.

11. Flores, J. A.; Komine, M.; Pal, K.; Pinter, B.; Pink, M.; Chen, C-H; Caulton, K. G.; Mindiola, D. J. *ACS Catal.* **2012**, *2*, 2066-2078.

12. Inkpen, M. S.; Du, S.; Hildebrand, M.; White, A. J. P.; Harrison, N. M.; Albrecht, T.; Long, N. J. *Organometallics* **2015**, *34*, 5461-5469.

13. Sunkel, K.; Weigand, S.; Hoffmann, A.; Blomeyer, S.; Reuter, C. G.; Vishnevskiy, Y. V.; Mitzel, N. W. *J. Am. Chem. Soc*. **2015**, *137*, 126-129.

14. Brown, K. N.; Gulyas, P. T.; Lay, P. A.; McAlpine, N. S.; Masters, A. F.; Phillips, L. *J. Chem. Soc., Dalton Trans.* **1993**, 835-840.

15. Bellows, S. M.; Brennessel, W. W. Holland, P. L. *Eur. J. Inorg. Chem.* **2016**, 3344-3355.

16. (a.) Long, A. K. M.; Yu, R. P.; Timmer, G. H.; Berry, J. F. *J. Am. Chem. Soc*. **2010**, *132*, 12228-12230. (b.) Timmer, G. H.; Berry, J. F. *Chem. Sci.* **2012**, *3*, 3038-3052.

17. (a.) King, E. R.; Hennessy, E. T.; Betley, T. A. *J. Am. Chem. Soc.* **2011**, *133*, 4917-4923. (b.) Hennessy, E.T.; Betley, T. A. *Science*, **2013**, *340*, 591-595. (c.) Iovan, D. A.; Betley, T. A. *J. Am. Chem. Soc.* **2016**, *138*, 1983-1993. (d.) Wilding, M. J. T.; Iovan, D. A.; Betley, T. A. *J. Am. Chem. Soc.* **2017**, *139*, 12043-12049. (e.) Wilding, M. J. T.; Iovan, D. A.; Wrobel, A. T.; Lukens, J. T.; MacMillan, S. N.; Lancaster, K. M.; Betley, T. A. *J. Am. Chem. Soc.* **2017**, **DOI:** 10.1021/jacs.7b08714

18. 42 Examples in the CCDC

19. (a.) Verma, A. K.; Nazif, T. N.; Achim, C.; Lee, S. C. *J. Am. Chem. Soc*. **2000**, *122*, 11013-11014; (b.) Thomas, C. M.; Mankad, N. P.; Peters, J. C. *J. Am. Chem.*

Soc. **2006**, *128*, 4956-4957; (c.) Nieto, I.; Ding, F.; Bontchev, R. P.; Wang, H.; Smith, J. M. *J. Am. Chem. Soc.* **2008**, *130*, 2716-2717; (d.) Klinker, E. J.; Jackson, T. A.; Jensen, M. P.; Stubna, A.; Juhasz, G.; Bominaar, E. L.; Munck, E.; Que, L. *Angew.Chem. Int. Ed.* **2006**, *45*, 7394-7397; (e.) Zhang, H.; Ouyang, Z.; Liu, Y.; Zhang, Q.; Wang, L.; Deng, L. *Angew. Chem. Int. Ed.* **2014**, *53*, 8432-8436.

20. (a.) Cowley, R. E.; Eckert, N. A.; Vaddadi, S.; Figg, T. M.; Cundari, T. R.; Holland, P. L. *J. Am. Chem. Soc.* **2011**, *133*, 9796-9811. (b.) Cowley, R. E.; Holland, P. L. *Inorg. Chem.* **2012**, *51*, 8352-9361.
21. Searles, K.; Fortier, S.; Khusniyarow, M. M.; Carroll, P. J.; Sutter, J.; Meyer, K.; Mindiola, D. J.; Caulton, K. G. *Angew. Chem. Int. Ed.* **2014**, *53*, 14139-14143.
22. For selective examples focusing on C-H and H_2 activation, see the following: (a.) Cummins, C. C.; Baxter, S. M.; Wolczanski, P. T. *J. Am. Chem. Soc.* **1988**, *110*, 8731-8733. (b.) Harlan, C. J.; Tunge, J. A.; Bridgewater, B. M.; Norton, J. R. *Organometallics*, **2000**, *19*, 2365-2372. (c.) Wicker, B.; Fan, H.; Hickey, A. K.; Crestani, M. G.; Scott, J.; Pink, M.; Mindiola, D. J. *J. Am. Chem. Soc.* **2012**, *134*, 20081-20096. (d.) Brown, S. D.; Peters, J. C. *J. Am. Chem. Soc.* **2004**, *126*, 4538-4539. (e.) Walsh, P. J.; Hollander, F. J.; Bergman, R. G. *J. Am. Chem. Soc.* **1988**, *110*, 8729-8731.
23. For selective examples see the following: (a.) Feldman, J.; Davies, W. M.; Schrock, R. R. *Organometallics*, **1989**, *8*, 2266-2268. (b.) Schrock, R. R.; Murdzek, J. S.; Bazan, G. C.; Robbins, J.; DiMare, M.; O'Regan, M. *J. Am. Chem. Soc.* **1990**, *112*, 3875-3886. (c.) Bazan, G.; Khosravi, E.; Schrock, R. R.; Feast, W. J.; Gibson, V. C. *Polym. Commun.* **1989**, *30*, 258-260.

24. For selective examples see the following: (a.) Catino, A. J.; Nichols, J. M.; Forslund, R. E.; Doyle, M. P. *Org. Lett.* **2005**, *7*, 2787-2790. (b.) Doyle, M. P; Hu, W.; Timmons, D. J. *Org. Lett.* **2001**, *3*, 933-935. (c.) Wehn, P. M.; DuBois, J. *J. Am. Chem. Soc.* **2002**, *124*, 12950-12951. (d.) Hinman, A.; DuBois, J. *J. Am. Chem. Soc.* **2003**, *125*, 11510-11511. (e.) Yu, X.-Q; Huang, J.-S.; Zhou, X.-G.; Che, C.-M. *Org. Lett.* **2000**, *2*, 2233-2236. (f.) Hennessy, E. T.; Betley, T. A. *Science* **2013**, *340*, 591-594.

25. Davies, H. M. L; Manning, J. R. *Nature* **2008**, *451*, 417-420.

26. (a.) Wilding, M. J. Y.; Iovan, D. A.; Betley, T. A. *J. Am. Chem. Soc.* **2017**, *139*, 12043-12049. (b.) King, E. R.; Hennessy, E. T.; Betley, T. A. *J. Am. Chem. Soc.* **2011**, *133*, 4917-4923. (c.) Kuijper, P. F.; Tiekink, M. J.; Breukelaar, W. B.; Broere, D. L. J.; van Leest, N. P.; van der Vlugt, J. I.; Reek, J. N. H.; de Bruin, B. *Chem. Eur. J.* **2017**, *23*, 7945-7952.

27. Wilding, M. J. Y.; Iovan, D. A.; Wrobel, A. T.; Lukens, J. T.; MacMillan, S. N.; Lancaster, K. M.; Betley, T. A. *J. Am. Chem. Soc.* **2017**, **DOI:** 10.1021/jacs.7b08714.

28. (a.) Aguila, M. J.; Badiei, Y. M.; Warren, T. H. *J. Am. Chem. Soc.* **2013**, *135*, 9399-9406. (b.) Wiese, S.; McAfee, J. L.; Pahls, D. R.; McMullin, C. L.; Cundari, T. R.; Warren, T. H. *J. Am. Chem. Soc.* **2012**, *134*, 10114-10121. (c.) Iovan, D. A.; Betley, T. A. *J. Am. Chem. Soc.* **2016**, *138*, 1983-1993. (d.) Cowley, R. E.; Eckert, N. A.; Vaddadi, S.; Figg, T. M.; Cundari, T. R.; Holland, P. *J. Am. Chem. Soc.* **2011**, *133*, 9796-9811.

29. (a.) Kilgore, U. J.; Basuli, F.; Huffman, J. C.; Mindiola, D. J. *Inorg. Chem.* **2006**, *45*, 487-489. (b.)Kriegel, B. M.; Bergman, R. G.; Arnold, J. *J. Am. Chem. Soc.* **2016**, *138*, 52-55.

30. (a.) Saeguesa, T.; Ito, Y.; Shimizu, T. *J. Org. Chem.* **1970**, *35*, 3995-3996. (b.) Cowley, R. E.; Eckert, N. A.; Elhaik, J.; Holland, P. L. *Chem. Commun.* **2009**, 1760-1762. (c.) Cowley, R. E.; Golder, M. R.; Eckert, N. A.; Al-Afyouni, M. H.; Holland, P. L. *Organometallics* **2013**, *32*, 5289-5298. (d.) Nguyen, A. I.; Zarkesh, R. A.; Lacy, D. C.; Thorson, M. K.; Heyduk, A. R. *Chem. Sci.* **2011**, *2*, 166-169. (e.) Laskowski, C. A.; Hillhouse, G. L. *Organometallics* **2009**, *28*, 6114-6120. (f.) Wiese, S.; Aguila, M. J. B.; Kogut, E.; Warren, T. H. *Organometallics* **2013**, *32*, 2300-2308. (g.) Yousif, M.; Tjapkes, D. J.; Lord, R. L.; Groysman, S. *Organometallics* **2015**, *34*, 5119-5128. (h.) Yonke, B. L.; Reeds, J. P.; Fontaine, P. P.; Zavalij, P. Y.; Sita, L. R. *Organometallics* **2014**, *33*, 3239-3242. (i.) Mindiola, D. J.; Waterman, R.; Lluc, V. M.; Cundari, T. R.; Hillhouse, G. L. *Inorg. Chem.* **2014**, *53*, 13227-13238.

31. (a.) Stokes, B. J.; Richert, K. J.; Driver, T. G. *J. Org. Chem.* **2009**, *74*, 6442-6451. (b.) Stokes, B. J.; Dong, H.; Leslie, B. E.; Pumphrey, A. L.; Driver, T. G. *J. Am. Chem. Soc.* **2007**, *129*, 7500-7501. (c.) Thornton, A. R.; Martin, V. I.; Blakey, S. B. *J. Am. Chem. Soc.* **2009**, *131*, 2434-2435.

32. (a.) Hessell, E. T.; Jones, W. *Organometallics* **1992**, *11*, 1496-1505. (b.) Mindiola, D. J.; Hillhouse, G. L. *Chem. Commun,* **2002**, 1840-1841. (c.) Glueck, D. S., Wu, J. Hollander, F. J.; Bergman, R. G. *J. Am. Chem. Soc.* **1991**, *113*, 2041-2054. (d.) Danopoulos, A. A.; Wilkinson, G.; Sweet, T. K. N.; Hursthouse,

M. B. *J. Chem. Soc., Dalton Trans.* **1996**, 3771-3773. (e.) Ishida, Y.; Kawaguchi, H. *J. Am. Chem. Soc.* **2014**, 1*36*, 16990-16993. (f.) Hanna, T. E.; Keresztes, I.; Lobkovsky, E.; Bernskoetter, W. H.; Chirik, P. J. *Organometallics* **2004**, *23*, 3448-3458. (g.) Chomitz, W. A.; Arnold, J. *Chem. Commun.* **2008**, 3648-3650.

33. Keane, A. J.; Farrell, W. S.; Yonke, B. L.; Zavalij, P. Y.; Sita, L. R. *Angew Chem Int. Ed. Engl.* **2015**, *54*, 10220-10224.
34. Chen, G. J.-J.; McDonald, J. W.; Newton, W. E. *Inorg. Chim. Acta.* **1980**, *41*, 49.
35. Fontaine, P. P.; Yonke, B. L.; Zavalij, P. Y.; Sita, L. R. *J. Am. Chem. Soc.* **2010**, *132*, 12273-12285.
36. Keane, A. K., Ph.D. Thesis, University of Maryland-College Park, **2015**.
37. Babcock, J. R.; Sita, L. R. *J. Am. Chem. Soc.* **1998**, *120*, 5585-5586.
38. Anslyn, E. V.; Doughtery, D. A.; *Modern Physical Organic Chemistry*, **2006**, p. 104
39. Kitching, W.; Olszowy, H. A.; Harvey, K. *J. Org. Chem.* **1982**, *47*, 1893-1904.
40. (a.) Baldwin, J. C.; Lappert, M. F.; Pedley, J. B.; Poland, J. S. *J.C.S. Dalton*, **1972**, 1943. (b.) Elschenbroich, Christoph; *Organometallics*, 3rd Ed., Wiley: New York, **2006** p. 173.
41. (a.) Thompson, R.; Chen, C.-H.; Pink, M.; Wu, G.; Mindiola, D. J. *J. Am. Chem. Soc.* **2014**, *136*, 8197-8200. (b.) Stevenson, L. C.; Mellion, S. Clot, E. Mountford, P. *J. Am. Chem. Soc.* **2015**, *137*, 10140-10143. (c.) Grant, L. N.; Pinter, B.; Kurogi, T.; Carroll, M. E.; Wu, G.; Manor, B.; Carroll, P.; Mindiola, D. J. *Chem. Sci.* **2017**, *8*, 1209-1224. (d.) Clough, B. A.; Mellino, S.; Clot, E.; Mountford, P. *J. Am. Chem. Soc.* **2017**, *139*, 11165-11183. (e.) Clough, B. A.; Mellino, S.;

Protchenko, A. V.; Slusarczyk, M.; Stevenson, L. C.; Blake, M. P.; Xie, B.; Clot, E.; Mountford, P. *Inorg. Chem.* **2017**, *56*, 10794-10814.

42. Townsend, E. M.; Kilyanek, S. M.; Schrock, R. R.; Muller, P.; Smith, S. J.; Hoveyda, A. *Organometallics* **2013**, *32*, 4612-4617.
43. Parr, R. G.; Yang, W. Density-functional theory of atoms and molecules; Oxford University Press: Oxford, **1989**.
44. Perdew, J. P.; Burke, K.; Ernzerhof, M. *Phys. Rev. Lett.* **1996**, *77*, 3865.
45. Laikov, D. N. *Chem. Phys. Lett.* **1997**, *281*, 151.
46. Laikov, D. N.; Ustynyuk, Yu. A. *Russ. Chem. Bulletin* **2005**, *54*, 820.
47. (a.) Stevens, W. J.; Basch, H.; Krauss, M. *J. Chem. Phys*. **1984**, *81*, 6026; (b.) Stevens, W. J.; Basch, H.; Krauss, M.; Jasien, P. *Can. J. Chem*. **1992**, *70*, 612; Cundari, T. R.; Stevens, W. J. *J. Chem. Phys*. **1993**, *98*, 5555.
48. Nexant, I. **2007**; Vol. 2012.
49. Coates, G. W. *Chem. Rev.* **2000**, *100*, 1223–1252.
50. Guan, Z.; Cotts, P. M.; McCord, E. F.; McLain, S. J. *Science* **1999**, *283*, 2059–2062.
51. Domski, G. J.; Rose, J. M.; Coates, G. W.; Bolig, A. D.; Brookhart, M. *Prog. Polym. Sci.* **2006**, *32*, 30–92.
52. Lee, I.; Geuthier, W. J.; Ball, J. M.; Iyengar, B.; Collins, S. *Organometallics* **1992,** *11*, 2115-2122.
53. Piccolrovazzi, N.; Pino, P.; Consiglio, G.; Sironi, A.; Moret, M. *Organometallics* **1990,** *9*, 3098-3105.
54. Leino, R.; Lehmus, P.; Lehtonen, A. *Eur. J. Inorg. Chem.* **2004,** 3201-3222.

55. Coles, M. P.; Hitchcock, P. B. *Organometallics* **2003,** *22,* 5201-5211.

56. Andell, O.; Maaranen, J. World Patent No. WO99/10353, **1999**.

57. Iwashita, A.; Chan, M. C. W.; Makio, H.; Fujita, T. *Catal. Sci. Technol.* **2014,** *4,* 599-610.

58. Kenyon, P.; Mecking, S. *J. Am. Chem. Soc.* **2017,** *139,* 13786-13790.

59. J. Saito, M. Mitani, J. Mohri, Y. Yoshida, S. Matsui, S. Ishii, S. Kojoh, N. Kashiwa, T. Fujita, *Angew. Chem., Int. Ed. Engl.* **2001,** *40,* 2918-2920.

60. M. Mitani, J. Mohri, Y. Yoshida, J. Saito, S. Ishii, K. Tsuru, S. Matsui, R. Furuyama, T. Nakano, H. Tanaka, S. Kojoh, T. Matsugi, N. Kashiwa, T. Fujita, *J. Am. Chem. Soc.* **2002,** *124,* 3327-3336.

61. J. Saito, M. Mitani, J. Mohri, S. Ishii, Y. Yoshida, T.Matsugi, S. Kojoh, N. Kashiwa, T. Fujita, *Chem. Lett.* **2001,** *30,* 576-577.

62. J. Saito, M. Mitani, M. Onda, J. Mohri, S. Ishii, Y.Yoshida, T. Nakano, H. Tanaka, T. Matsugi, S. Kojoh, N.Kashiwa, T. Fujita, *Macromol. Rapid Commun*. **2001,** *22,* 1072-1075.

63. Tian, J.; Hustad, P. D.; Coates, G. W. *J. Am. Chem. Soc.* **2001,** *123,* 5134-5135.

64. Mason, A. F.; Tian, J.; Hustad, P. D.; Lobkovsky, E. B.; Coates, G. W. *Isr. J. Chem.* **2002,** *42,* 301-306.

65. Edson, J. B.; Wang, Z.; Kramer, E. J.; Coates, G. W. *J. Am. Chem. Soc.* **2008,** *130,* 4968-4977.

66. Weberski, M. P.; Chen, C.; Delferro, M.; Zuccaccia, C.; Macchioni, A.; Marks, T. J. *Organometallics* **2012,** *31,* 3773-3789.

67. Weberski, M. P.; Chen, C.; Delferro, M.; Marks, T. J. *Chem. Eur. J.* **2012,** *18*, 10715-10732.

68. Makio, H.; Kashiwa, N.; Fujita, T. *Adv. Synth. Catal.* **2002,** *344*, 477-493.

69. Elkin,T.; Aharonovich, S.; Botoshansky, M.; Eisen, M. S. *Organometallics* **2012,** *31*, 7404-7414.

70. The exception to this was the living-systems wherein fluorination solely occurred in either the 2- or 2,6-positions.

71. Jayaratne, K. C.; Sita, L. R. *J. Am. Chem. Soc.* **2000**, *122*, 958-959.

72. Jayaratne, K. C.; Keaton, R. J.; Henningsen, D. A.; Sita, L. R. *J. Am. Chem. Soc.* **2000**, *122*, 10490-10491.

73. Keaton, R. J.; Jayaratne, K. C.; Fettinger, J. C.; Sita, L. R. *J. Am. Chem. Soc.* **2000**, *122*, 12909-12910.

74. Keaton, R. J.; Jayaratne, K. C.; Henningsen, D. A; Koterwas, L. A.; Sita, L. R. *J. Am. Chem. Soc.* **2001**, *123*, 6197-6198.

75. Zhang, Y.; Keaton, R. J.; Sita, L. R. *J. Am. Chem. Soc.* **2003**, *125*, 9062-9069.

76. Zhang, Y.; Sita, L. R. *J. Am. Chem. Soc.* **2004**, *126*, 7776-7777.

77. Zhang, Y.; Reeder, E. K.; Keaton, R. J.; Sita, L. R. *Organometallics.* **2004**, *23*, 3512-3520.

78. Harney, M. B.; Keaton, R. J.; Fettinger, J. C.; Sita, L. R. *J. Am. Chem. Soc.* **2006**, *128*, 3420-3432.

79. Harney, M. B.; Zhang, Y.; Sita, L. R. *Angew. Chem. Int. Ed.* **2006**, *45*, 2400-2404.

80. Harney, M. B.; Zhang, Y.; Sita, L. R. *Angew. Chem. Int. Ed.* **2006**, *45*, 6140-6144.

81. Wei, J.; Hwang, W.; Zhang, W.; Sita, L. R. *J. Am. Chem. Soc.* **2013**, *135*, 2132-2135.

82. Kissounko, D. A.; Zhang, W.; Harney, M. B.; Sita, L. R. *Adv. Synth. Catal.* **2005**, *347*, 426-432.

83. Zhang, W.; Sita, L. R. *J. Am. Chem. Soc.* **2008**, *130*, 442-443.

84. Zhang, W.; Wei, J.; Sita, L. R. *Macromolecules* **2008**, *41*, 7829-7833.

85. Wei, J.; Zhang, W.; Wickman, R.; Sita, L. R. *Angew. Chem. Int. Ed.* **2010**, *49*, 9140-9144.

86. Wei, J.; Zhang, W.; Sita, L. R. *Angew. Chem. Int. Ed.* **2010**, *49*, 1768-1772.

87. Blakely, C. G., Ph.D. Thesis, University of Maryland-College Park, **2013**.

88. Knapp, C.; Lork, E.; Watson, P. G.; Mews, R. *Inorg. Chem.* **2002**, *41*, 2014-2025.

89. Wedler, M.; Knosel, F.; Noltemeyer, M.; Edelmann, F. T.; Behrens, U. *J. Organomet. Chem.* **1990**, *388*, 21-45.

90. Recknagel, A.; Knosel, F.; Gornitzka, H.; Noltemeyer, M.; Edelmann, F. T.; Behrens, U. *J. Organomet. Chem.* **1991**, *417*, 363-375.

91. Krasnopolski, M.; Hrib, C. G.; Seidel, R. W.; Winter, M.; Becker, H.; Rogalla, D.; Fischer, R. A.; Edelmann, F. T.; Devi, A. *Inorg. Chem.* **2013**, *52*, 286-296.

92. Sita, L. R.; Babcock, J. R. *J. Am. Chem. Soc.* **1998**, 5228-5230.

93. Davidson, J. L.; Green, M.; Nyathi, J. Z.; Stone, F. G. A.; Welch, A. J. *J. Chem. Soc., Dalton Trans.* **1977**, 2246-2255.

94. Koola, J. D.; Roddick, D. M. *Organometallics* **1991**, *10*, 591-597.

95. Loizou, D. C.; Castillo, J. Oki, A. R.; Hosmane, N. S.; Morrison, J. A. *Organometallics* **1992**, *11*, 4189-4193.

96. Taw, F. L.; Scott, B. L. Kiplinger, J. L. *J. Am. Chem. Soc.* **2003**, *125*, 14712-14713.

97. Huang, H.; Hughes, R. P.; Rheingold, *Organometallics* **2010**, *29*, 1948-1955.

98. Tamura, K.; Mizukami, H.; Maeda, K.; Watanabe, H.; Uneyama, K. *J. Org. Chem.* **1993**, *58*, 32-35.

99. Uneyama, K.; Kobayashi, M. *J. Org. Chem.* **1994**, *59*, 3003-3014.

100. Scharf, A. B.; Betley, T. A. *Inorg. Chem.* **2011**, *50*, 6837-6845.

101. Dureen, M. A.; Welch, G. C.; Gilbert, T. M.; Stephan, D. W. *Inorg. Chem.* **2009**, *48*, 9910-9917.

102. Krummenacher, I.; Cummins, C. C. *Polyhedron* **2012**, *32*, 10-13.

103. Rasika Dias, H. V.; Jin, W.; Kim, H.; Lu, H. *Inorg. Chem.* **1996**, *35*, 2317-2328.

104. Cole, M. L.; Evans, D. J.; Junk, P. C.; Smith, M. K. *Chem. Eur. J.* **2003**, *9*, 415-424.

105. Groom, C. R.; Bruno, I. J.; Lightfoot, M. P.; Ward, S. C. *Acta. Cryst.* **2016,** *B72*, 171-179.

106. Koterwas, L. A.; Fettinger, J. C.; Sita, L. R. *Organometallics* **1999**, *18*, 4183-4190.

107. Parr, R. G.; Yang, W. Density-functional theory of atoms and molecules; Oxford University Press: Oxford, **1989**.

108. Perdew, J. P. ; Burke, K.; Ernzerhof, M. *Phys. Rev. Lett.* **1996**, *77*, 3865.

109. Laikov, D. N. *Chem. Phys. Lett.* **1997**, *281*, 151.

110. Laikov, D. N.; Ustynyuk, Yu. A. *Russ. Chem. Bulletin* **2005**, *54*, 820.

111. (a.) Stevens, W. J.; Basch, H.; Krauss, M. *J. Chem. Phys*. **1984**, *81*, 6026; (b.) Stevens, W. J.; Basch, H.; Krauss, M.; Jasien, P. *Can. J. Chem*. **1992**, *70*, 612; Cundari, T. R.; Stevens, W. J. *J. Chem. Phys*. **1993**, *98*, 5555.

112. (a.) Scharf, A. B.; Betley, T. A. *Inorg. Chem.* **2011**, *50*, 6837-6845. (b.) Bogart, J. A.; Lewis, A. J.; Boreen, M. A.; Lee, H. B.; Medling, S. A.; Carroll, P. J.; Booth, C. H.; Schelter, E. J. *Inorg. Chem.* **2015**, *54*, 2830-2837. (c.) Inkpen, M. S.; Du, S.; Hildebrand, M.; White, A. J. P.; Harrison, N. M.; Albrecht, T.; Long, N. J. *Organometallics* **2015**, *34*, 5461-5469. (d.) Chen, C.; Bellows, S. M.; Holland, P. L. *Dalton Trans.* **2015**, 16654-16670.

113. (a.) Rodriguez, M. M.; Bill, Eckhard, B.; Brennessel, W. W.; Holland, P. L. *Science* **2011**, *334*, 780-783. (b.) Anderson, J. S.; Rittle, J.; Peters, J. C. *Nature.* **2013**, *501*, 84-87. (c.) Keane, A. J.; Yonke, B. L.; Hirotsu, M.; Zavalij, Sita, L. R. *J. Am. Chem. Soc.* **2014**, *136*, 9906-9909. (d.) Searles, K.; Carroll, P. J.; Chen, C.; Pink, M.; Mindiola, D. J. *Chem. Commun.* **2015**, *51*, 3526-3528. (e.) Kuriyama, S.; Arashiba, K.; Nakajima, K.; Matsuo, Y.; Tanaka, H.; Ishii, K.; Yoshizawa, K.; Nishibayashi, Y. *Nat. Commun.* **2016**, *7*, 12181-12189.

114. (a.) Yandulov, D. V.; Schrock, R. R. *Science* **2003**, *301*, 76-78. (b.) Arashiba, K.; Miyake, Y.; Nishibayshi, Y. *Nat. Chem.* **2011**, *3*, 120-125. (c.) Chalkely, M. J.; Del Castillo, T. J.; Matson, B. D.; Roddy, J. P.; Peters, J. C. *ACS Cent. Sci.* **2017**, *3*, 217-223.

115. Hirotsu, M.; Fontaine, P. P.; Zavalij, P. Y.; Sita, L.R. *J. Am. Chem. Soc.* **2007**, *129*, 12690-12692.

116. Laplaza, C. E.; Johnson, M. J. A.; Peters, J. C.; Odom, A. L.; Kim, E.; Cummins, C. C.; George, G. N.; Pickering, I. J. *J. Am. Chem. Soc.* **1996**, *118*, 8623-8638.

117. (a.) Tran, B. L.; Pinter, B.; Nichols, A. J.; Konopka, F.; Thompson, R.; Chen, C.; Krzystek, J.; Ozarowski, A.; Telser, T.; Baik, M.; Meyer, K.; Mindiola, D. J. *J. Am. Chem. Soc*. **2012**, *134*, 13035-13045. (b.) Scheibel, M. G.; Askevold, B.; Heinemann, F. W.; Reijerse, E. J.; de Bruin, Bas; Schneider, S. *Nat. Chem.* **2012**, *4*, 552-558.

118. (a.) Schoffel, J.; Rogachev, A. Y.; DeBeer, S.; Burger, P. *Angew. Chem. Int. Ed.* **2009**, *48*, 4734-4738. (b.) Long, A. K. M.; Yu, R. P.; Timmer, G. H.; Berry, J. F. *J. Am. Chem. Soc*. **2010**, *132*, 12228-12230.

119. Hirotsu, M.; Fontaine, P. P.; Epshteyn, A.; Zavalij, P. Y.; Sita, L. R. *J. Am. Chem. Soc*. **2007**, *129*, 9284-9285.

120. Decker, J. M.; Geib, S. J.; Meyer, T. Y. *Organometallics* **1999**, *18*, 4417-4420.

121. Epshteyn, A; Zavalij, P. Y.; Sita, L. R. *J. Am. Chem. Soc*. **2006**, *128*, 16052-16053.